UNIVERSITÀ DELLA CALABRIA

UNIVERSITA' DELLA CALABRIA

Dipartimento di Ingegneria Meccanica, Energetica e Gestionale – DIMEG

Scuola di Dottorato

"Pitagora"

Dottorato di Ricerca in Ingegneria Meccanica

CICLO

XXVIII

Titolo della tesi

ENHANCING IN PORTHOLE DIE EXTRUSION.

Influence of geometric and process parameters on the quality of aluminum alloys profiles

Settore scientifico disciplinare: ING-IND/16 Tecnologie e Sistemi di Lavorazione

Coordinatore: Ch.mo Prof. LEONARDO PAGNOTTA

Supervisore: Ch.mo Prof. LUIGINO FILICE

Dottoranda: Dott.ssa TERESA CITREA

Anni 2012/2015

UNIVERSITA' DELLA CALABRIA

Dipartimento di Ingegneria Meccanica, Energetica e Gestionale – DIMEG

Scuola di Dottorato

"Pitagora"

Dottorato di Ricerca in Ingegneria Meccanica

CICLO

XXVIII

Titolo della tesi

ENHANCING IN PORTHOLE DIE EXTRUSION.

Influence of geometric and process parameters on the quality of aluminum alloys profiles

Settore scientifico disciplinare: ING-IND/16 Tecnologie e Sistemi di Lavorazione

Coordinatore: Ch.mo Prof. Leonardo Pagnotta

Firma

Supervisore: Ch.mo Prof. Luigino Filice

Firma

Dottoranda: Dott.ssa Teresa Citrea

Firma _Teresa Citrea_

Anni 2012/2015

The work detailed in this thesis is the result of my engagements as a PhD researcher at the Mechanical, Energy and Management Department at University of Calabria and as Research Assistant at the Institute of Forming Technology and Lightweight Construction at Technische Universität of Dortmund (October 2013-June 2014).
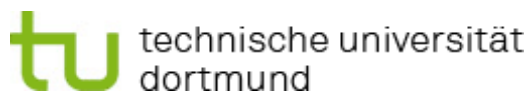
Alla mia famiglia ed

a coloro che anche oggi hanno vinto insieme a me

ACKNOWLEDGEMENTS

Please, let me do the acknowledgements on my own way.

I ringraziamenti sono sempre i più difficili da fare se non si vuol essere scontati. Devo avvertirvi che la mia lista è abbastanza lunga, spero voi abbiate quindi la pazienza necessaria. La mia sfida inizia otto anni fa, quando con l'appoggio dei miei genitori decisi di iscrivermi all'Università. È proprio a loro, ai loro consigli ed ai loro sacrifici che devo ciò che sono oggi. Ho incontrato tante persone lungo il mio percorso di studi universitario, ma poche sono quelle rivelatesi veri amici. Ne cito alcune, sperando che quelle che dimenticherò per la mia solita sbadataggine non me ne vogliano. Un grazie particolare va a Katia, mia amica nonché coinquilina, sempre pronta ad ascoltare le mie preoccupazioni e a trovare una soluzione ai miei problemi; a Romina, l'amica che tutti vorrebbero avere e per la quale nutro profonda stima, sempre con il sorriso sulle labbra e sempre pronta a sopportare le mie birbanterie. E poi un grazie alla mia Bionda, a Fabio, a Natalia ed a Carmen che mi hanno dimostrato che la vera amicizia dura anche se si è distanti; a Basilio, amico di corsa, di shopping e di complotti anti-autisti! Un grazie ad Enrico ed a tutto lo staff del bar di ingegneria che alla mattina mi davano la giusta carica per iniziare la giornata ed anche a tutti i conoscenti che hanno comunque segnato il libro della mia vita. Ed ora la cosa si fa più seria quindi massima concentrazione ;-p. Non uno, ma mille grazie vanno a coloro che fanno parte del mio gruppo di ricerca, che più che collaboratori sono amici e maestri di vita: al Prof. Filice che con cura e costanza ha seguito la mia crescita professionale, ma ciò che è più, quella personale; che quindi mi ha dato la possibilità di apprendere e aumentare le mie conoscenze e che mi ha dato anche la possibilità di scoprire nuovi mondi, gente eccezionale e posti spettacolari. A Giusy che con i suoi saggi consigli e la sua preparazione contribuisce a mandare avanti la baracca (ma sì, direi che possiamo anche darle il pieno merito di ciò), al magnifico trio composto dal Prof. Umbrello, Serafino e Stano che rendono le giornate più allegre; ad Ernesto, Renato e Diego, i tecnici più in gamba che conosca. Thanks to Professor Tekkaya for give me the opportunity to work in his Institute in Dortmund, working with knowledgeable and experienced people; to Professor Misiolek for his collaboration and friendship and to all of my dear German colleagues as well as lovable friends Martin, Christoph, Stephan, Eilina, Oliver, Matthias, Alessandro, Soeren. E per finire, non perché sia meno importante, il mio Grazie va a te, Fràààà..a

te che sei stato la mia guida, a te che sei stato mio amico, a te che sei stato mio consigliere, a te che, con i tuoi modi bizzarri e divertenti, mi hai insegnato sempre ad andare avanti ed a non arrendermi mai. A te che mi hai lasciata in mezzo ad una stazione in Germania, a te che mi hai fatto portare una valigia di ben 25 chili da sola, a te che hai scommesso un centesimo, a te che mi hai sempre spianato la strada e a te che me ne hai dette di tutti i colori :-(, sono convinta per il mio bene (anzi lo spero!!). Grazie anche a te, Giovanni che nel tuo piccolo riesci a regalarmi momenti irrinunciabili. Inutile dirvi che in questi tre anni di dottorato sono molto cambiata, non sono più la ragazzina di un tempo, timida ed insicura; sono oramai una donna colta, pronta a combattere per ciò che vuole e pronta a lavorare onestamente per ottenerlo. Forse ho esagerato con gli elogi, ma oggi concedetemelo! Tutto ciò è merito di voi tutti e di questa bellissima esperienza che mi avete dato la possibilità di vivere.

CONTENTS

LIST OF FIGURES

LIST OF TABLES

INTRODUCTION

Industrial needs are becoming always more complex pushed by an ever more demanding market and an increasingly fierce competition. Innovation and new products are the way forward if customers' attention has to be captured. On this direction, extrusion processes can be properly designed for the manufacture of complex shape parts. Furthermore, taking into account the current requirements related to the reduction of weights and volumes for fuel saving in the automotive field, the production of components with thinner thickness is increasingly on demand. Therefore, the process complexities have been growing up but, at the same time, companies have to assure quality and productivity in a more and more competitive scenario. Extrusion process consists of pressing a material of a billet inside a matrix container, forcing it to flow through an orifice built inside the final part of the matrix, named bearing land. The final profile has a shape with the same cross section reproduced by the orifice. Actually, porthole die extrusion of lightweight alloys is used for producing profiles that may have complex and hollow cross section geometries. Porthole die extrusion consists of splitting the material flow in several streams inside the matrix by using a porthole die in which there is a central mandrel linked to the die walls by means of bridges. The material streams flow into the feeders between the bridges and weld together behind them in the welding chamber, with a longitudinal seam weld. Moreover, also a charge weld will be present between two consecutive billets if the process is a continuous billet to billet process. The bonding is a solid welding so only a few materials can be used and particular extrusion conditions have to be guaranteed. The material considered in this thesis is the aluminum alloy AA6060 because its properties and its requests in industrial applications. Currently, the market demand of long profiles with thin cross sections and highly strength brings to manufacture profiles reinforced with elements such as wires. Composite extrusion with continuous reinforcing elements has other advantages: low process load due to the reinforcements inserting directly into the welding chamber from outside; reduced die wear and fracture generation; limited decohesion. Instead, some disadvantages, related to the settled process and geometric parameters, are: inclusion of air and not complete covering of the wire; reinforcing elements cracking; inhomogeneous material flow due to the reinforcements; positioning deflection of the wires. Properly, this thesis aims at investigating the influence of continuous reinforcing elements on

the material flow during composite extrusion. In such a way, guidelines are provided for a correct die design minimizing the distortion and the extrusion loads, manufacturing competitive products with the minimum effort. A particular die geometry, using a mandrel with curved feeding channels, is designed to fill the reinforcing elements directly into the material flow inside the welding chamber. Since the experience in case of composite extrusion is still limited, and in order to build that kind of die and to adequately set the process variables, a thorough knowledge about the porthole die extrusion principles and its criticalities is necessary. The most critical aspects are related to the seam welds quality, to the profile distortion and inhomogeneous material flow inside the profile at the die exit, and to the superficial and internal extrusion defects. Therefore different analysis are performed to investigate the influence of geometric and process parameters variations on the extrusion process characteristics in order to obtain undistorted profiles with good mechanical properties and without defects. It is also been attempted to generalize the extrusion process considering the simultaneous extrusion of non-symmetric profiles. Adding the obtained results with what is known in literature, the influence of reinforcing elements on the material flow distortion is analyzed extruding a profile with high reinforcing volume.

Methods and approaches used to reach the fixed goals are different. Numerical analysis and experimental campaigns are carried out in order to have more accurate and truthful results. Microstructural analysis and tensile tests are performed to increase the outcomes reliability and to better understand the phenomena that can occur during the process with particular extrusion conditions. Deform^{TM} and Altair HyperXtrude® are the software used during numerical investigations. Experimental campaigns, microstructural analysis and tensile tests are performed with the equipment in the Laboratory of Department of Mechanical, Energy and Management Engineering at University of Calabria (UNICAL) and in the Laboratory of Institute of Forming Technology and Lightweight Construction (IUL) at Technische Universität in Dortmund during a collaboration. Moreover, researchers of Lehigh University in Bethlehem, Pennsylvania, contributed analyzing microstructural properties of extruded specimens.

Following there is a brief description of the work done in this doctoral program, which will be discussed in detail in this thesis composed as below summing up.

- *Introduction_* An overview about the topic of interest and the objectives that this thesis aims to satisfy in the same area are briefly described.

- *Chapter 1: Main aspects of extrusion process_* Extrusion process is in detail explained focusing attention on the porthole die extrusion variant and reinforced profiles. Critical aspects of the process are highlighted: more in detail, welding phenomena in case of continuous billet to billet extrusion process, and profile distortion due to a inhomogeneous material flow inside the matrix and at the die exit; several studies regarding their evolution are also listed. Finally, some improvements and new challenges in the manufacture of profiles as lightweight and sustainable as possible are also mentioned.

- Chapter 2: *Investigated material, numerical approaches and experimental equipment_* AA6060 aluminum alloy is the material considered in this thesis because the mechanical and thermal characteristics and high weldability also in sound conditions. The most relevant features of this aluminum alloy are underlined and the evolution of its microstructure during extrusion process is investigated because the relation with the mechanical properties of the material. Another critical aspect to consider during extrusion process is related to external defects on the profiles surface due to some temperatures and speed fields. In this chapter the principal defects that could be visible with AA6060 aluminum alloy and the reasons are pointed out. Moreover, the numerical approaches used during the thesis are mentioned and the equipment utilized during the experimental tests and for outcomes analysis is disclosed.

- *Chapter 3: Investigation of seam welds phenomenon in porthole die extrusion_* In this chapter are described different analysis that are performed in order to investigate the seam welds evolution and the extrusion load, changing process and geometric parameters, in order to improve profile quality and avoid die wearing and breaking using presses with not so high capability, respectively. The outputs considered are pressure and temperature conditions inside the welding chamber, velocity distribution in the final extruded profiles and extrusion load reached during the process at regime. The focus lies firstly on the bridge volume of the extrusion porthole die, which influences the reinforcing elements feeding and the material entry in the welding chamber. The influence of the flow distortion on the contact pressure

inside the welding chamber is investigated designing a special test die with three mandrel supporting legs, each one of a different width. With the output considerations of the above cases of study, the effect of some geometric and process parameters on the seam weld quality is analyzed, because the influence on the welding pressure value and contact time inside the welding chamber between the material streams, respectively. The considered geometric parameters were the leg size and the extrusion ratio related to the profile thickness changes; whereas, the ram speed is the process parameter taken into account. The welding line quality is analyzed by means of the weld width that is one of the possible indicator of the weld soundness. Finally, the influence of the above process and geometric parameters on the profile quality and on the seam weld strength is investigated extruding a 'I' shaped section with the welding line in the middle of the central tongue by means of microstructural observation and tensile tests, respectively.

- *Chapter 4: Investigation of profile properties and distortion in porthole die extrusion_* High productivity and thin and complex profile shapes are a consequence of the process speed increment and the profile thickness reduction, respectively. Increasing the ram speed there is an increase of the temperature that can lead to superficial defects, such as hot shortness. Whereas, reducing the profile thickness there are strain and stress states that can originate ductile fractures such as shear tearing or speed cracking on the external profile surface. In this chapter results about defects growth are shown considering a ductile fracture criterion to highlight the relation between thickness reduction and punch velocity changes with superficial defects in extruded components.

Moreover, the material flow distortion and the process load in steady state conditions are analyzed in case of non-symmetric profiles evaluating the most influential geometric parameters.

*Chapter 5: Influence of reinforcing elements on the material flow distortion during composite extrusion_* The composite extrusion is taken into account, which aims at improving the mechanical properties of extrudates by embedding continuous reinforcing elements into profiles using a modified porthole die. The influence of the reinforcing elements on the material flow during the composite extrusion with high reinforcing volumes is evidenced. An

experimental campaign is carried out and a modeling approach is identified in order to simulate the composite extrusion process. Several issues are highlighted regarding the unbalanced material flow inside the final profile and the high load on the reinforcing elements that can bring to their breaking.

- *Conclusion_* A summary regarding the work done in this thesis is presented in the last chapter, accenting the quality and usefulness of the obtained results in the extrusion field and proposing some future developments.

1. MAIN ASPECTS OF EXTRUSION PROCESS

Extrusion is an innovative forming process that allows the manufacturing of complex profiles cross-sections (Fig. 1.1) characterized by good mechanical properties ensuring a lightweight product.

Billet aluminum   **Bearing**   **Final product**
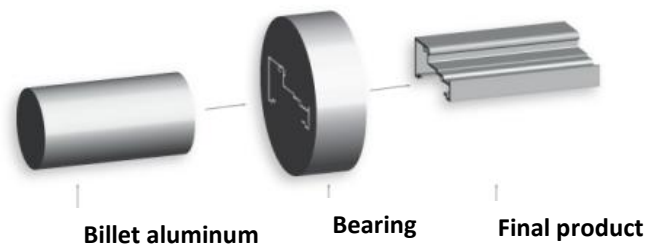
Figure 1.1. Extruded profile with complex shape

It consists of pressing a billet inside a container by means of a ram, sometimes with a hydraulic press. As pressure is first applied, the billet is pushed against the die, becoming shorter and wider until its expansion is constrained by full contact with the container walls. Then, as the pressure increases, the softer billet material, but still solid, begins to flow through the orifice of the bearing, at the die end, to emerge on the other side as a fully formed profile (Fig. 1.2). About 10% of the billet, including its outer skin, is left inside the container. The extruded profile is cut off at the die exit, and the remainder of the metal is removed to be recycled. The friction at the interface between the material and the die walls decelerates the material in these locations modifying the mechanical properties and generating some defects [1] on the profile surface and central bursting inside the extrudate. It is possible to avoid the problems with a right combination of lubricant and designing a die with a conical angle belonging to proper range to save the process energy [2]. The last one is given by three components: ideal energy, spent to reduce the cross section of the billet to get the final profile; distortion energy, spent to change the material lines flow before the orifice in the bearing land; and friction energy, due to friction opposition against the material flow along the extrusion direction. The optimal angle that reduces process energy belongs to the range 40-60 °, [3].
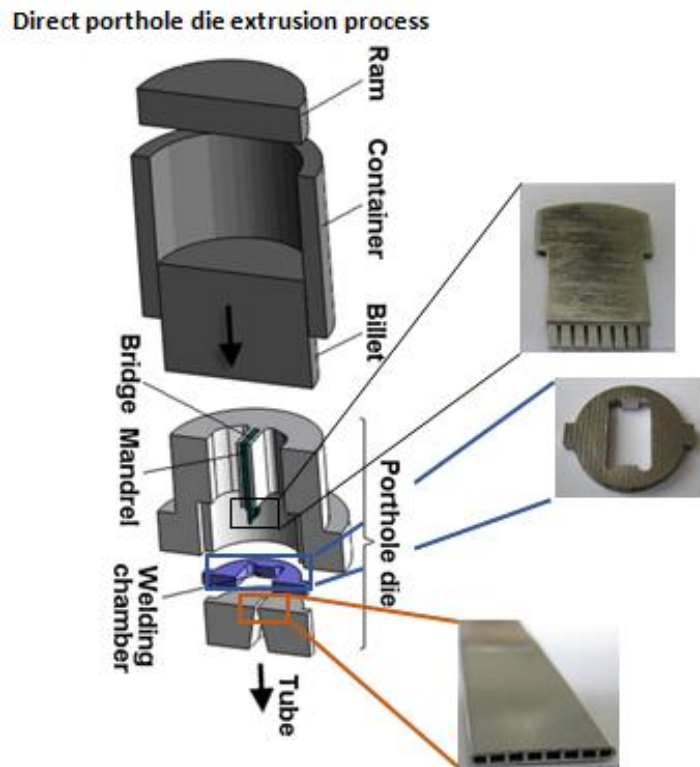
Figure 1.2. Extrusion process equipment

Extrusion rates vary, depending on the used alloy and the shape of the die. A hard alloy will flow slower than the soft one. The profile that leaves the die can undergo quenching, mechanical treatments and aging. Depending on the alloy, the semi-solid extrudate is cooled after emerging from the die: natural aging occurs at room temperature, while artificial aging takes place through controlled heating in an aging oven and it is sometimes referred to precipitation heat-treating. The aging process ensures the uniform precipitation of fine particles through the metal, yielding maximum strength, hardness, and elasticity for the specific extrusion alloy. Four are the variants of the process: direct, backward, hydrostatic and impact extrusion. More recent, but not less important, is the porthole die extrusion. The extrusion could be considered, in the same time, continuous referring to the extruded profiles and semi-continuous because the ram stroke, as well as the time work, is constrained by the billet volume.

There are several advantages of the modern process, such as: variety of possible profile shapes that can be complex and hollow, improvement of grain structure and strength properties, close tolerances and little amount of wasted material. Moreover, brittle materials can be processed because the only compressive and shear stresses.

Parts with an excellent surface quality and geometric accuracy, reducing other subsequent operations, can be manufactured. However, in order to have a good extruded profile, its cross section should be uniform and the material flow must be homogeneous throughout its length. The tool used to manufacture extruded profiles and the choice of process parameters depend of the material to work that can be a solid metallic billet, plastic granules or powder; also depending on that, the process can take place in hot or cold conditions. Cold conditions are typical to extrude small profiles with a simple shape and with processable materials. The process offers some advantages, such as: high mechanical properties after cold work hardening, high productivity, better dimensional tolerances control so that less surface treatments are needed, better quality surface and oxide layers absence. Some of the metals that can be extruded in cold conditions are lead, tin, aluminum alloys, copper, titanium, steel. On the other hand, hot conditions getting plastic deformation but without reaching the temperature corresponding to material melt, decrease strength and rise ductility, because the recrystallization phase. Oxide layers could wear the die-workpiece interface, which will lose its mechanical properties, so that a proper lubrication condition is very difficult, and the high temperature could also frazzle the die. Hot extrusion process is used in automotive and construction applications, window frame members, railings, aircraft structural parts. It permits to extrude metals such as aluminum, which can also be extruded without lubricant.

The principal disadvantage of extrusion process is the huge force required to extrude the billet because of frictional forces between billet material and walls along the entire length of the container. The load required is great at the beginning of the process; after that, it slowly decreases until the end of the billet volume and then it increases again because the billet is thin and the material must flow radially to reach the die orifice, so that the final volume of the billet is considered waste material. Most theoretical analysis of the process show that it is composed of two different stages, namely transient state at the beginning and steady state in the rest of the process cycle [4].

Dies are grouped as flat if they produce solid shapes and porthole dies if produce hollow or semi-hollow shapes. An important characteristic of both is that the effective local bearing lengths control the metal flow in order to homogenize it, so they can be set differently. The resistance to the material flow is greater with longer bearing

length, so the stream through thick parts of the profile can be slowed using longer bearing local lengths to match the speed of the material across the thinner parts with short local bearing lengths.

1.1 DIRECT PORTHOLE DIE EXTRUSION

Hollow profiles are manufactured with porthole die extrusion that is highly productive for manufacturing parts of small length and cross-section. The die consists of two parts: a mandrel to define the inner geometry of the profile and a die plate that determines the outer geometry (Fig. 1.3).
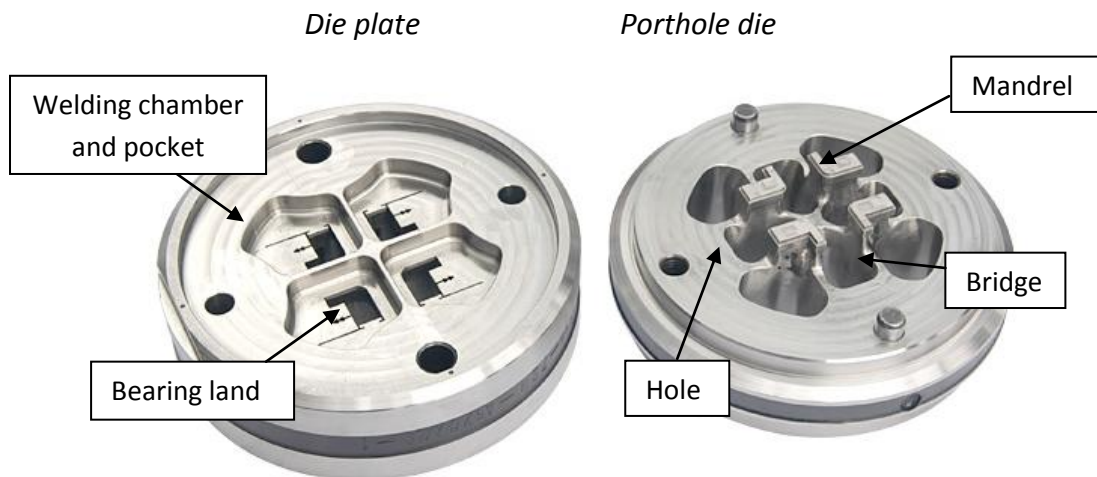
Figure 1.3. Extrusion porthole die

Some bridges, which support the core or mandrel, split the aluminum flow in several streams as many as the feeder holes (Fig. 1.4), that weld together in the welding chamber. Sometimes there is a region between the welding chamber and the bearing land, named pocket, which is designed in order to homogenize also the material flow.
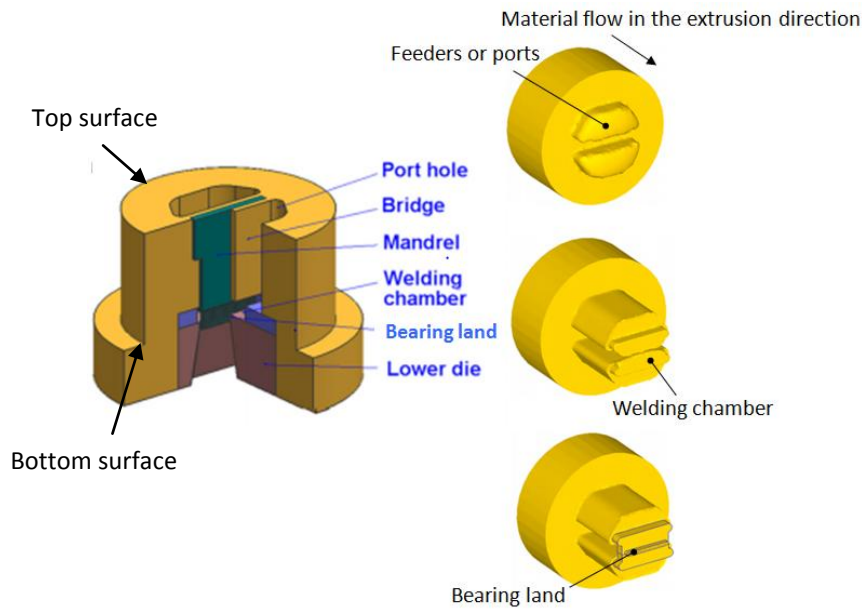
Figure 1.4. Material flow during ectrusion process, [5]

The process window is limited by two factors: the maximum extrusion load and the maximum exit temperature (Fig. 1.5).
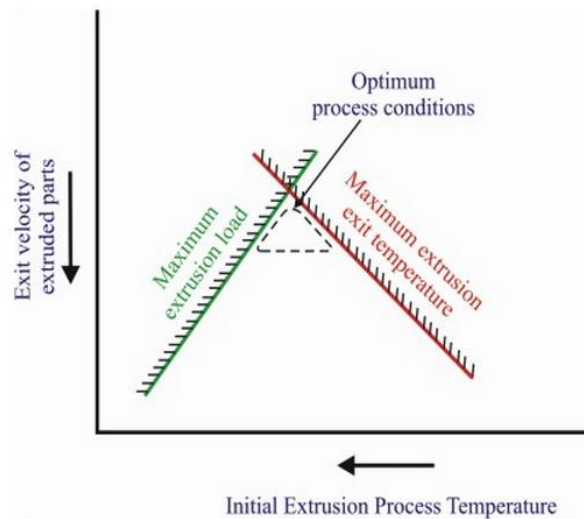
Figure 1.5. Extrusion process window

The maximum extrusion load is either imposed by the die strength and by the maximum capacity of the extrusion press. The extrusion load is low increasing the initial temperature of the billet; however, this is limited by the maximum exit temperature of the material into the profile. When this temperature gets too high, surface defects or even melting of the material can occur. So that, an optimization of the process is choosing an optimum initial temperature.

At the top of the porthole (Fig. 1.5), the material undergoes important deformation and microstructural recrystallization so that could be in an improvement of the material mechanical properties. At the bottom of the porthole, behind the bridges the streams weld together in solid longitudinal welding. Also corresponding to the seam weld the microstructure is different from the rest of the profile increasing the extrudate strength. As said, only some materials can create solid seam welds, such as aluminum or magnesium, with special temperature and pressure conditions and only a right set of geometric and process parameters permits to manufacture a profile without defects or air inclusion. Geometrical parameters are referred to die design therefore to portholes, welding chamber and bearing shape and volume; process parameters regard punch speed, temperature for billet and die and in general the boundary conditions. The process conditions depend also by the extrusion ratio; if it is higher than the quality of the extrusion is better [6].

In the design of porthole dies, another challenge is to obtain uniform exit velocity over the entire cross section of the profile in order to get an undistorted extrudate, with good mechanical properties, with both controlling and changing the bearing area and designing appropriately the welding chamber, feeder holes and pocket region.

Porthole is also the die used to manufacture reinforced extruded profiles. Composite extrusion with continuous reinforcing elements has different advantages: high strength with thin profile sections, low process load due to the reinforcements inserting directly into the welding chamber from outside; reduced die wear and fracture generation; limited decohesion. Instead, some disadvantages, related to the settled process and geometric parameters, are: inclusion of air and not complete covering of the wire; reinforcing elements cracking; inhomogeneous material flow due to the reinforcements; positioning deflection of the wires. The knowledge about the effects of continuous reinforcing elements on the material flow during composite extrusion is still limited. A particular die geometry, using a mandrel with curved feeding channels, is designed to fill the reinforcing elements directly into the material flow inside the welding chamber. In order to provide guidelines for a correct die design minimizing the distortion and the extrusion loads, manufacturing competitive products with the minimum effort, and to adequately set the process variables, a thorough knowledge about the porthole die extrusion principles and its criticalities is necessary. The most critical aspects are related to the seam welds quality, to the

profile distortion and inhomogeneous material flow inside the profile at the die exit, and to the superficial and internal extrusion defects.

1.2 WELDING IN PORTHOLE DIE: CHARGE AND LONGITUDINAL WELDS

During a porthole die extrusion process there are two kinds of welds: charge and longitudinal ones. The first welds appear between two billets consequently loaded into the container during the process; whereas, the second ones, between the material flows, previously split by the bridges, which weld together behind the porthole region, inside the welding chamber.

1.2.1 Charge welds

Charge welds result from interface between consecutive billets. The end of the previous billet, containing the contaminated and highly sheared residual material, should be removed properly and the use of lubricants should be avoided because it could remain entrapped in the charge weld [7]. While the charge weld is initially transverse to the extrusion direction, it is highly elongated and parallel to the longitudinal weld, so parallel to the profile contour, over most of the extrusion length. Particularly, in hollow extrusions they are so close to the longitudinal welds as to be indistinguishable from them [8], unless near to their initial location, as shown in Figure 1.6. With the presence of charge welds, there is a drop of elongation and a drop of ultimate and yield strength of the material [9].
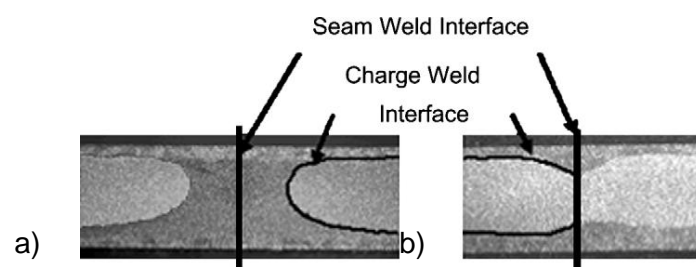
Figure 1.6. Charge and seam welds on the profile cross section, across the profile length a) at the beginning of the process and b) during extrusion, [8]

As the billet crosses the feeder and the die, the interface between the billets does not remain flat (Fig. 1.7), as already mentioned. Old material remains into the dead metal zone in the die corners (Fig. 1.8), subsequently flowing surrounding the new one into the profile as a coated surface, reducing the thickness of its layer with punch stroke advancing.
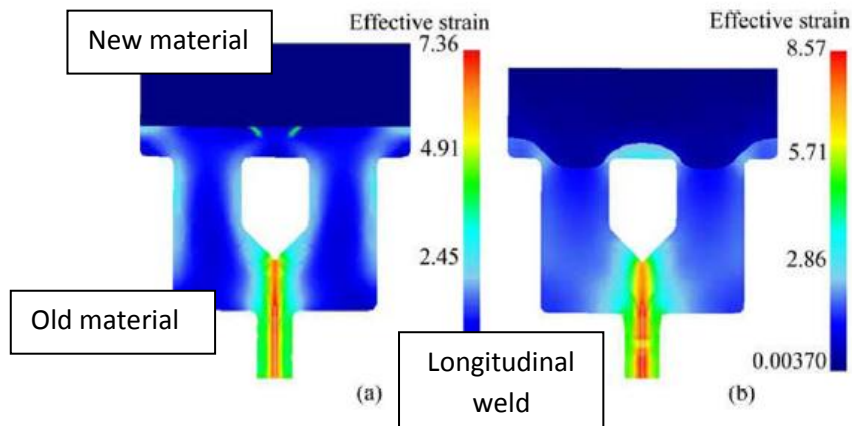
Figure 1.7. Transverse welding formation and effective strain distribution increasing simulation steps. Contact surface initially a) flat, and then b) curved, [10]

Not only near the die walls, but also in the middle of the extrudate, behind the bridge, there is the transverse weld [10]: during the process, the thickness of the layer formed by previous billet in the middle of the profile decreases, but never disappears, as shown in Figure 1.8.
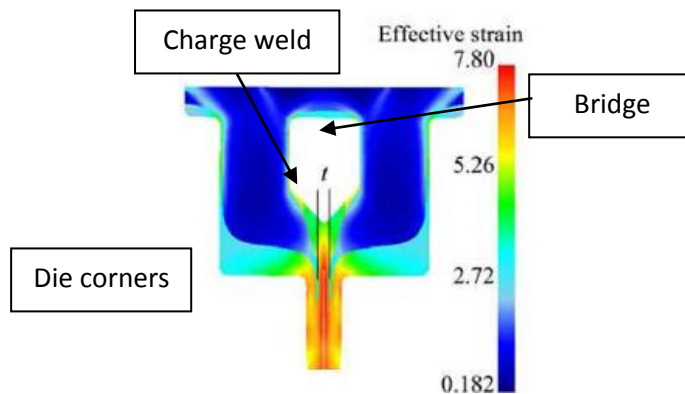
Figure 1.8. Effective strain distribution inside the profile and old material that, from the dead metal zone behind the bridge and at the die corners, flows in the middle and on the external surface of the extrudate, [10]

The transverse welding length and thickness depend on how fast the material from the previous billet flows out at the die corners; therefore, the geometry of feeder and die can significantly affects them. If a tapered feeder configuration is used, the center of the billet passes through the die earlier than the regular feeder configuration, [11]. During the entire extrusion, the previous billet material left inside the regular feeder geometry is much larger than that left in the tapered feeder (Fig. 1.9) because the different metal flow pattern relative to the geometry.
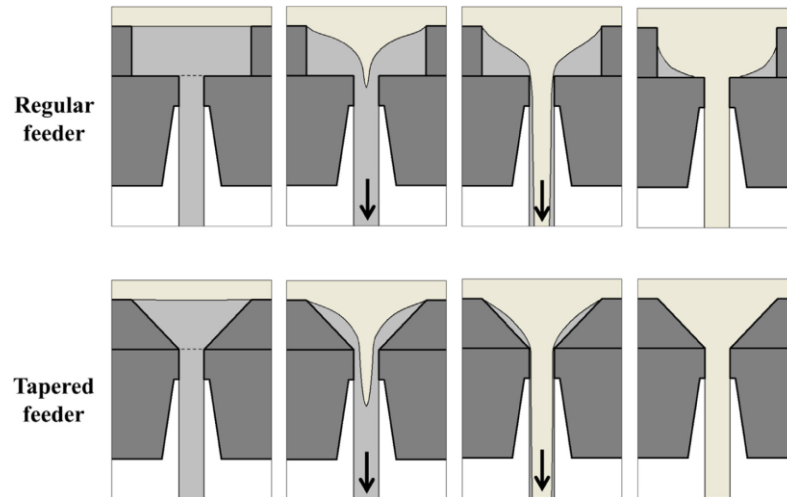
Figure 1.9. Effect of feeder geometry on the shape of transverse weld, increasing the ram stroke, [11]

Using a tapered shape, the length of product contaminated by the transverse weld defect and the clad thickness due to the previous billet, significantly decrease. Not only the shape, but also the volume of the feeder has a significant effect on the transverse weld extension (Akeret in [12]). Moreover, the charge weld length is longer if the extrusion ratio is higher.

During billet to billet process also some inclusions could be on the surface between the final part of the previous billet and the top part of the consecutive billet because the contact with air and punch. Increasing the pressure, the oxide layer of the interface would be broke into island-shaped flakes during heavy plastic deformation (Fig. 1.10), because it is generally considered less ductile than the bulk aluminum metal.
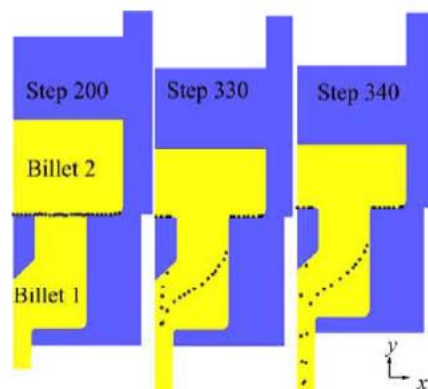
Figure 1.10. Distribution of oxides represented by black dots during billet to billet extrusion, considering subsequent simulation steps, [10]

Part of clean metal of the two bodies in contact will extrude through the holes between the oxide flakes.

1.2.2 Longitudinal welds

During porthole die extrusion, the material flows, previously split by the bridges into the feeder holes, are welded with a longitudinal welding at the end of the bridges into the welding chamber, with particular temperature and pressure conditions [13]. The welding line is the weakest point of the extrusion product and its strength depends also by the extrusion ratio, portholes number, bearing length, billet temperature, mandrel shape, welding chamber design. To guarantee pressure and temperature conditions suitable for a solid seam weld generation different works were conducted in order to investigate how the geometric and process parameters can influence those variables. For example, if the welding chamber height is too high, pressure and time contact increase, but the effective stress and strain decrease. The pressure value decreases until the bearing land, after that it increases because the material is pressed to make the final profile shape. Moreover, if the welding chamber height is elevated, also the extrusion load increases [14]. On the other hand, if that height is not so high the seam weld will be just a false bonding; therefore, a compromise is needed [15]. The bridge design is also important to avoid gap between the material flows, because the region behind bridges is the region of the welding chamber that is filled later than the bottom of the chamber [16]: if the bridge at the end is not flat, the dead metal zone is not so relevant and there are better pressure conditions. Another parameter to consider for a good welding is the process velocity because its effects on temperature, extrusion pressure, effective stress, contact time [17]. If the velocity is too low, the contact time between the hotter material and the colder container increases so that the material cools more rapidly. On the other hand, increasing the velocity there is an increase of productivity, but also the stored thermal energy is high and defected surfaces and welds can appear due to recrystallization [18].

1.2.3 State of the art about welding phenomena

Pargin, in 1988 started to investigate the charge welds; more in detail, the effects of temperature, deformation and welding chamber height on the length of the charge weld in a tubular and circular extrudate, were analyzed.

Subsequently, Akeret [12], in 1992, focused his study on the influence that the extruded material alloy and the die design parameters had on the charge weld

length. Moreover, the mechanical properties into the profile were analyzed, far from the stop mark. The last one is the visible sign between two profiles, left at the interface profile-die at the bearing exit, when the ram is stopped. The profile corresponding to this region and to the zone in which the charge weld starts has to be discarded because it represents a discontinuity. Some experimental tests were performed with the disadvantage to have results related to a particular die geometry. Also the work of Johannes, in 1996, was experimental. He stated that the profile length unwrapped can be reduced changing the ratio between the orifice volume into the bearing and its cross section area. The back-end defect started corresponding to an extruded billet length of 85%; in particular, the skin of the previous billet left into the container, because the friction at the interface billet-container walls, started to extrude covering the profile made up of the new material billet. In 2000, Saha [19] proposed an empirical equation in order to evaluate the evolution of the charge welds for different die geometries. In particular the length of the profile unwrapped, considering the stop mark, depended from the ratio between the volume of the portholes and welding chamber and the product between the area of the cross section of a single profile and the number of profiles simultaneously extruded from the die. Sheppard [20] noted that the interface between two consecutive billets into the feeders and the bearing, so the charge weld, did not remain flat during the extrusion, but it bended due to the material flow, creating a coating surface layer.

Meanwhile, Valberg [21] analyzed the extrusion of small H shape profiles using a porthole die, with a seam weld in the middle section evaluating the bonding strength. Afterwards, Bourqui [22] studied the pressure requirements within the die for obtaining sound welds and Kim [13] investigated the welding pressure with respect to the changes of welding chamber length, H4 and H5 in Figure 1.11, and bridge shape, H1, H3 and Hp in the same Figure.
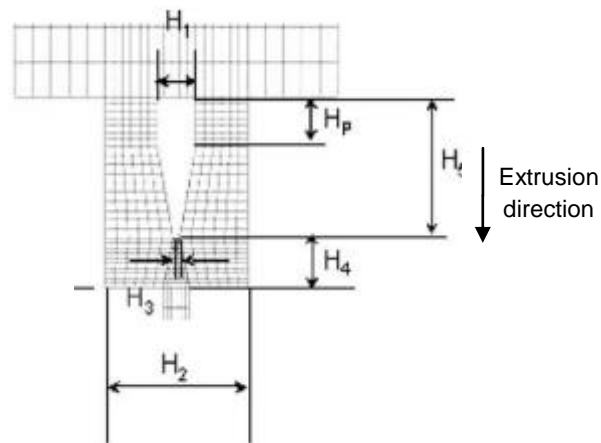
Figure 1.11. Two-dimensional model of the welding chamber, [13]

The top surface of the bridge did not influence the welding pressure inside the welding chamber, while the bottom tip had a big control of it. In fact, whit a shorter H3 parameter, the welding pressure was higher. Also increasing Hp, therefore the angle of the bridge bottom surface, there was an increase of welding pressure near the tip. Regarding the welding chamber, increasing its height also the welding pressure and contact area increased. With those changes the welding line had an improved strength. Another aim [23] was to investigate the metal flow into profiles with tubular shape (Fig. 1.12a), in steady state extrusion starting from 6 rings-shaped billet into which thin wires were inserted (Fig. 1.12b).

a)   b)
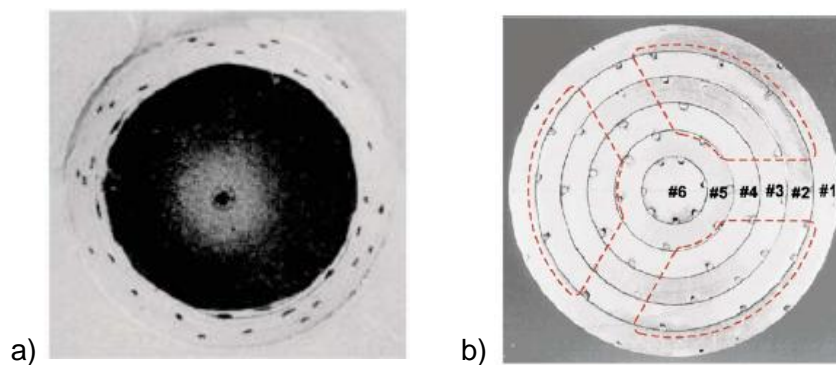
Figure 1.12. 6 Rings-shaped billet for detecting metal flow: a) tubular profile and b) positions of inserted wires, [23]

By using that billet, characterized by alternative layers of different materials AA1050 and AA1100, the attention was focused on which part of the billet flowed into the die exit and welding plane. By keeping track of the boundaries between the first billet and the ring-shaped billet (the second one) on all the transverse sections observed, the

transition of dead metal zone shape and deformation zone shape was clarified. The metal flow behavior in respect to the location inside the billet was understood by examining boundaries between adjacent rings. At the end, it was clear that no billet surface flowed into the welding plane in the steady-state extrusion, unlike that in the later stage of extrusion.

In 2003, Jo [14] enriched the research examining how billet temperature, bearing length and product thickness affected the welding strength, analyzing the welding pressure. The considered profile was a hollow and circular extruded made up of Al7003. By the numerical and experimental outcomes it was possible to observe that increasing the initial billet temperature, the extrusion load decreased with an increase of the welding pressure. Changing the bearing length, both the extrusion load and the welding pressure slightly and gradually raised. The reason why the extrusion load was nearly constant according to the bearing length was because the relatively small friction area in the bearing in comparison with the total friction area. In relation to the product thickness changed in order to have a constant extrusion ratio, extrusion loads and welding pressure made no difference. Finally, the pressure on the welding plane was the greatest when the billet temperature was high, the bearing length long, considering the same extrusion ratio, as later accorded by the expanding test using a conical punch. Billet temperature had a high influence also on the occurrence of surface defects.

In the same year, Li [24] analyzed the charge welds stating that their length depended on how quickly the previous billet material flowed in the bearing corners, surrounding the new billet material. He stated that using conical dies, the dead metal zone disappeared more quickly unlike occurred with a flat die (90 °). Numerical methods were used to analyze the charge weld formation and behavior; the FEM software firstly used was Deform2D^{TM}, simulating the extrusion of an aluminum alloy, AA6061. As already known, it was possible to see that when the charge welds moved into the profile, the surface started to be not orthogonal to the extrusion direction. A gap was at the tip of the charge weld (Fig. 1.13) and there was a difference between the two material flows velocity: the metal of the new billet flowed faster than the old one generating a sliding phase on the welding interface. The velocity discrepancy decreased when the metal reached the bearing orifice due to

sticking condition at the welding interface depending of temperature, energy and distance from the bearing exit.
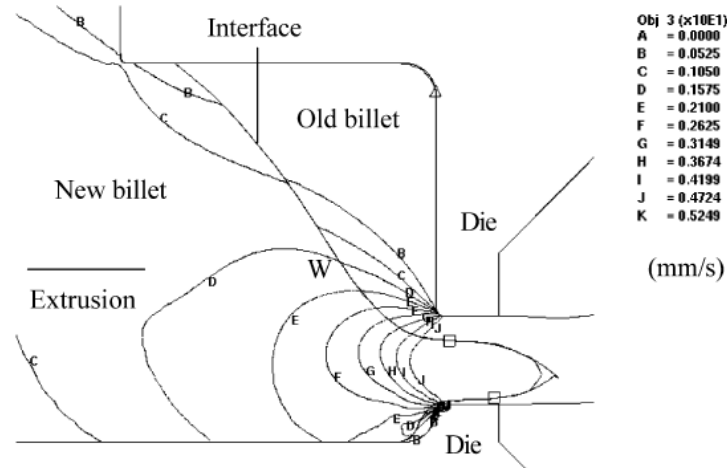
Figure 1.13. Gap between two consecutive billets surface corresponding to the charge weld surface, [24]

Also microstructural analysis were added to the numerical and experimental tests; Loukus [25] focused his attention on AA6082 microstructure and stated that the regions with charge welds were not ductile as the region without welds. Moreover, Mg_2Si precipitates were visible on the charge weld surfaces, leading to premature failure of the profile at such points. The study was extended also to porthole die extrusion, analyzing the welding line microstructure. A big difference in the dimensions of the grains on the weld sides (Fig. 1.14) was revealed due to the old and new materials.
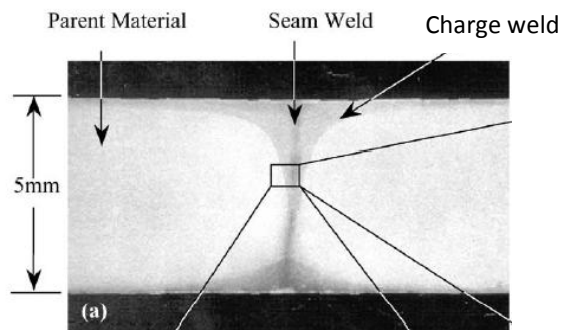
Figure 1.14. Microstructure corresponding to the charge weld surface, [25]

Considering several samples with different inclination respect the welding line, also an analysis of the tensile strength was performed, highlighting a fracture typically

brittle. The research continued also on the front of seam welds. In fact, Donati and at. [26] determined the criteria that could discriminate good welds from poor ones, that was improved in [27] taking into account also the temperature influence. Donati and at. [28], provided then to analyze the extrusion of AA6082 profiles (Fig. 1.15a), with a central seam weld line suitable for mechanical testing. Different processing conditions were tested, varying the dimensions of the die feeder (Fig. 1.15b), the length of the welding chamber, indicated as H in the next Figure 1.15, the billet pre heating temperature and the process speed.
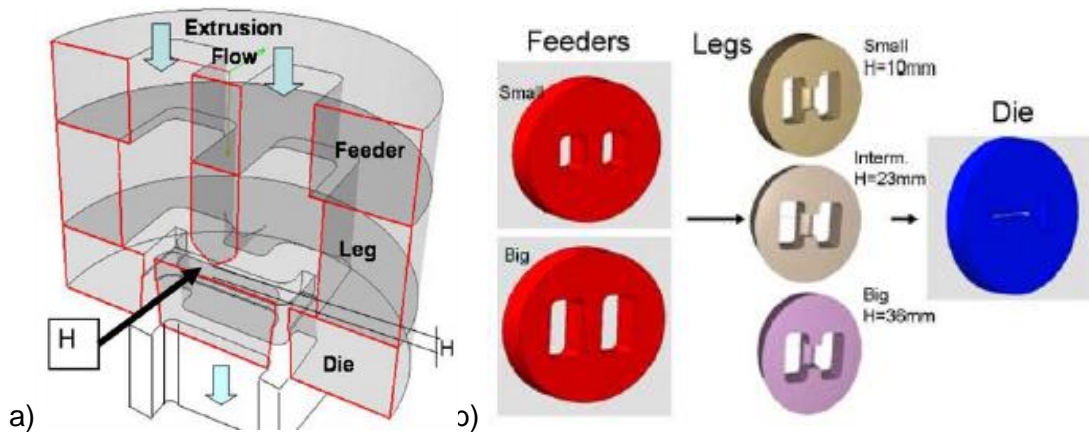
Figure 1.15. a) Die assembly and profile shape and b) geometry variations, [28]

For each condition, the workability area was defined by detecting tearing defects in the production stage. Considering a general extrusion limit diagram (Fig. 1.16), different types of limitations must be taken into account: pressure requirements and press speed limits, occurrence of poor product mechanical properties, appearance of profile defects.
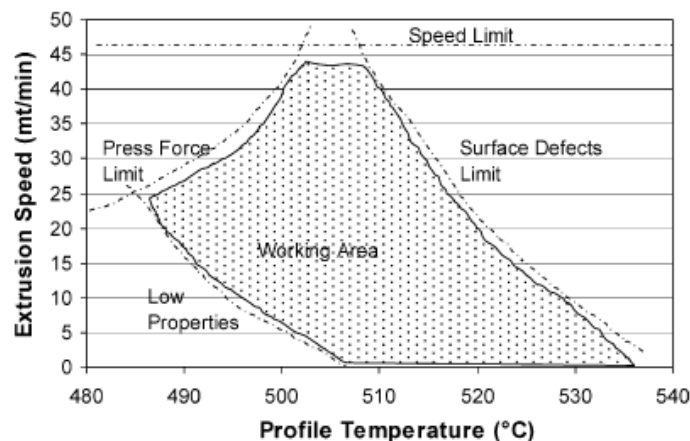
Figure 1.16. Extrusion limit diagram by Johannes and Jowett, [28]

The first mentioned limit depends on the type of press used, the second one is typical of very low process temperatures and speeds, and usually appears during the first extrusion stage, when many oxides are present in the die and on the billet. Instead, the occurrence of profile defects is related to die geometry. The welding chamber volume was the parameter that mainly affected the residence time of the material in the welding chamber and the maximum pressure at the top of the chamber; the feeding ports sections regulated the strain in the final stage of extrusion and hence the strain inside the welding chamber. Tensile strength and equivalent fracture strain were evaluated on the final product to assess the effectiveness of welding. The ultimate stress was independent of die geometry. Concerning the strain at fracture: a small welding chamber provided the lowest strain while the bigger one determined a fracture strain close to that typical of the no weld condition. Moreover, big feeders determined a fracture strain that was less sensitive to welding chamber variations than small ones. Bigger feeder allows a high increase in production speeds, but its dimensions are usually limited by the dimensions of the bridges supporting the mandrel, fixed by metal pressure. Also friction and strain rate have to be considered: a smaller welding chamber decreased the friction surface, but strongly increased local strain rate, and consequently the flow stress and extrusion loads [29]; on the other hand, a bigger welding chamber allowed a marked decrease in strain and consequently in flow stress, thus allowing a strong reduction in extrusion loads.

Bingol [30] analyzed the influence of temperature and ram speed on the welds macro-structure properties after the extrusion of AA6063 profiles. Increasing the billet temperature and the profile temperature, coarse grains were present and the visibility of the seam region was reduced. Whereas, increasing the ram speed, the grains structure was finer and the charge weld was well distinguishable, Figure 1.17.
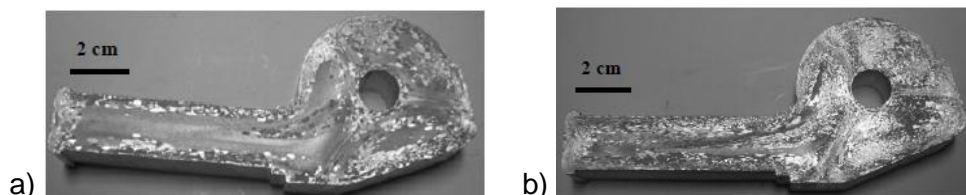
Figure 1.17. Specimens with both seam welds and transverse weld; a) Tbillet=470 °C, V=10 mm/s, Tprofile=500 °C; b) Tbillet=490 °C, V=15 mm/s, Tprofile=520 °C, [30]

Moreover, he observed that the alloys after heat treatments shown a higher yield stress with a decrease of the material strength in the thermal affected zone.

Afterwards, Zhu [31], in 2007, took into account the influence of the charge welds between two thermally treated specimens made up of AA6063 and AA6061, respectively. In order to analyze the influence of different pre heating temperatures of billet, production rates, welding chamber heights and feeders surface, on the weld quality, a "I" shaped profile of AA6082 was extruded by means of a porthole die extrusion in the work of Pinter [32]. Experimental tests were carried out and microstructural analyses were performed to explain fracture mechanisms. Also in this case, no correlation was found between the ultimate tensile stress, die design and production rates. Fracture strain was found to decrease with increasing speed and specimens extracted from higher welding chamber height and bigger cross section area of the feeder showed greater deformability. Crack propagation tests were performed to discriminate seam weld quality. The best weld qualities, almost comparable to the behavior of the unwelded profiles, were obtained with die geometry characterized of big feeder ports and high welding chamber height.

Subsequently, in 2009, Khan [33] analyzed the AA6082 material flow into the extrusion porthole die both numerically, with Deform2D, and experimentally aiming at homogenizing the structure of the charge welds and the other parts inside the profile. To get a good welding line, an extrusion pressure was needed higher than the yield stress of the asperity between the surfaces destroying the oxide layer on the same surface. In order to avoid the dead metal zones that make comfortable the charge welding phenomena (Fig. 1.18) a bridge with a tip at the bottom was required.
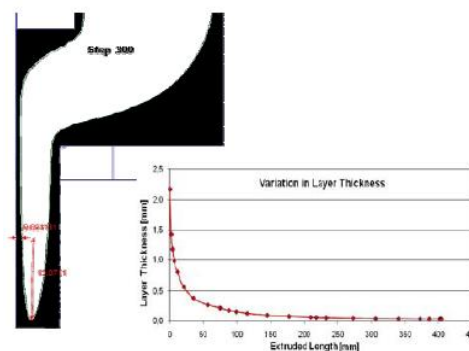
Figure 1.18. Numerical outcomes regarding the flow distribution of two consecutive billets. More in detail, the black region represents the dead metal zone and the graph represent its thickness variation along the profile, [33]

In 2010, Hatzenbichler [34] also used the FEM code Deform to analyze the process parameters influence on the charge weld extension and on the back-end defect, and

Khan analyzed the material flow in a porthole die with two portholes of different dimensions, [35]. Two models of porthole die with different porthole sizes were created by displacing pointed bridge from the center line of welding chamber as shown in Figure 1.19. In order to approximate the real case, a meshed material was initially set up into the welding chamber. The numerical outputs shown that the contact surface between the two billets started to bend especially where the feeder was bigger.
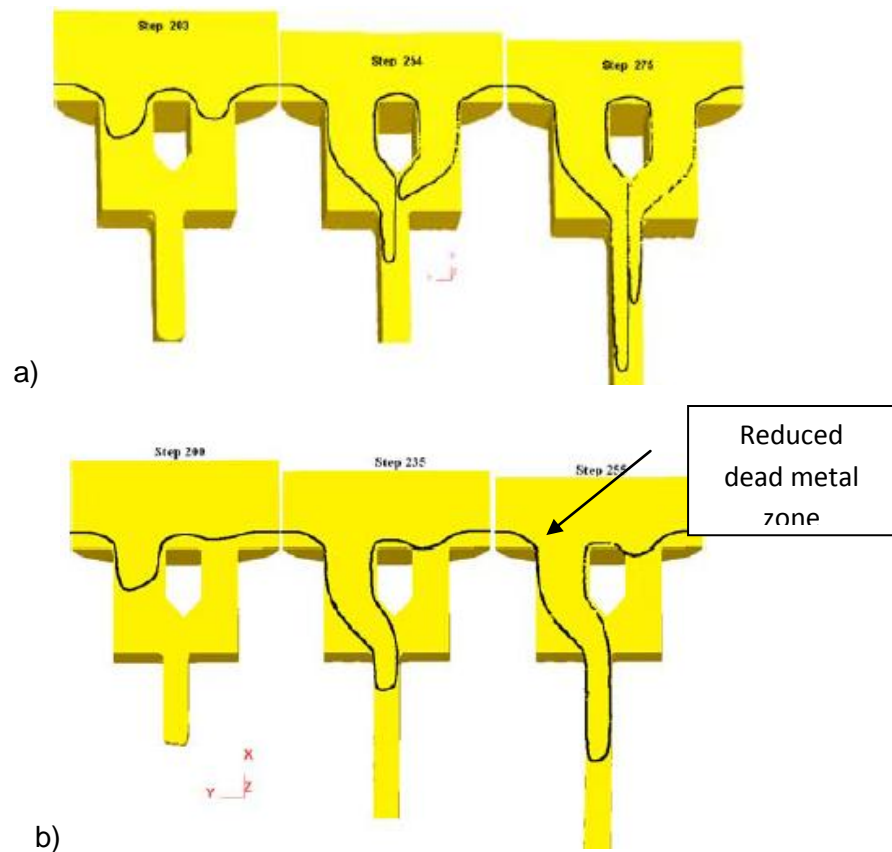
Figure 1.19. 3D models of porthole die with different porthole sizes created by displacing pointed bridge a) 2 mm, b) 4 mm, from the center line of welding chamber, and contact surface between two consecutive billet, [35]

The material of the old billet flowed into the profile around the new material until it disappeared. There were changes also in the dead metal zone on the top of the bridge that was more reduced if the feeders were not symmetrically located (Fig. 1.19b). The strain rate, related to the flow speed, was higher in the wider feeder (bridge 4 mm far from the center line of the welding chamber); instead, pressure distribution was irregular in that case and was difficult to define a welding plane between two flows that joined behind the bridge with very different velocity values.

Jowett [36] carried out experimental tests and stated that the old material was in the profile until the end of the process, influencing the new one. Moreover, Zhang in [10], analyzed the microstructure of seam and charge welds highlighting the presence of oxide layers, in case of extrusion of two billets with different materials, AA1100 and AA6061, as shown in Figure 1.20.
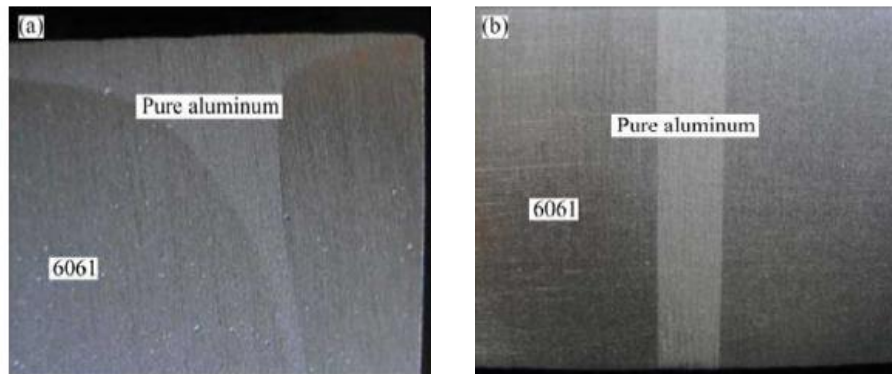
Figure 1.20. Macrograph of welding zone: a) transverse section; b) longitudinal section, [10]

The microstructure of the seam welds was characterized by a dark band with big grains with irregular shape due to the abnormal grains growth with high shear deformation and high temperatures (Fig. 1.21, Point 2). The microstructure of the charge welds was characterized by finer and equiaxic recrystallized grains due to the dynamic recrystallization and the grain growth during extrusion process and aging treatment (Fig. 1.21, Point 1).
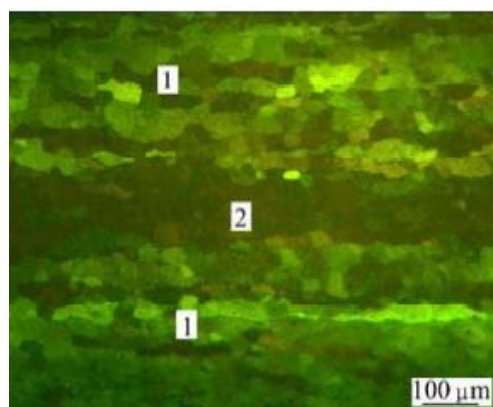
Figure 1.21. Microstructural analysis of charge welds (Pont 1) and seam weld (Point 2), [10]

Recently, Reggiani [37] investigated the evolution of the charge welds, considering different kinds of friction models, with microstructural analysis and numerical tests by means of Altair HyperXtrude® software. The friction influenced the flow of the material in contact with the walls inside the die that had eight feeders and permitted

to extrude four non-symmetric profiles made up of AA6060 in the same time (Fig. 1.22).
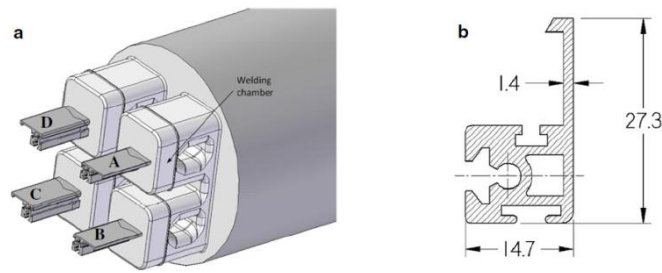
Figure 1.22. a) Extrusion of 4 non symmetric profiles; b) profile cross section, [37]

The hollow profile had a shape with a thinner part X and a thicker one Y, as shown in Figure 1.23, so the material flow was not homogeneous.
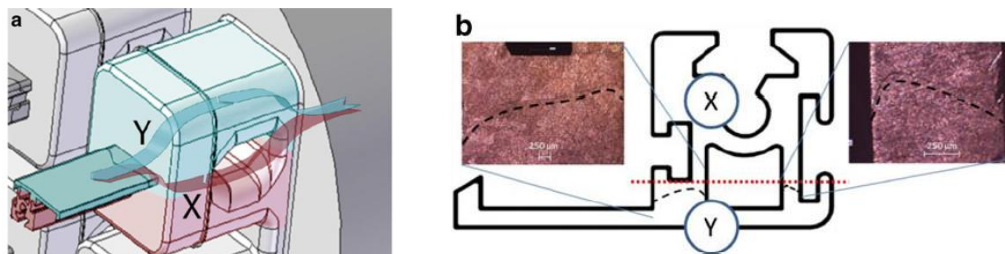
Figure 1.23. a) 3D view of metal flow; b) position of the bridge (dotted line) and experimental seam welds (dashed lines) for one profile at 200 mm from the tip, [37]

In the following Figure 1.24, is possible to distinguish the *stop mark* that represented the end of the ram stroke when the new billet filled the container, generated on the profile surface at the exit of the bearing. *'ds'* is the region in which there was still the material of the previous billet and after that the charge weld started. After the distance *'de'* the charge weld was considered disappeared, so the profile was made up of the only material of the new billet.
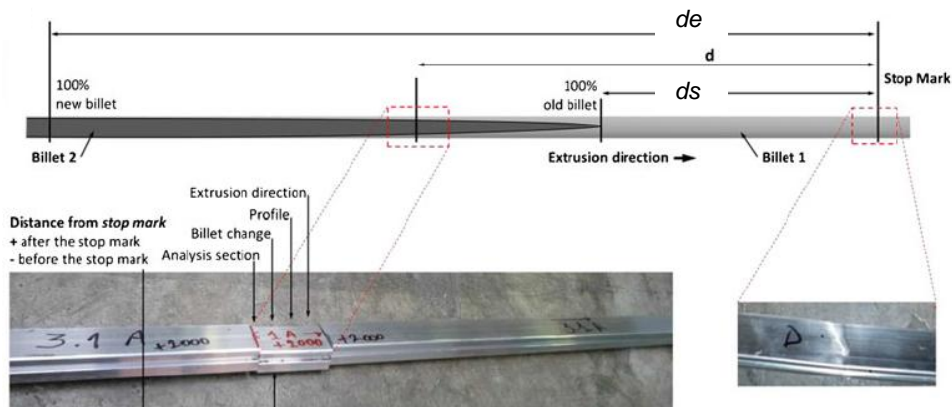
Figure 1.24. Charge weld evolution during an extrusion process, [37]

The analysis was performed into the profile before the stop mark to observe the seam weld characteristics inside the first extrudate and after the mark to evaluate the back-end effect inside the second extrudate. As expected, the material was faster in the thicker region of the profile cross section replacing easily the material of the previous billet. The flows of the new billet coming from the two portholes were then joined in a seam weld (Fig. 1.23b). Considering all profiles located as in Figure 1.22, the results obtained about the charge welds evolution, are shown in Figure 1.25 and Table 1.1.
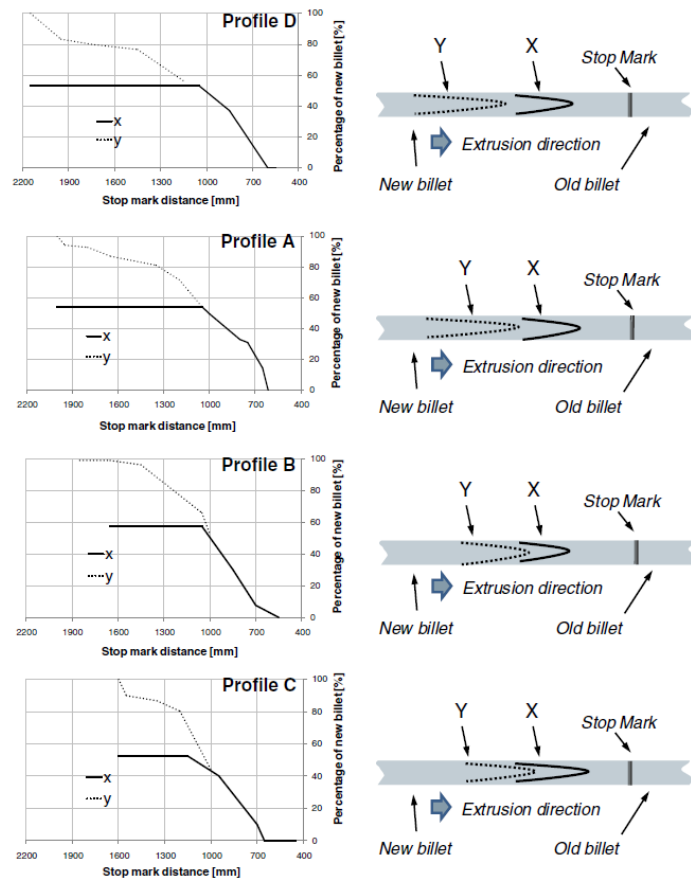
Figure 1.25. Charge weld evolution into the 4 profiles, [37]

Profile	Start–stop distance from stop mark [mm]	X [mm]	Y [mm]
A	565–1,950	565–1,000	1,090–1,950
B	500–1,600	500–1,000	900–1,600
C	400–1,550	400–1,150	950–1,550
D	500–2,100	500–1,000	1,080–2,100

Table 1.1. Results concerning the charge welds start points and their extensions along the profiles length, [37]

In all profiles the charge welds started 400-550 mm far from the stop mark; the material flowed faster in the thicker region (X) than in the other (Y), so the charge welds appeared first in the X zone. The extension of the charge welds depended of the velocity; if it is higher than the charge weld extension is shorter. The charge weld in the thinner region was visible first into the profile closer to the die center (B-C, Fig. 1.22), and also its extension was shorter. In the other two profiles (A-D, Fig. 1.22), the flow was unbalanced so the charge welds were not contemporary and the extension of the defected zone into the profile was longer. As consequence, there was the need to homogenize the material flow so that the charge welds can appear at the same time after the stop mark, reducing the waste. Moreover, the friction model that better approximated the experimental results was the sticking model because took into account the initial phase of billet upsetting inside the container; on the other hand, the viscoplastic model was also good to predict the faster flow into the thicker region of the profile. Moreover, it was demonstrated that the equation in Saha's work (2000) underrate the length of the profile to be wasted.

A numerical model was also set to analyze AA3003 hot extrusion with a simple die (Fig. 1.26) after the extrusion of a billet made up of AA6060 in order to make more visible the charge weld, in the study of Mahmoodkhani [38].
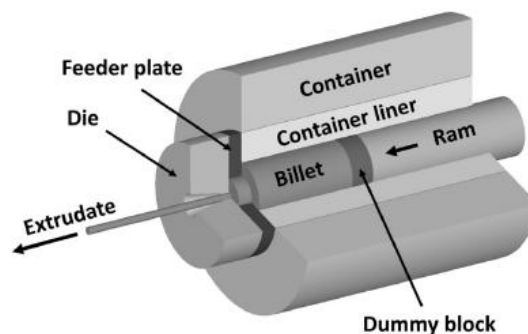
Figure 1.26. 3D view of the extrusion die model, [38]

The used software was Deform2D with the support of Matlab algorithms [39]. The Matlab algorithm was developed in order to change the numerical outputs about the flow velocity distribution in quantitative data regarding the charge weld shape and the coat layer thickness of the old billet material around the new one inside the profile (Fig. 1.27).
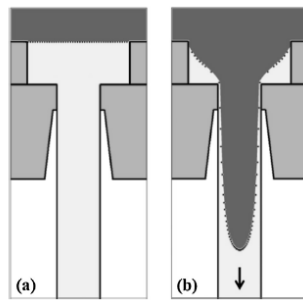
Figure 1.27. Grid of points in Matlab to analyze the evolution of the charge weld, [38]

The analyzed parameters were the extrusion ratio and the feeder geometry. The study confirmed that if the final part of the die is not flat than the charge weld is shorter because the dead metal zone is reduced and the metal flow is faster. Moreover, with a flat feeder, if the extrusion ratio increases than the charge weld extension is longer.

If the weld conditions are not so good then a gas pocket could be behind the bridge, as shown in [40]. With a seam weld into AA6060 profile the ductility was reduced and the minor critical case was with higher height of the chamber (Fig. 1.28d). The welding line was well visible by means of microstructural investigations (Fig. 1.28). Actually, thanks to Schwane's work [41] the gas pocket formation can be predict.
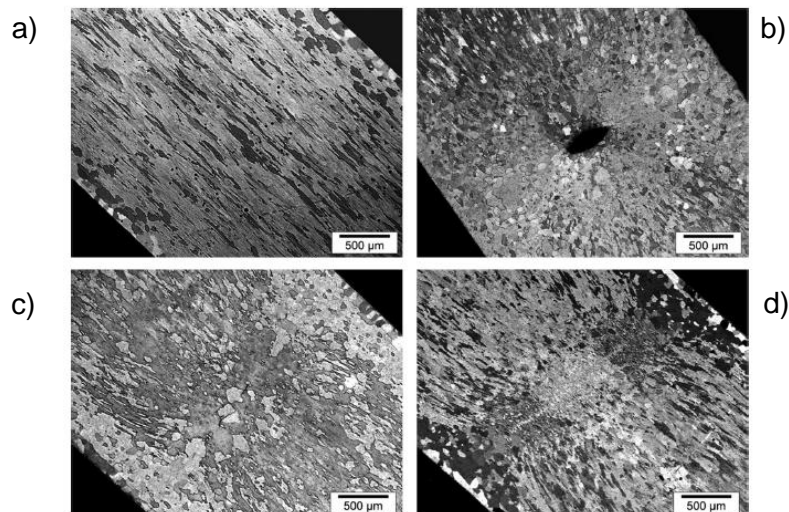
Figure 1.28. Cross sectional microstructures of AA6060 extrudates produced at 450 °C with die a) without an obstruction, b) with 2 mm welding chamber height, c) 10 mm welding chamber height, d) 15 mm welding chamber height, [40]

The research is constantly evolving and also in the last year some works were conducted in order to investigate the welding phenomena in porthole die extrusion. In

fact, the Ring Hoop Tension Test (RHTT) and Digital Image Correlation (DIC) were used to investigate the mechanical behavior (strength and ductility) of the seam welds [42] in AA6061-T4 profiles. Using Digital Image Correlation to probe the strain fields, was discovered that the cold-welded seam was stiffer than the remainder of the material. That region exhibited higher strength and was less ductile than the surrounding base region. Meanwhile, Pinter [43] analyzed the influence of a porthole die with an increasing number of bridges (Fig. 1.29) with different ports dimensions, on the die deflection and welds generation, during the extrusion of a tubular profile.

2-legs   3-legs   4-legs
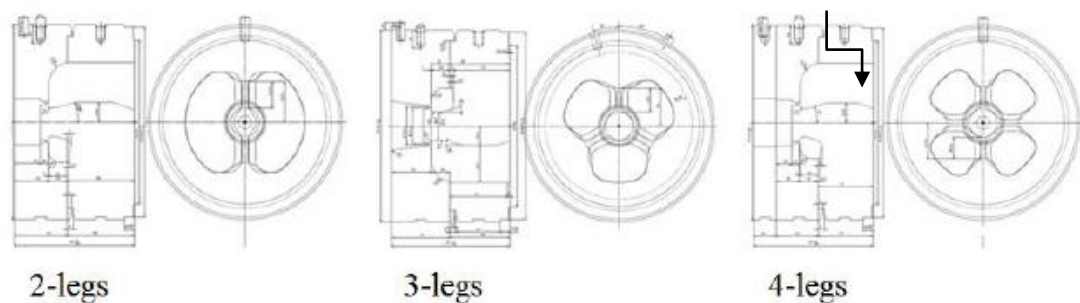
Figure 1.29. Porthole die with 2, 3 and 4 bridges, with different ports dimensions, [43]

The influence of the bridges number on the seam welds was analyzed by pressure, temperature and velocity field into the welding chamber; while the effect on the charge weld was analyzed considering the fraction of new billet material inside the extruded profile after the stop mark in order to estimate the waste material in transient steady condition. Mandrel deflection was related to the cycled load because billets were consequently inserted inside the container and the influence on die deformation was analyzed by the pressure and temperature values. Also the effects of ram speed, billet length and kind of alloys, were taken into account on die deformation after different extrusion cycles. Designing properly the die [43], it was observed that there was a slight load increase rising number of the bridges because the bigger friction opposition to the flow, which get unbalanced. Moreover, if the holes section was bigger then also the pressure inside the welding chamber was higher. On the other hand, if the holes were flat, the load peak was related to total bridges surface and friction. With a tapered die, the friction had a low influence and the load peak was inversely correlated to the ports area. The pressure increase was more sensible to the variation of the welding chamber height than the ports sizes. It was also observed that using 1 mm of fillet radius at the entrance of the bearing, the peak load was reduced because there was a strain distribution also near the die exit and

the pressure into the welding chamber was lower. Negligible was the difference in the temperature distribution. Regarding the charge weld, if a porthole with two legs was used, the weld starting and ending points were delayed. In this way bigger is the distance from the stop mark and consequently higher is the profile volume to be discarded. This is because with a porthole with two bridges configuration, the dead metal zone increases so the influence of the old billet material on the new one is more evident and the charge weld length increases. Currently, non-destructive methods such as ultrasonic or eddy current [44], are used to analyze the charge welds. The extruded material, instead, was the parameter that had more influence on die deflection. Extruding hard alloys, there were critical die deflection conditions in all the porthole configurations.

1.2.4 Seam weld quality criteria

There are different criteria to consider the quality of the welding line [26], as previous mentioned and following summarized.

Maximum pressure criterion: proposed by Akeret [45] and [12], considers as a discriminating parameter the only maximum pressure inside the welding chamber. Once the elements *i* of the welding chamber are known, than: $P_m = max(p_i)$; if this value exceeds a critical limit, which depends on the physical state of the material in that point, the welding could be assessed as sound: $P_m=max(p_i)>Cost$.

Pressure-time criterion: proposed by Plata and Piwnik [46], is based on the integral on time of contact pressure (P), normalized on the actual effective stress, along a generic path for a welding element; the value obtained must exceed a critical limit experimentally determined. In analytical terms: $w=\int \frac{P}{\sigma eff}>w_{lim}$, where σ is the actual effective stress and w_{lim} is determined by means of experimental tests; w depends of pressure and temperature, but it does not take into account the contact time and the extrusion velocity. If the height of the welding chamber is high, the time contact and the pressure increase, so there are better welding conditions. However, w cannot be too small otherwise the material flows are not joined together [27].

Pressure-time-flow criterion: it gives great emphasis to dead zones of the welding chamber. Consequently, the speed was introduced as a correction factor, meaning that the flow of material through a generic point must also be considered: $\int_t \frac{P}{\sigma} dt *$

$v = \int_L \frac{P}{\sigma} dl \geq Cost$; L is the path from the back side of the die leg up to the die exit, where pressures are zero.

Finally, Ceretti at al. [27] identified the material welding limit stating that the conditions at which solid bonding occurs depend not only on the interface pressure, but also on the temperature at which the contact takes place: $w_{lim} = 4.9063 e^{-0.0017T}$, for $T \geq 320$ °C.

1.3 PROFILE DISTORTION AND QUALITY

In order to get a good weld quality, a homogeneous material flow has to characterize the profile at the bearing die exit. Sometimes, related to the flow material, defects inside the profile and on its surface may occur. As already known, right die designs, particularly pocket and bearing configurations, are set to homogenize the material flow avoiding poor profile properties and defects, in case of porthole die extrusion. In addition to that, also high temperature can create cracks on profile surface. Careful studies were done to better understand the phenomena.

1.3.1 Geometric parameters influence during extrusion

The variation in metal flow speed is due to the variable thickness of the profile cross section and to the friction along the container walls. The material is faster in the areas corresponding to the thicker bearing sections and close to the die center. The lengths of the bearing are locally adjusted so that the frictional forces act to balance any symmetry of the velocity field. The disadvantage of this method is that the bearings generate heat due to friction, which limits the extrusion speeds attainable before poor surface quality or localized tearing of the extrudate [47], (Fig. 1.30). This is more evident when the bearing lengths are too long.
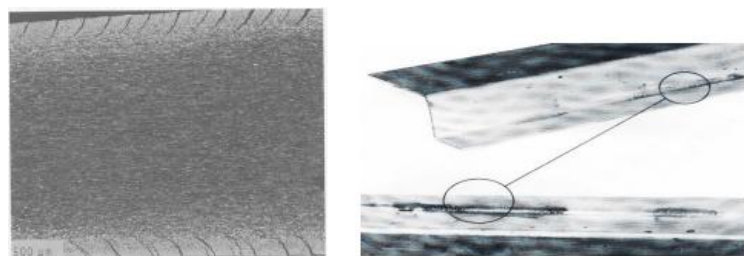
Figure 1.30. Hot shortness and surface tearing, [47]

For this reason, it is beneficial to use the shortest bearings possible. Bearings are also extremely sensitive to slight changes in angle due to their deflection or rounding during polishing. To enable the use of short bearings and to minimize impact of the bearing angle, material flow can also be controlled primarily using a shaped pocket (or welding chamber) in front of the die. Pockets have the additional advantage of defending bearings from damage and reducing deflection of critical areas by protecting the bearing land face from the full extrusion pressure [48]. For a constant depth pocket, if the pocket width approaches the size of the die orifice, the extrusion load can increase significantly [49]. The volume of the pocket has to be bigger corresponding to the regions in which the profile velocity has to be faster as well as the bearing length must be shorter. Speed decreasing from the center of towards the die walls (Fig. 1.31) has also to be taken into account choosing the set of geometric parameters [50].
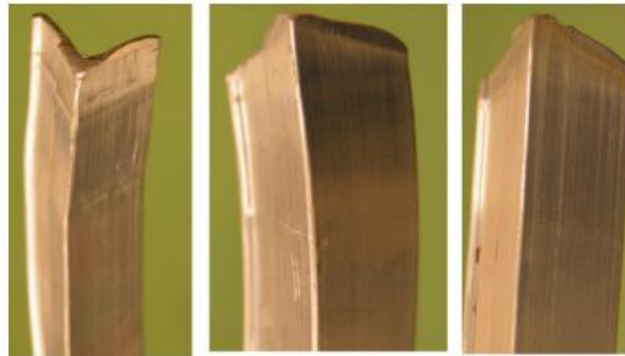
Figure 1.31. Distorted profile, faster material flow into the central zones, [50]

Addition to the pocket cross section, the pocket angle can be changed and also its height, building a multistep pocket (Fig. 1.32). The metal in the area where the pocket angle is larger flows faster and if the number of pocket steps increases the velocity becomes more homogeneous [50]. However, a conical pocket is more effective in increasing metal flow velocity compared with stepped pocket; in fact, the material flows easily and with less shear and internal friction occurring within it because the metal died zone is absent. Friction coefficient has an influence on the pocket qualitative role because the friction will slow down the edge part of the billet, whereas the central one will travel faster; if the friction coefficient is high, larger is the flow velocity discrepancy between center and edge [51].
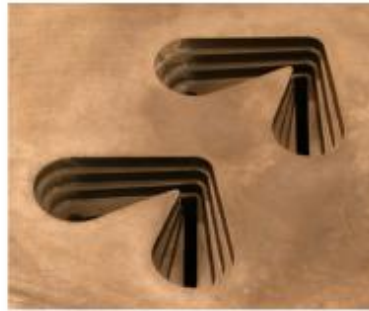
Figure 1.32. Multistep pocket, [50]

Of interest is the peak pressure required, which indicates if the extrusion process will be possible with the existing extrusion press [52]. This peak pressure decreases rising the number of pocket steps when the total pocket depth is unchanged [53]; although the contact area, and thus the friction, increases in the case of multi-step pocket die, the easier metal flow through the pocket leads to a lower pressure requirement as well as to a lower temperature.

1.3.2 Process parameters influence during extrusion

The major process parameters to consider during the extrusion process are the punch speed and the initial temperature of billet and die; these are influencing the profile velocity at the bearing exit and the thermal history during the extrusion. Temperature determinates the quality of the product and indicates the possibility of increasing extrusion speed and productivity. When it exceeds a critical value, surface defects appear in form of hot shortness or cracking (Fig. 1.30), as previously mentioned. Even below this critical value, high temperature may lead to local recrystallization and grain growth, harmful for the mechanical properties of the extruded product [54, 55]. Meanwhile the metal is filling the pocket, the temperature of the material is lower than the initial billet temperature [56]. This thermal phenomenon is because at the beginning of extrusion the hotter billet contacts the colder extrusion die and heat dissipation takes place. At the stage of filling the pocket, deformation is very small and, as consequence, the rise of local temperature due to plastic deformation, is marginal. The lowest extrudate temperature is in the multi-step pocket because the metal flows more easily and the contact area between the billet and the die pocket is larger, leading to more heat dissipation into the initially colder die. When the metal crosses the bearing, the workpiece temperature increases rapidly as result of large deformation. The rapid temperature raise and its

magnitude, as combined result of large deformation and friction, are in relation to die bearing length and ram speed. As mentioned, the maximum temperature occurs at the bearing die inlet, indicating that the converted heat from deformation is more pronounced that the heat generated from the friction at the die bearing, [57]. Severe deformation and friction at the die bearing would lead to a further temperature increment at the bearing outlet, but if the profile is exposed to room temperature is not the case. With a temperature that exceeds a critical value is possible to see some cracks on the profile surface, which are less visible with lower ram speed. Regarding the extrusion pressure, the effects of the die design and ram speed are marginal, [56].

1.3.3   State of the art about extrusion parameters effects on profile quality

In order to investigate the improvements on the material flow during an extrusion process, different studies were performed. Several parameters such as billet temperature, bearing length and product thickness, were firstly examined by Jo et al. [14], in 2003. In detail, the flow was monitored by 3D transient state simulations and then compared with experimental results, for AA7003 extruded profiles. Afterwards, the extrusion process of an aluminum AA1100 rectangular hollow pipe was simulated using finite volume method based software Msc/SuperForge by Wu et al. [58]. The simulation results indicated that the extruded workpiece had non-uniform deformation distribution and high load peak if using a die without pockets. Lesniak [48], in 2007, investigated pocket influence on the material flow considering two bearing sections, Profile 1 and Profile 2 (Fig. 1.33), having diversified wall thickness. The extruded material was AA6060 aluminum alloy.
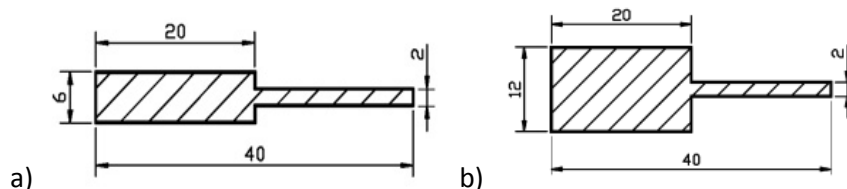
Figure 1.33. Shapes with different thickness corresponding to the thicker region of a) Profile 1, 6:2mm; b) Profile 2, 12:2 mm, [48]

Extruding profiles with varying thickness, a non-uniform metal flow and a high velocity gradient in the die opening occur. Three pockets were designed in order to investigate the influence of the two profiles shape and volume on the material flow. The pocket cross sections had particular dimensions in relation to the profile shape

and to the velocity of the material flow inside the pocket and at the bearing exit. The aim of Lesniak's work was to check the effects of pocket dies geometry on the formation of cracks and geometrical stability of extrudate. The pockets used for Profile 1 are shown in Figure 1.34, the others for Profile 2 are shown in Figure 1.35.

Figure 1.34. Three pocket designs for Profile 1, [48]

The cross section that significantly changed was the section corresponding to the thinner part of the profile.

Figure 1.35. Three pocket designs for Profile 2, [48]

By means of experimental tests and macrostructural observations, was clear that pockets affected the range of dead metal zones in the billet, and thereby, enabled to even the metal velocity distribution within the deformation zone, resulting in the improved geometrical stability of the extruded profile (Fig. 1.36).
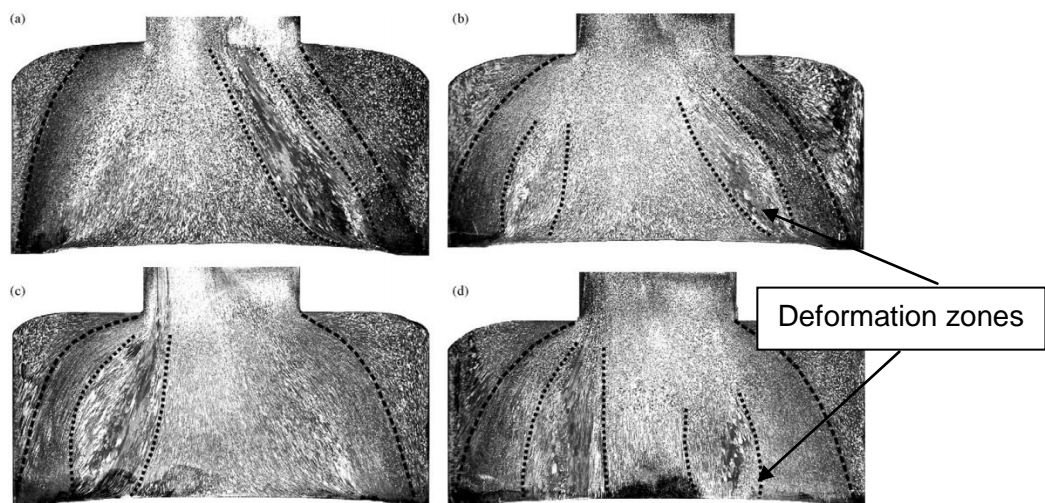
Figure 1.36. Macrostructures of material in the billet rest while extruding Profile 2 by using different die configurations: a) without pocket; b), c) and d) with increased pocket sizes, [48]

There was a narrow range of pocket widths, which caused considerable changes on metal flow (Fig. 1.37) and extrusion loads. Increasing the pocket width just over the mentioned range slightly influences the metal flow, which was confirmed by the measurements of extrudates bending.

Figure 1.37. Comparison of the Profile 2 curvature, when applying a flat die (on the left), an intermediate pocket (in the middle) and a bigger pocket (on the right), [48]

There was also a small increase in the extrusion force, using die with pockets compared to flat dies without pocket, due to additional friction and changes in dead zone geometry. The maximum extrusion load was extruding Profile 1 because the higher extrusion ratio and corresponding to the pocket whose cross shape was close to the bearing shape, as expected. In both profiles there was a minimum load corresponding to the intermediate pocket sizes (Fig. 1.38). Furtherly increasing the dimension of the pocket, its influence tended to decrease because it approaches the flat die conditions.
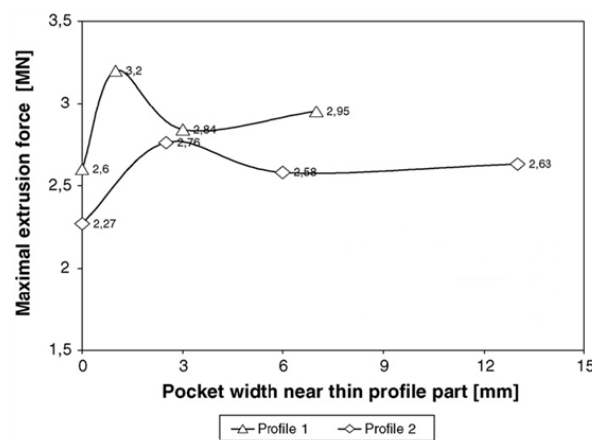
Figure 1.38. Extrusion load versus pocket width, [48]

The use of pocket dies is also associated with the beneficial state of stresses in the die orifice, leading to higher material deformability and better surface quality of

extrudates. An optimal pocket die geometry can be found from the criterion of the volume rate control. In addition, applying either too narrow or too wide pockets can worsen the extrudates surface quality (Fig. 1.39).

a)   b)
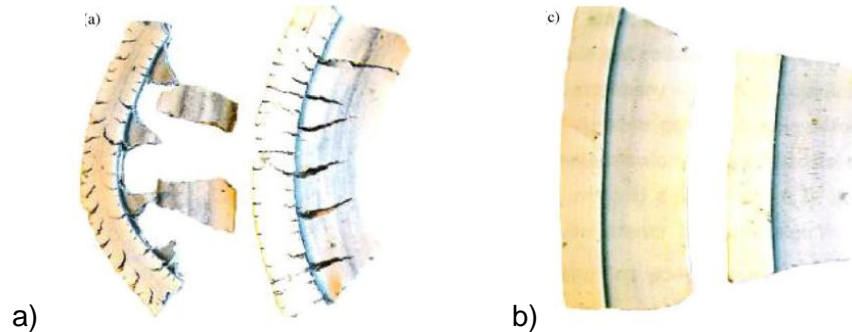
Figure 1.39. Material cracking on extrudates surface when applying dies a) flat and b) with an intermediate and optimized pocket, [48]

Finally, higher values of micro-hardness were obtained while using the pocket dies with the medium and large widths.

In order to investigate the pockets effects on the metal flow, also two different multi-hole porthole dies, with and without pockets, for H-type solid extrusion of AA6061 were designed by He et al. [59]. The simulation results shown that the pockets could be used to effectively adjust the metal flow especially under the bridges. In fact, multi-hole pocket dies are a type of extrusion tooling used in aluminum extrusion industry for efficient production of solid aluminum profiles. Subsequently, Fang et al. [60], in 2009, did multi-holes pocket dies FEM simulations and extrusion experiments for AA6063 billet material, and found that multi-steps in die pocket could be effectively used to regulate the metal flow through multi-holes dies. In 2012, Aue-u-lan and Khansai [61] focused their attention on the effect of the factors that could shortening die life, such as flow behavior, extrusion load, velocity field and temperature distribution. FEM was employed to simulate and investigate the effect of those factors on die stress for AISI H-13 die material. DEFORM3D^{TM} was used to simulate the hot extrusion process of AA6063 with square hollow profile. The numerical outcomes concerning the die stress were predictable and coherent with failure in real die used to produce aluminum profile. Fang, [62], investigated die design and process optimization to manufacture a complex AA7075 solid profile with large differences in wall thickness, by means of 3D FEM simulation and experimentation instead of the traditional trial and error approach. The effects of die

bearing length and extrusion speed on temperature and extrusion pressure were predicted. Hsu et al. [63, 64, 65], in 2011 and 2012, studied solid welding conditions, square tube and hollow complex profile extrusion process of AA7075.

Extrusion ram speed is an important parameter that directly influences the profile quality and the extrusion equipment choice because increasing ram speed, the temperature of the extrudate and required extrusion load increase. The welding quality of extrudate could be improved just as shown by Zhang et al. [66]; they analyzed analytically the extrusion of a hollow profile with constant wall thickness and varying ram speed, using a porthole die with five portholes (Fig. 1.40) adopted to balance the metal flow, using also a bearing with different local lengths.

a)   (a) Porthole layout   b)   (a) Upper die   (b) Lower die
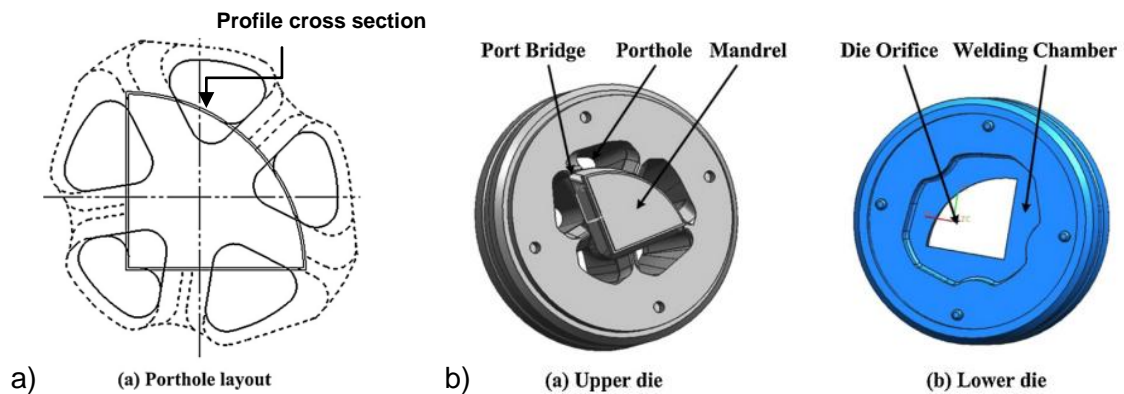
Figure 1.40. a) Bottom view of porthole die and profile cross section; b) extrusion die design, [66]

Six different ram speeds were considered in the range 0.1÷1.5 mm/s, and the velocity discrepancy on the profile cross section at the die exit was taken into account to represent the metal flow uniformity. Smaller is this value and better is the extruded quality. It was possible to see that the velocity discrepancy was minimum corresponding to an intermediate, but low, ram speed value, as shown in Figure 1.41.
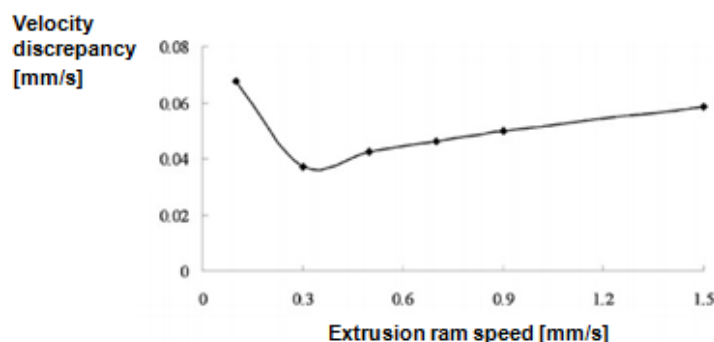
Figure 1.41. Velocity discrepancy on profile cross section increasing the ram speed, [66]

As known, in the extrusion process, the temperature evolution of the extrudate is mainly influenced by heat transfer, frictional heat and plastic deformation heat. Increasing the ram speed, the extrudate temperature gradually raises, as shown in Figure 1.42. It needs to consider that the maximum temperature of extrudate should not exceed the critical temperature, otherwise surface defects such as over burning and heat cracking will appear in the extrudate; thus, the extrusion ram speed should be less than a special value.
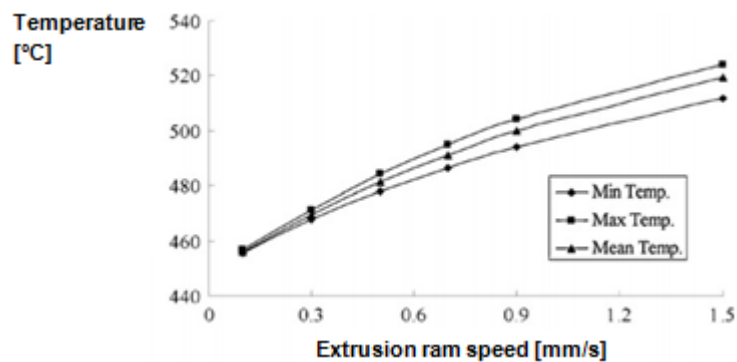
Figure 1.42. Billet temperature increasing the ram speed, [66]

Regarding the extrusion load, it was observed that at low punch speed, the required extrusion force increased (Fig. 1.43). Moreover, with a lower ram speed, the heat generated by plastic deformation and friction work is less, the strain rate played a more effect on flow stress than forming temperature rise and a higher flow stress or extrusion force is required for a certain deformation. At larger punch speed, the temperature rise and the flow softening of aluminum alloys is intensified, leading to drops of flow stress. The effects of strain rate and temperature on flow stress tend to a balance, and the required extrusion force is typically characterized by a rise to a plateau followed by a relatively steady state [67].
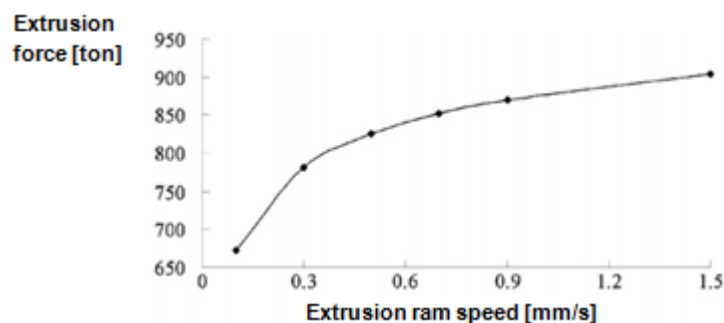
Figure 1.43. Extrusion load increasing the ram speed, [66]

Due to the five portholes in the extrusion die, five seam welds appeared in the profile and the pressure in the welding zones is relatively lower than in other zones. The average pressure in the welding chamber, therefore the welding quality of profile, increased with increasing ram speed, as shown in the next Figure 1.44.
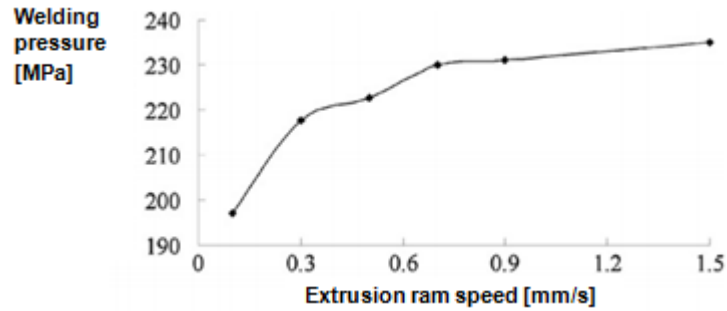
Figure 1.44. Welding pressure increasing the ram speed, [66]

Finally [68], a hollow extruded AA7075 product with complex and non-symmetric cross section was considered (Fig. 1.45).
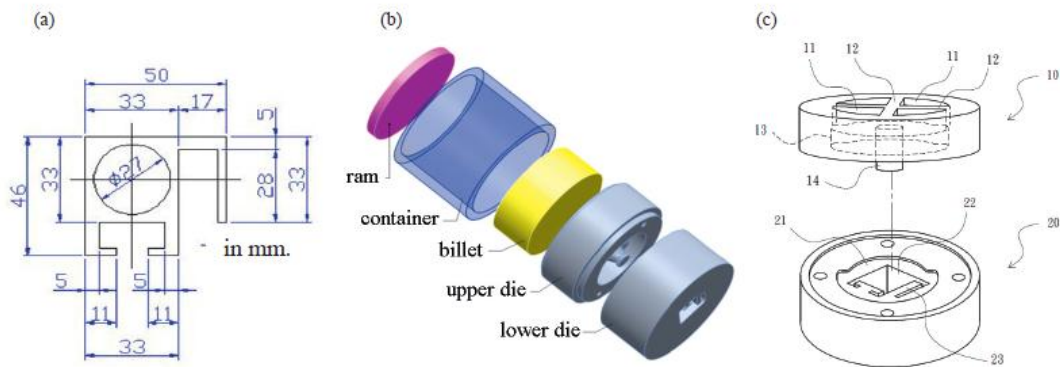
Figure 1.45. a) Hollow extruded product with complex profile; b) die configuration for porthole extrusion; c) upper die and lower die detail, [68]

Three different pockets were designed as shown in Figure 1.46.
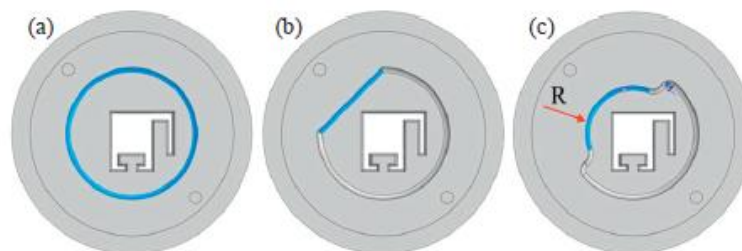
Figure 1.46. Three different types of welding chamber pocket: a) original type, b) cut edge type and c) double arc type, [68]

Moreover, two types of die bearing with different local lengths were considered for welding chamber with double arc type pocket that had another small arc (labelled as R in Fig. 1.46c) besides the original diameter, because the outlet profile geometry was more uniform. A smaller radius R of pocket geometry was preferred because the lower extrusion load. Analyzing the velocity distribution of material flow along the ram direction, four marked regions, showing four welding planes, were highlighted (Fig. 1.47).
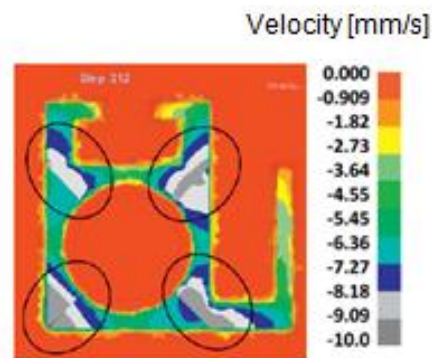
Figure 1.47. Profile cross section and velocity distribution inside the profile: the circled parts represent four welding planes; the remainder parts represent four divided flows of billet, [68]

The material flow was investigated, changing three parameters: bridge shape in upper die, pocket corner radius and chamfer angel in lower die, as shown in Figure 1.48.
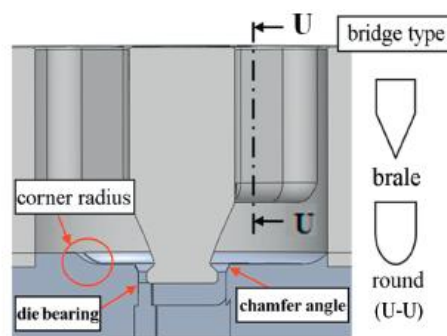
Figure 1.48. Control factors for die design used Taguchi method, [68]

An experimental plan was performed, following Taguchi approach, where the output parameters were maximum ram load, maximum die stress in upper die and lower die and the objective was to seek their minimum values. The most influential parameter for ram load and upper die stress was the bridge type, and for lower die stress was the chamfer angel. Moreover, unequal bearing lengths made better billet fluidity.

1.4 COMPOSITE EXTRUSION PROCESS

Another way to improve the extruded properties, maintaining reduced sections and lightweight, is feeding reinforcing elements inside the material flow during the process. In fact, using the reinforcing elements is possible to combine the good mechanical properties of composite and lightweight materials. In some cases, the specific tensile strength of the profile can be increased by nearly 50%, as well as the bending stiffness in comparison to profiles without reinforcing elements. However, the issue to consider is the influence of the reinforcing elements on the material flow distortion. Three kinds of composite extrusion process can be distinguished resulting in profiles with varying metallurgical and mechanical properties, as below summarized.

1) Extrusion of short fibers composite billet

In a powder metallurgical process, short fibers or whiskers are embedded and compacted into billets. Extruding these billets leads to short fiber reinforced profiles with undirected reinforcements [69]. If short fibers or whiskers are inside the profile there is an increase of extrusion load and die wear, consequently the extrusion will be expensive. In the following picture is possible to see the fibers orientation in an extruded profile [70].
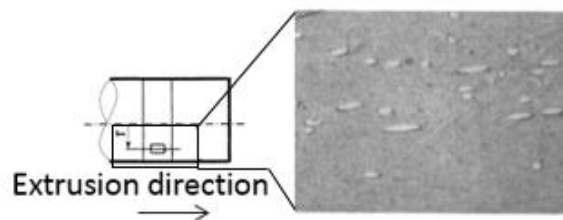
Figure 1.49. Fibers orientation in an extruded profile, [70]

2) Coextrusion of bi-material billets

A solid inner billet is joined to a hollow outer billet of a different material [71], (Fig. 1.50); during the process, profiles consisting of a core material and a different skin material are extruded.
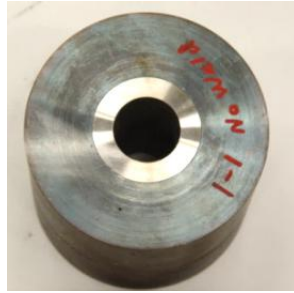
Figure 1.50. Front view of bimetallic billet with stainless steel core and plain carbon steel sleeve, [71]

The bimetallic extrusion guarantees high compressive deformation, shape changing in one step and the possibility to vary the deformation zone varying tool design. During the extrusion of a billet characterized by a core and a coating made up of different materials, the two regions can undergo no homogeneous strain due to the materials characteristics. The difference between the velocities of the internal and external materials along the extrusion direction and a low pressure at the interface core/coating, can lead to the profile decohesion and fracture. The coating generates loads on the material core that increase with the friction at the interface core/coating ensuring a necessary pressure for the joining and consequently for getting a homogeneous material flow [72]. Working in cold conditions there are some advantages: energy conservation, small dimensional tolerances and good quality surface. Metallic massive glass with Zr, as coating, and aluminum 7075, as core, can be coextruded to get profiles with high yield strength and corrosion resistance [73], with low temperature and strain rate, because intermetallic compounds and defects did not appear, but aluminum and magnesium are the more appropriate materials to satisfy the current lightweight request of the industrial products. An aluminum core and discontinuous reinforcements can increase stiffness and ductility of a magnesium coating. The interface Mg-Al has a strength higher than the materials considered individually. The Mg coating is brittle, the interface is ductile, and finally, the Al core has a mixed behavior. The join integrity is due to the good wettability, workability in hot conditions and to the creation of solid solutions at the interface [74]. Another combination for bi-materials extruded is zirconia (ceramic resistant to heat and corrosion), and ductile stainless steel, respectively in the inner and outer layer [75]. Residual stress as well as fractures across the interface between the materials are due to different thermal expansion and conductivity of both. During the extrusion of bi-material profiles particular attention has to be focused on the velocity distribution

of both material flows to avoid that one entering inside another [76]. Analyzing the behavior and failure types of different kinds of wires and wire ropes (Fig. 1.51) of high strength steel was stated that solid wires showed the highest process stability [77]. In the case of wire ropes, the elongation depends on the angle of braiding, which has to be not so high otherwise the stiffness in longitudinal direction decreases. Increasing the number of wires into the rope, the cross section becomes smaller, while the lateral surface becomes bigger, therefore the last one undergoes a lower load.
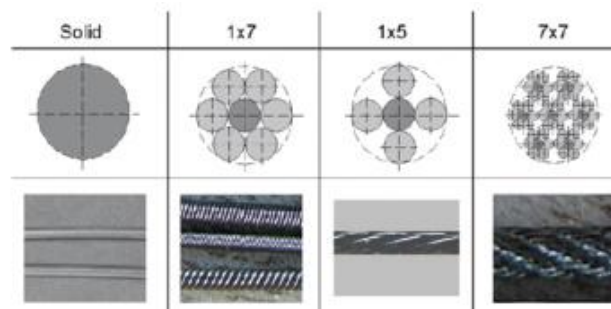
Figure 1.51. Examples of wire ropes, [77]

Nowadays, a challenge is extruding rope conductors made up of aluminum wires in order to increase the electrical conductivity of the same conductors, and consequently replace the existing cables made up of copper, that is a more expensive material.

3) Extrusion with continuous wires as reinforcement embedding

By using special die geometries endless reinforcing elements, such as wires or wire ropes [78], are introduced into the material flow (Fig. 1.52) and embedded thanks to special extrusion pressure and temperature reached during the process.
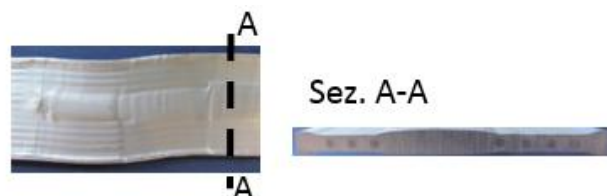
Figure 1.52. IUL work: a) extruded profile reinforced with 7 reinforcing elements; b) cross section corresponding to the cut section AA, [78]

An increase in resistance, using high strength material as reinforcement, and stiffness, using materials with high Young's modulus, can be achieved, as well as an increase in functionality [79]. Special extrusion porthole dies (Fig. 1.53) are used to

feed reinforcing elements in form of high strength steel wires separate from the material flow [80], directly into the welding chamber of the die. Here, both materials bond together to a composite profile.
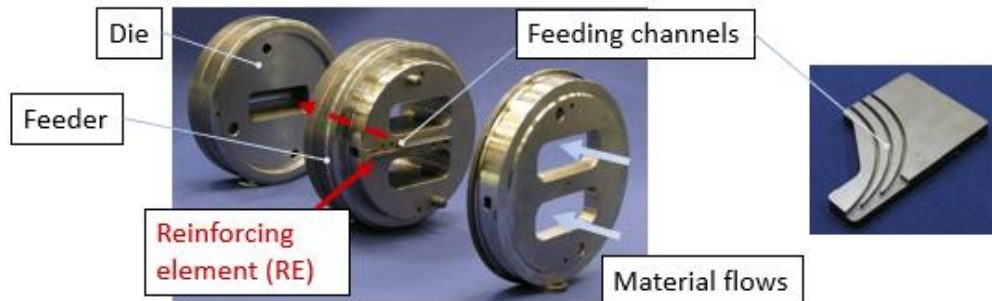
Figure 1.53. Porthole die used in composite extrusion with continuous reinforcing elements, IUL Laboratory, [77]

More in detail, cartridges are built in the bridges (Fig. 1.53), which divide the material flow and carry the mandrel in hollow profile extrusion, for supplying the steel wires. To prevent the reinforcement from cracking, adapted regions inside the welding chamber are also utilized. The reinforcing element has a proper diameter and has to be flexible enough to flow through small and bended feeding holes into the tool; moreover, it has to support the extruded profiles in loaded condition. The reinforcing elements are located not so close to each other to save the die, that could be not rigid enough, and to permit the material to surround them transfering the load. The technology of composite extrusion by continuous feeding of a second material in the extruded base material by means of modified tools is the most used extrusion process variant and offers advantages like reduced wear during extrusion, reduced punch forces, and high flexibility in cross-section design. In this case, in contrast to coextrusion only one material is deformed within the process and the second one is fed in the material flow.

1.4.1 Influence of reinforcing elements on profile distortion

The main advantages of using wires reinforcing elements (REs) are different. In fact, complex and thin sections can be manufactured and the profile has high strength maintaining a reduced shape. If high strength spring steel wires are considered inside an aluminum matrix, there is also an increase of stiffness and impact resistance of the profile. Moreover, the extrusion load reached during the process is

not so high because the REs are fed directly into the welding chamber and not at the beginning of the process (as in the case of short fibers), consequently die wear and fracture generation are limited. Also the decohesion does not represent a real problem.

On the other hand, there are also some bottlenecks, as below described.

- Inclusion of air and not complete covering of the wire due to die geometry (Fig. 1.54); in particular way, due to small welding chamber height in which the material streams and the REs have no time and no space to better weld together [77].
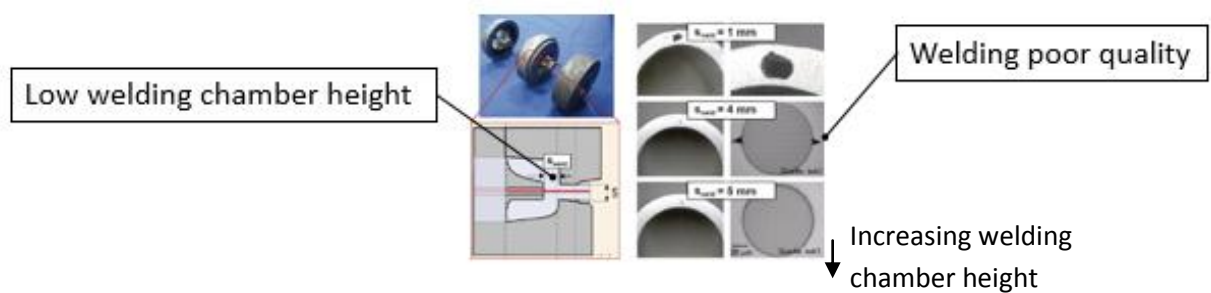
Figure 1.54. Reinforcement enclosure defects, [77]

However, when the welding chamber height is too high, there is the risk of high thermo-mechanical shear loading and cracking of the reinforcement. Moreover, wire deviations and cracking occurs when feeding the reinforcement too early.

- REs cracking due to equivalent stress inside the reinforcement (Fig. 1.55). In fact, the wire is subjected to a compressive orthogonal stress due to hydrostatic pressure applied through the material that is compressing inside the small die opening clamping the element, and also to tensile stress in longitudinal direction due to inhomogeneous velocity distribution in the composite development area. These stresses are higher when the welding chamber height is higher.
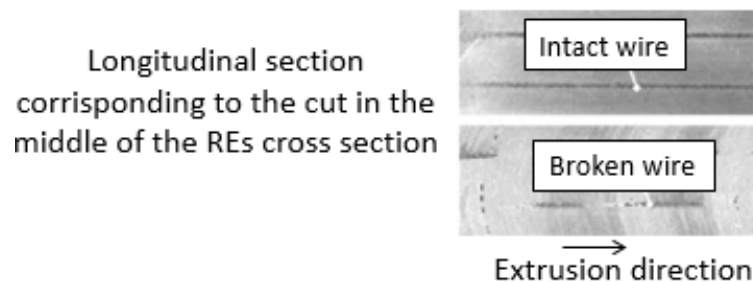
Figure 1.55. Broken wires inside an extruded profile due to high stress, [77]

Two dead zones exist due to the die geometry and the mandrel. While the zone near the die exit does not influence the composite development area, the dead zone at the mandrel lies at the position of the reinforcement introduction. Following the aluminum flow from the mandrel tip, the billet material velocity increases until it reaches exiting velocity. While, after the welding chamber filling, the values of the velocity and stress remain constant. Introducing the reinforcement leads to a change in the velocity distribution because the reinforcement pulls with sticking conditions the aluminum through the welding chamber till the die opening. The base material's speed is about zero when a first contact with steel reinforcement happens; in this area, the reinforcement gets clamped and the difference between clamping and pulling leads to high tensile stresses in longitudinal reinforcement direction. In addition to the high compressive stresses, acting orthogonally on the reinforcement due to the hydrostatic pressure in the welding chamber, high equivalent stresses occur, which can lead to experimentally determined reinforcement cracking [81]. The maximum equivalent stress concentration occurs in the reinforcement element right in the composite development area before leaving the die that can result in reinforcement cracking [82]. The friction and the relative movement of the functional elements in the developing dead metal zone behind the mandrel also lead to additional shear stresses [83].

- Moreover, temperature and die geometry can deflect the REs position (Fig. 1.56) because their influence on the material flow. Sometimes the reinforcements are pushed towards the die walls wearing the die and themselves manufacturing a profile with bad quality.
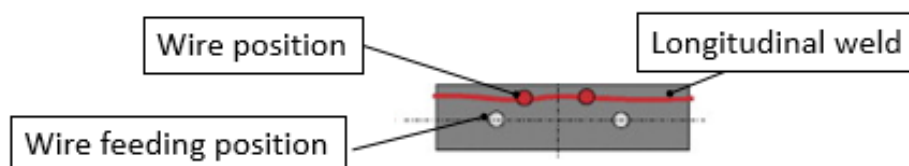
Figure 1.56. Horizontal and vertical deflection of the wires, [77]

To reduce possible deviations, an accurate control of the material flow and process influencing parameters, such as temperature field or die geometry, is necessary. In the case of vertical deflection, parameters influencing the flow are mainly the geometry of the tool and the temperature distribution inside the die. In detail, if the mandrel has feeders with different volume, the material of the smaller feeder flows

slower and the seam weld is pushed out of the symmetry plane, due to the constancy of inflow and outflow. The horizontal deflection, instead, is due to the position of the wire feeding holes inside the die in relation to the material flow lines. Due to the narrowing inside the welding chamber of extrusion tools towards the profile's exit, the material flows along stream lines deflecting the wires stronger corresponding to a big distance to the vertical symmetry plane (Fig. 1.57).
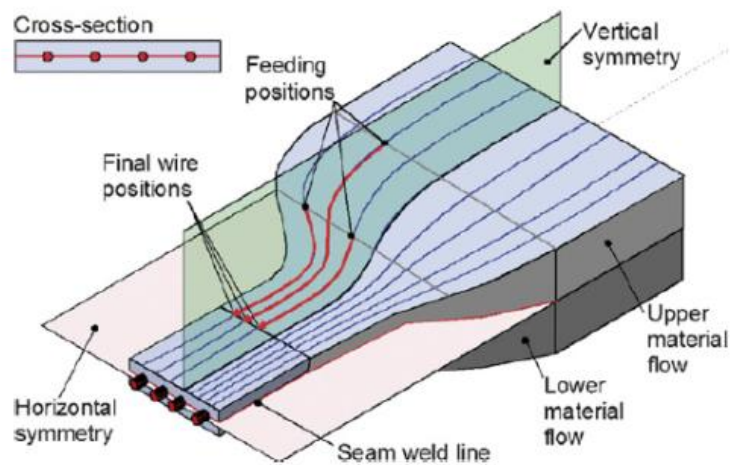
Figure 1.57. Principal of horizontal wire deflection based on the feeding position, [77]

- Finally, introducing the reinforcements, the material flow can be influenced by their position and their amount, [78], (Fig. 1.58).
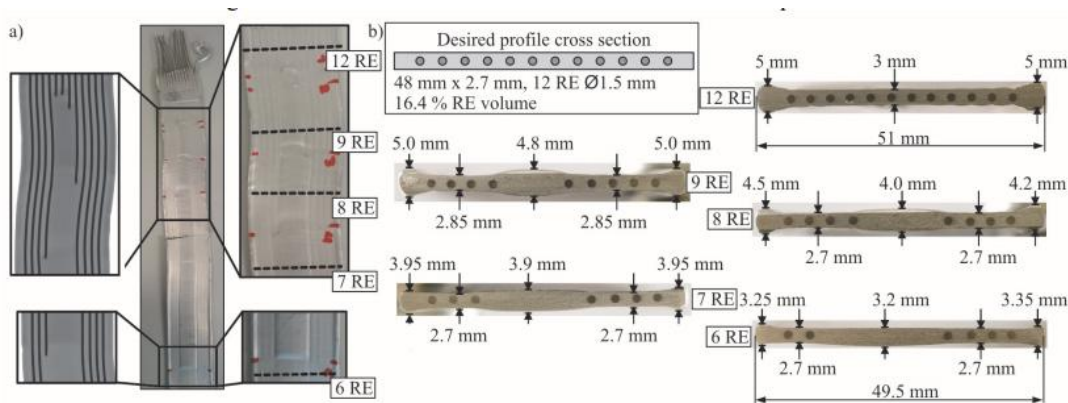
Figure 1.58. IUL work: a) extruded profile with 12 REs; b) cross section view and thickness increase because speed rising due to reduction of REs into the same profile, [78]

1.4.2 State of the art about composite extrusion process

To facilitate the understanding of the mechanical and thermal conditions during the process with reinforced profiles, finite element methods have been utilized to support

the investigations and a brief state of the art about that is reported in the work of Schwane et al. [78]: in 2006, Schikkora and Kleiner [84] used a simple axisymmetric FEM model to investigate the influence of the die geometry on the material flow and on stresses acting in the reinforcing element (RE) during the extrusion of a round bar with a single RE in the center. Furthermore, Pietzka et al. [85] considered a simplified approach in order to determine the deflection of the RE in a rectangular, flat profile. A slender strip with two wires was modeled to mimic the material flow near the symmetry plane of the profile. Due to the numerical effort and high computational time, only the very initial stage of the process with little punch movement was simulated. In both of the previous research works, Lagrangian FEM codes were used. In order to overcome the limitations of Lagrangian codes, in particular with regard to model complexity and necessary computation time, FEM based on the Eulerian formulation was applied. Schikkora and Kleiner used Altair HyperXtrude for the steady-state simulation of an I-beam profile [86]. The position of the longitudinal seam weld was determined by optical inspection of flow lines and by the distribution of the equivalent stresses. As the REs are embedded, the seam weld location gives an indication of the REs position in the profile cross section. The analysis of the composite extrusion process by Eulerian formulation was further improved by Kloppenborg et al. [87], in 2010, who introduced the particle tracing method. By means of this method, the wires position in the profile cross section could be exactly determined [88]. In detail, the reinforcing elements are not considered physically in the Eulerian models, but only by virtual particles traced through the computed velocity field. However, the method provided reliable results for profiles with a low reinforcements volume and a high wire diameter to profile thickness ratio [78]. Some experimental investigations [77] shown that welding chamber height is the main parameter to guarantee a perfect embedding and that wires made of high strength spring steel AISI 301 [89] are the best choice in case of an aluminum matrix, in terms of strength to high temperatures and to thermal impact.

1.5 RECENT EXTRUSION PROCESS ENHANCEMENTS

Subsequently are summarizing some improvements and innovations in the extrusion field.

1.5.1 ECA extrusion

Equal Channel Angular Extrusion (ECAE) is a variant of the extrusion process [90] that joins metals and alloys with low plasticity because the higher compressive stress in the die characterized by channels inclined between each other (Fig. 1.59).
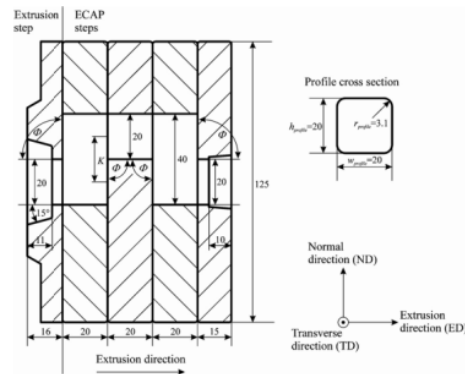
Figure 1.59. ECAP die with four turning, and profile cross section, [90]

This process guarantees good dimensional accuracy [91] and high profile strength because fine microstructure and ductility due to the high compressive load reached during extrusion. The material passes through the die exit and then it flows into the ECA die where undergoes shear stress without changing its cross section shape. The strength increases of 45% in the case of ECAE, while 31% in the conventional extrusion process. With ECAE also chip extrusion and composite extrusion are processed; in the last case, the bonding between the core and the skin is more resistant than in the common extrusion.
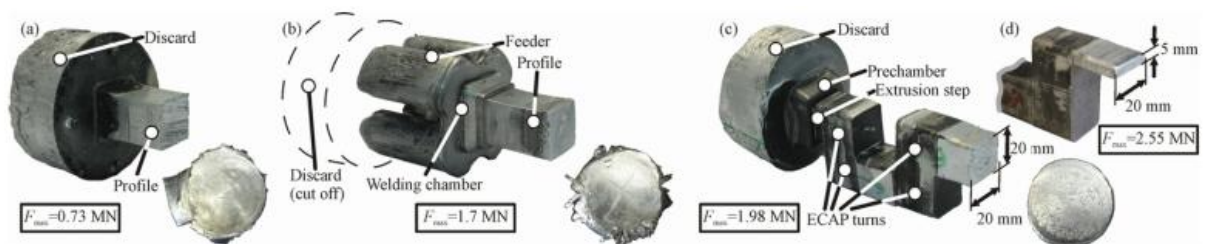
Figure 1.60. Process load during extrusion with a) flat die, extrusion ratio of 8.6; b) porthole die, extrusion ratio of 8.6; c) ECAP die with an extrusion ratio of 8.6; d) ECAP die with an extrusion ratio of 34, [90]

An increase of the extrusion ratio or punch speed brings to strength and ductility decrease into the profile, which becomes soft because the temperature rise. On the other hand, if the compression load and the application time increase, also the chips

consolidation is better. Afterwards, the profiles can be processed by means of plastic manufacturing processes as forging and rolling [90].

1.5.2 Extrusion of profiles with variable cross section

The variable section extrusion process is a new process that changes the section of the extruded material by using molds moving in the direction perpendicular to the direction of extrusion (Fig. 1.61), during the general extrusion process of rods or tubes. Since the section changes during the extrusion process, the successive processes, such as hydroforming and bending, can be eliminated as well as aluminum parts can be manufactured with low production cost and high reliability [92].
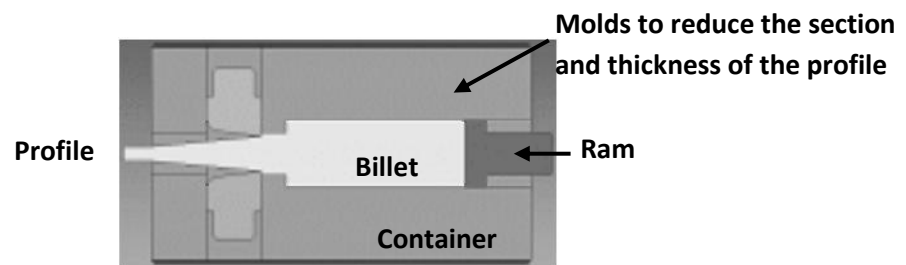
Figure 1.61. Profile with variable section and thickness, [92]

A combination of curved profiles extrusion and extrusion of profiles with variable cross section is also developed, Figure 1.62 [93].
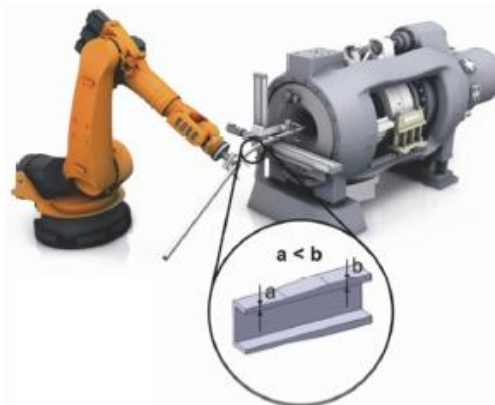
Figure 1.62. Curved extruded profile with variable cross section, [93]

In this case, the variation of the wall thickness is achieved by means of a wedge that is driven by a massive screw from the front of the press, which is used to change the position of the bearings. An advantage of this process is manufacturing profiles with a customized shape without extrusion press modification and with reduced weight.

1.5.3 Recycling in the extrusion process

Another current challenge is manufacture extruded profiles starting from billet made up of chips in order to avoid waste, and consequently costs, energy consumption and working time, safeguarding the environment. More attention is focused on aluminum chips because the difficult to recycle them; this is due to the elongated spiral shape, small dimensions, oxides and oils surface contamination. Usually, chips are cutting in granulated material, pressed in hot condition (Fig. 1.63a) and extruded (Fig. 1.63b), avoiding the melting phase [94]. The profiles manufactured from chips billet do not have similar yield strength [90]. If chips of different materials are considered, the mixture has a value of strength that is the intermediate of the virgin material values.
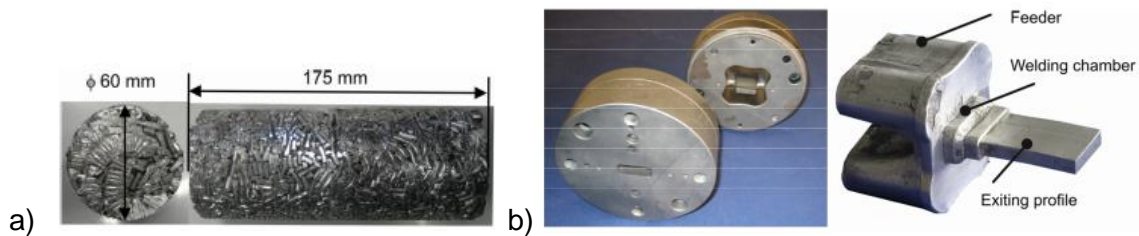
Figure 1.63. a) Aluminum billet of pins and chips; b) extrusion die with two bridges used in chips extrusion and material flow inside the die, [94]

The critical aspects of the process are the quality of solid bonding and the absence of pores that influence the profile mechanical properties. In order to have a good welding, the oxide layers on the chips surface have to be destroyed. With low extrusion ratio is useful working in hot conditions, while the cold compacting before hot extrusion is enough to guarantee a good welding with high extrusion ratio. Other parameters that influence microstructural properties and porosity are high extrusion temperature, which makes easy the material flow into the pores and voids, low ram speed, in order to increase the pores filling time, and the particles orientation inside the press [95]. During chips extrusion, the top part of the exit profile is characterized by non-welded chips because the low deformation in this region (Fig. 1.64). Moreover, some defects are in the central region of the profile when the aspect ratio (ratio between the bigger and smaller profile size) is high, Figure 1.64, [96].
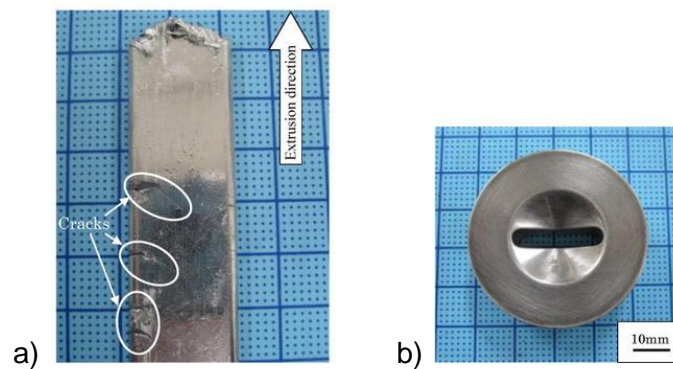
Figure 1.64. a) Extruded specimen with defects; b) die geometry for aspect ratio of 1:3.8, [96]

1.6 KEY POINTS INVESTIGATED IN THIS THESIS

In order to investigate the quality of the seam welds, the pressure and temperature conditions as well as the time contact between the material streams inside the welding chamber, have to be considered. These conditions are mainly influenced by the process and geometric parameters. Several studies, previously mentioned, are the base of the analysis performed in this thesis. in fact, different shapes of the top and bottom surface of the bridges will be considered in order to find the configuration that give the best welding conditions as Kim's work [13], in which welding pressure with respect to the changes of welding chamber length and bridge shape was investigated. In order to analyze the influence of different pre heating temperatures of billet, production rates, welding chamber heights and feeders surface, on the weld quality, a "I" shaped profile of AA6082 was extruded by means of a porthole die extrusion in the work of Pinter [32]. AA6060 profile with the same shape was subsequently analyzed in this thesis considering the influence of geometric and process parameters on welding pressure and time contact, respectively. Designing properly the die [43, 48, 66, 67, 68], a homogeneous flow at the bearing exit and a low process load can be get. Also in this thesis the sensitivity of the flow and maximum extrusion load to the variation of some geometric parameters is investigated. The material flow can be influenced also by the position and amount of reinforcing elements, where introduced, [78], as explained in this thesis.

2. INVESTIGATED MATERIAL, NUMERICAL APPROACHES AND EXPERIMENTAL EQUIPMENT

In this chapter, aluminum characteristics are shown and aluminum application camps are highlighted, especially regarding extrusion field. An overview of the numerical models and the equipment used in this research activity is reported. Numerical investigations are performed by means of Altair HyperXtrude® software that easily and quickly can simulate the extrusion process permitting to validate the experimental results or to highlight the critical issues. The experimental campaigns are carried out with the equipment available in the Laboratory of the Department of Mechanical, Energy and Management Engineering at University of Calabria and at the Institute of forming Technology and Lightweight Construction, in Dortmund. Microstructural observation are performed also at the Lehigh University in Bethlehem, Pennsylvania.

2.1 ALUMINUM AND EXTRUSION PROCESS

As previous mentioned, the material whose behavior is investigated in this thesis is aluminum and its alloys. The ductility and malleability characteristics allow the manufacture of extruded profiles that can be used in various fields. The aluminum extrusions permit in fact the maximum degree of modular assembly, in addition to great flexibility and robustness ensuring great design possibilities and a considerable rapidity and economy of production. In the extrusion field is possible to manufacture profiles with particular sections in order to have more metal in the greatest stress areas, and with shapes that facilitate subsequent processing and applications. For this reason extruded profiles are used also in the modern architecture and in different buildings. Moreover, the aluminum and its alloys can be bonded in solid state. In this study, the considered aluminum alloys belong to the series 6000 (Mg+Si), in detail AA-6060 or UNI 3569, because the request in several industrial applications. Its chemical composition is reported in Table 2.1; it is a low chrome (Cr) alloy and this is important because Cr is a recrystallization inhibitor.

Cu max	Fe max	Si	Mg	Mn max	Zn max	Ti max	Cr max	Global impurities	Al
0.1	0.35	0.2-0.6	0.45-0.85	0.1	0.1	0.1	0.1	0.3 max	Rest

Table 2.1. Chemical composition of the analyzed AA-6060

2.1.1 Aluminum properties and application fields

Aluminum is the most abundant metallic element in the earth; however, it is not chemically inert and it can be found in nature only combined with oxygen and various minerals, in the form of silicates and aluminum oxide (Al_2O_3). Aluminum use in industrial production started in 1886, when the American Charles Martin Hall and the French Heroult discovered the first practical electrolytic method to produce aluminum in large quantities. Aluminum is now of industrial importance secondarily only to steel, [97]; Italy is the second country in Europe for production and for consumption (the first is Germany), with a growth rate of 7.5% in ten years (compared to + 4.5% of Germany).

As previous said, aluminum is becoming the most important material because its lightweight characteristics that permit to reduce products weight and to save energy and fuel consumption. It has also other properties, such as:

- mechanical strength, in a range of 60-530 N/mm^2 (from the lead strength to the steel one). An aluminum element can replace a steel element reducing weight of almost 50-60% ensuring the same mechanical properties;

- corrosion-resistant, it has a high corrosion strength to the chemical reagents and it is the cheapest metal with this property. Aluminum alloys typically should have this characteristic in industrial and rural field, but only high-purity alloys, or the magnesium or magnesium-silicon, show a high resistance to marine and salt water. As consequence, alloys with high copper content are not recommended for naval uses or applications near the sea;

- reflexivity, the high reflexivity makes favorable the aluminum application in the lighting sector, for the reflector bodies. Because the high ability to reflect heat and infrared rays it is used in the civil and industrial constructions;

- thermal conductivity, is higher if other materials (magnesium, copper, steel, titanium) are considered. For this property, the aluminum is used to manufacture thermal radiators;

- non-magnetic properties, that permit to use aluminum in the control rooms of ships, because it does not lead to any change in the compass reading and detection. In many fields of electronics there is also a growing demand;

- non-toxic characteristic, aluminum and its salts are completely non-toxic;

- no sparks, this is the reason to using aluminum in flammable and explosive sectors;

- excellent workability, its technological properties make it particularly adapted for all the machining processes obtaining products with various shapes with minimum dimensional tolerances. In fact, it can be laminated in very thin thickness, less than 0.005 mm. Moreover, it can be brazed, welded or joined with all the normal mechanical systems;

- aesthetics, the aluminum has a white color and can undergo different surface treatments.

The aluminum is actually used in different application fields, from the electronics or aerospace industry to the most common ones with the manufacturing of doors and windows, up to car wheels, or horseshoes. This is due to metal qualities and properties, such as: lightness (almost a third of steel), electrical conductivity (second only to copper) and thermal, mechanical characteristics especially regarding its alloys, weather resistance, plasticity, formability, durability in contact with food and almost all the liquid, and the aesthetic qualities. Also the design field uses aluminum to get particular shapes. Important is the application of extruded profiles and recycled aluminum material. Some examples of recycled aluminum are the automotive industry and that of the cans.

2.1.2 Aluminum alloys and machining

To get an improvement about the mechanical properties, the aluminum is mixed with other metals. There are two different kinds of alloys: casting and hardening. The latter are those of type 1000 (at least 99% aluminum), 2000 (cupper), 3000 (manganese), 4000 (silicon), 5000 (magnesium), 6000 (magnesium and silicon),

7000 (zinc), 8000 (steel and silicon). The aluminum is easily worked by machining, but attention needs the metal behavior with different equipment. So that softer alloys can "mix" and can rise long chips with all the problems related to the surface finishing treatments and the possibility to use automatic machines.

2.1.3 6XXX aluminum alloys microstructure

Aluminum alloys, especially 6XXX series, are widely used in the production of high performance and lightweight components by means of bulk forming processes. In particular, hot aluminum extrusion process is used for manufacturing profiles in aerospace, automotive and other high performance sectors. The mechanical properties of the profiles are related to the final grain shape and size as described by the Hall-Petch relation [98]. During hot extrusion process different phenomena are involved [18]: heating of a homogenized billet, dynamic recrystallization of the grains during deformation, high frictional conditions, high strains achieved in the material, which will then undergoes several degrees of static recrystallization depending on the quenching treatment. In some cases, PCG (peripheral grain coarsening) may occur thus leading to profile scrapping. The onset of dynamic or static recrystallization mechanism is related to the presence or absence of deformation, respectively, as explained in the work of Donati et al. [18]. In particular, the dynamic recrystallization mechanism is strictly related to the type of material: low stacking fault energy materials promote conventional dynamic recrystallization DRX (nucleation and growth of new undeformed grains during deformation as found in pure aluminum), while high stacking fault energy materials (6XXX series aluminum alloys) exhibit different behaviors. In 6XXX series aluminum alloys, grains are surrounded by High Angle Grain Boundaries (HAGB, conventionally set over 15° of misorientation between two adjacent grains), while Low Angle Grain Boundaries (LAGB, below 15°) surround the subgrains within the grain. Grain shape is deeply influenced by the local state of strain, while subgrain size is mainly dominated by the temperature and strain rate field. Continuous dynamic recrystallization theory claims that during deformation the misorientation angle of a subgrain is subjected to change so that LAGB can be transformed into HAGB thus generating the appearance of a new grain. McQueen, 2011, proposed that during deformation, the original grains flatten and elongate as consequence of deformation up to a level where grain boundaries become highly serrated: when grain thickness is in the order of 2-3 times the subgrain size, the grain

is pinched-off and two or more smaller grains are generated from the original one. Such phenomenon is called geometric dynamic recrystallization. When aluminum alloys are casted no evidence of subgrains can be found in relation to the dendritic structure of the alloys: as the material is subjected to strain, subgrains will appear and evolve following processing conditions. Castro-Fernandez and Sellars (1990) showed that although grains elongate under deformation, subgrains remain equiaxed and their dimension is correlated with the Zener-Hollomon parameter. Extruding 6060 aluminum alloy, different levels of deformation of grains are within a single billet [18]: almost undeformed grains are found in the so called dead metal zones located at the die face and next to the ram, while shear zones are characterized by elongated grains, as shown in Figure 2.1.
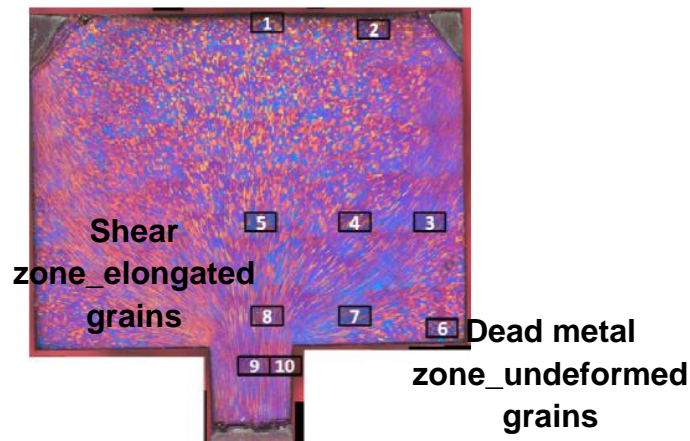
Figure 2.1. Grains configuration of AA6060 aluminum alloy during an extrusion process, [18]

The profile microstructure is characterized by very elongated grains with onset of serration and grains pinch-off: thinner grains are found on the profile surface due to the double action of the high friction at the bearing zones, and of the highly deformed material flowing from the shear zones into the profile surface, thus contributing to the highest deformation levels. Grain thickness continuously decreases with strain up to a steady state condition (2-3 times the subgrain size), while grain length initially increases up to a maximum, then abruptly decreases in relation to the onset of grain pitch-off. The length decrease ends at another critical level of strain (100% pinched off material) in which the grain thickness reaches a constant value.

As said before, quenched specimens (Fig. 2.2a) revealed elongated grains with serration and pinch-off in proximity of the punch, where the highest strain was

reached; while, almost undeformed equiaxed grains are found in proximity of die corners.
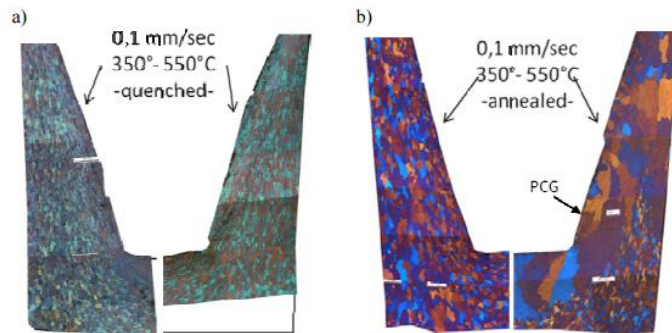
Figure 2.2. Half section of extruded specimens with a punch speed of 0.1 mm/s, at 350 °C on the left, and at 550 °C on the right, a) quenched immediately after extrusion; b) after annealing, [18]

Finally, during deformation no static recrystallization phenomena occur, but immediately at the end of the deformation, grains start to recrystallize. In case of immediate quenching the size of the grains is like frozen, while if no quenching is performed recrystallization occurs (Fig. 2.2b). Nucleation and growth of new grains can start from three different locations: from particles, from pinched off grains and from zones with high misorientation boundaries. Because in extrusion very high strains are reached, only the last two mechanisms occur [18]. The variation of the local extrusion ratio and thus the final velocity, as well as the profile temperature during the experiments, lead to a significantly different microstructure, especially in thin-walled sections [99].

In porthole die extrusion, since both longitudinal and charge welds pass through the thickness of the hollow extrudate, where most of the stress is concentrated, recrystallization will occur more readily and larger grain sizes occur in the weld regions. The seam weld shows a darker band including the largest grains with irregular shape due to the abnormal grain growth under the heavy shear deformation and high temperature (Fig. 2.3). The transverse welding zone consists of oxides and equiaxed recrystallized grains which are a little finer than those in the longitudinal welding seam (Fig. 2.3), [10].
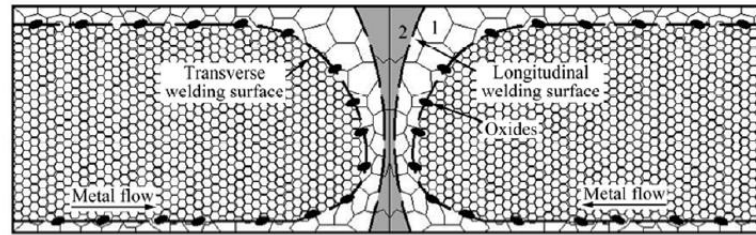
Figure 2.3. Scheme of the extrusion welding on the profile cross section, [10]

More in detail, equiaxed grains are observed in the transverse welding zone on both sides of the longitudinal welding, and they have dimension bigger than the initial one (Fig. 2.4b-c, Point 1). This may be explained by the complete dynamic recrystallization effect and grain growth during extrusion and aging. The longitudinal welding zone is recognizable as a darker etching band (Fig. 2.4b-d, Point 2) with the largest grains in it. The grains are bigger than before and bigger than the grains in the transverse welding zone and they have irregular shape indicating a heavy deformation or high temperature affected zone presented under the die webs.
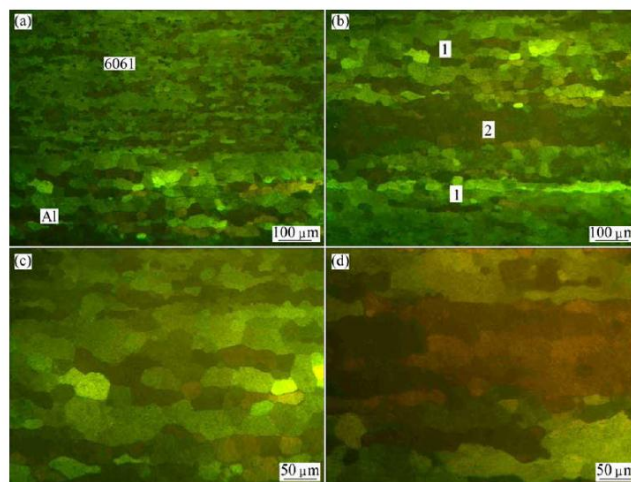
Figure 2.4. Microstructure corresponding to the welding surface into the profile, parallel to extrusion direction; a) grain size comparison; b) welding zone: 1-charge welding zone, 2-longitudinal welding zone; c) charge welding zone corresponding to Point 1; d) longitudinal welding zone corresponding to Point 2, [10]

2.1.4 Extrusion defects of 6XXX aluminum series

Defects in extruded aluminum profiles are related to mechanical characteristics, surface aspect and dimensions [100].

1- Mechanical characteristics. The problems regarding the final mechanical properties depend of the thermal treatments adopted in billet casting phase and during extrusion, quenching and aging.

2- Surface aspect. It depends of non-uniform cooling time in the different parts of the extruded sections. On the profile surface could be some areas with higher concentration of precipitates of alloying elements and intermetallic compounds that have a surface appearance different than the rest of the surface poor of these particles. These areas can also have different mechanical properties.

3- Dimensions. The dimension and shape defects depend of the extrusion die geometry and its wear.

Typical extrusion defects (Fig. 2.5) are:

- Surface cracking, which occur when the surface of an extrudate splits. This is often due to high extrusion temperature, friction, or high speed. It can also happen at lower temperatures if the extruded product temporarily sticks to the die. Another reason can be the quality or roughness of the die or some residues of the extruded material that can stick to the die surface producing embossed lines.

- Pipe, when a flow pattern draws the surface oxides and impurities to the center of the product. Such a pattern is often caused by high friction at the interface material-walls or fast cooling of the outer regions of the profile.

- Internal cracking or central bursting, when the center of the extrusion develops cracks or voids. These cracks are attributed to hydrostatic tensile stress at the centerline corresponding to deformation zone in the die.
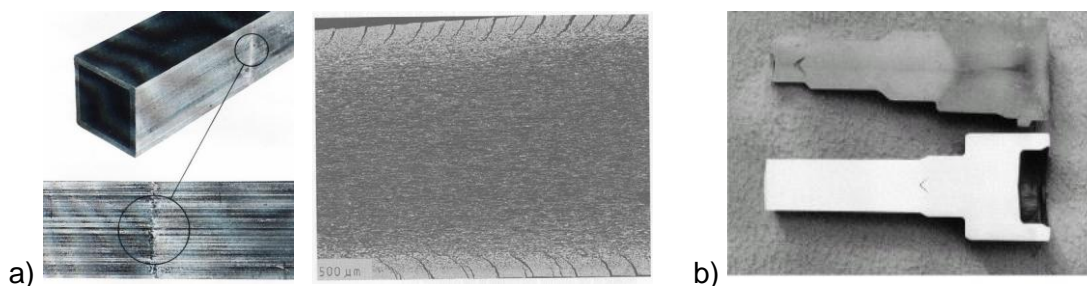
Figure 2.5. Extruded specimens with a) surface defects, [101]; b) central bursting defects

Afterwards, a more detailed description about the extrusion defects, in case of AA6060 aluminum extruded profiles, is presented.

Stop mark

It is represented with reliefs over the entire cross-section associated with tearing. It is due to an accidental stop of the press during extrusion or when the press has to be stopped to load a new billet inside the container. The material has to be discarded.
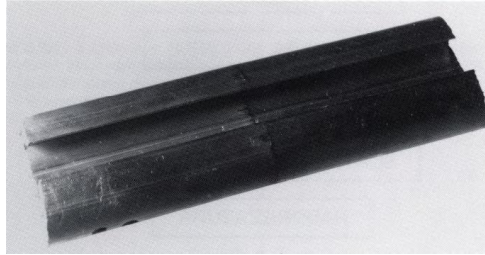
Figure 2.6. Stop mark defect, [100]

Transverse cracks

This defect is visible on the profile edges. Sometimes the cracks have a thin section so it is difficult to observe them. They are due to a wrong temperature or ram speed value for the considered billet material and die design. Also in this case the material is wasted.

Figure 2.7. Transverse cracks, [100]

Tearing

The tearing consists of material removed from the profile sharp edges. Also in this case the reason of its formation is the temperature and ram speed condition and the material cannot be used. The tearing is favored by the presence of heterogeneous particles under the skin extrudate, which promote the detachment of portions of the external layer.
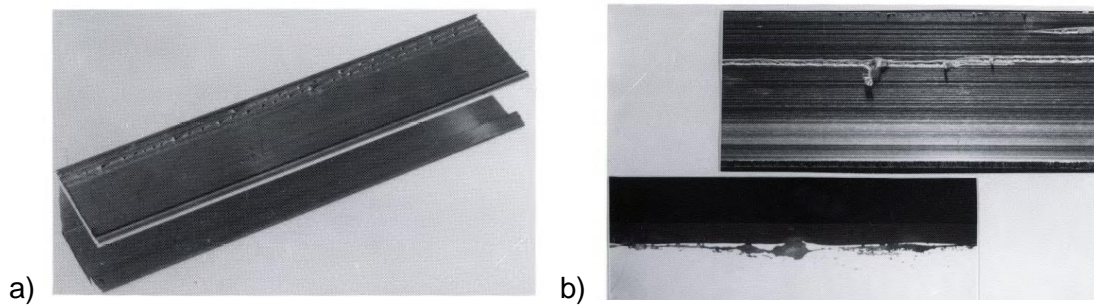
Figure 2.8. a) Tearing defect and b) sectional view of the defect, [100]

Bondings

On the surface sometimes tearing and surface reliefs are evident, associated with scratches. They are due to high ram speed and temperatures. It is possible try to recover the profile by deep grinding, but usually this is not enough.
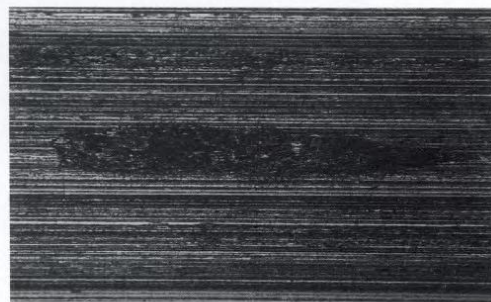
Figure 2.9. Detailed view (100x) of bonding defect, [100]

Extrusion grooves

On the profiles surface there are grooves that could be confused with the bands of the structure. They are due to extrusion die wear and it is possible recover the material by frosting.
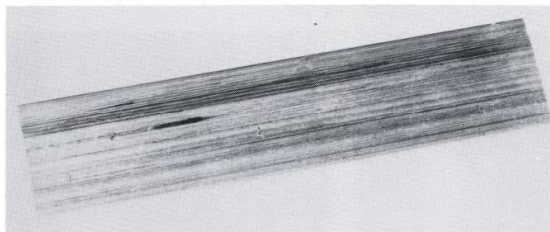
Figure 2.10. Extrusion grooves defect, [100]

Blistering on the surface

This is a visible defect on the surface. The external layers are inflated along the extrusion direction due to oxides, particles or gas inclusion. Sometimes, after surface polishing they can be transformed into tearing. The material is wasted.
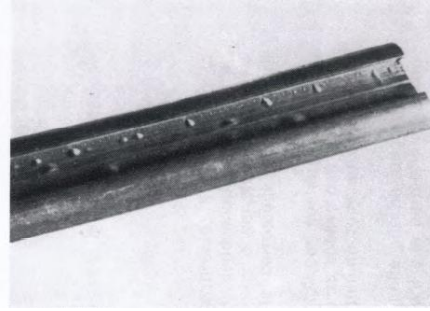
Figure 2.11. Blistering defect on the profile surface, [100]

Deep blistering

Also in this case, the defects are evident but more isolated and more elongated than the blistering on the surface. The reason is the presence of gas or dross inside the billet that flows along the center zone of the extrusion section. The material can not be utilized.
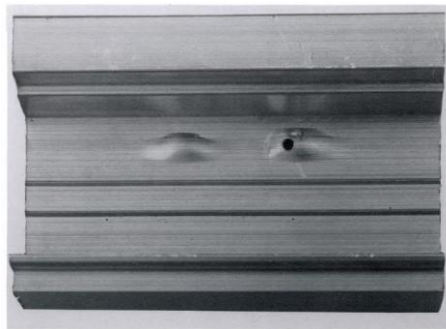
Figure 2.12. Deep blistering defect on the profile surface, [100]

Signs of straightening

This defect is characterized by a series of shinier stretches, parallel or inclined respect the extrusion axis. It can also occur as deep carvings having a zebrine aspect after anodizing. The signs depend on an incorrect material flow between not well adjusted straightening rollers. A very pronounced dysregulation leads to cuts. If the defect is slight, it can be easily removed by sanding.
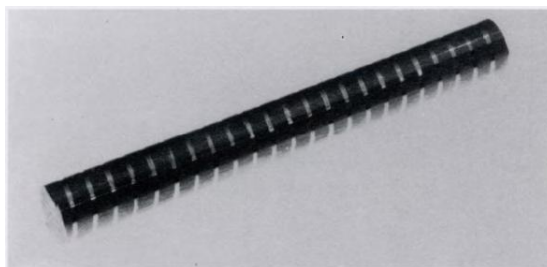
Figure 2.13. Straightening signs, [100]

Bands or Streaks

This kind of defect is not detectable before the pickling, during which zones with different reflectivity appear. It can be visible also after anodizing treatment with darker or lighter bands depending on the observation direction. It usually will appear on a long profile. It is due to intermetallic phases or particles inside the billet or to extrusion modality. The final aspect depends on mechanical polishing. Usually, the profile is wasted. In hollow profiles, the bands appear on the welding plane, especially on the lateral surfaces or external tongues.
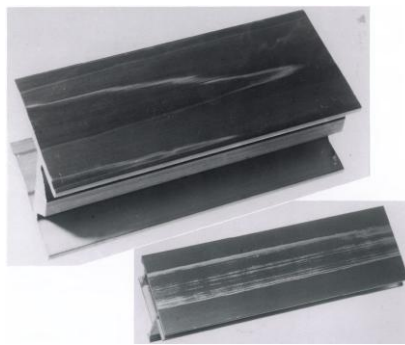
Figure 2.14. Bands or Streaks defect, [100]

In the following picture it is possible to see the microstructure of a band defect on both parallel (Fig. 2.15a) and orthogonal (Fig. 2.15b) plans to the defected surface, after the oxide layer removing.

a)   b)
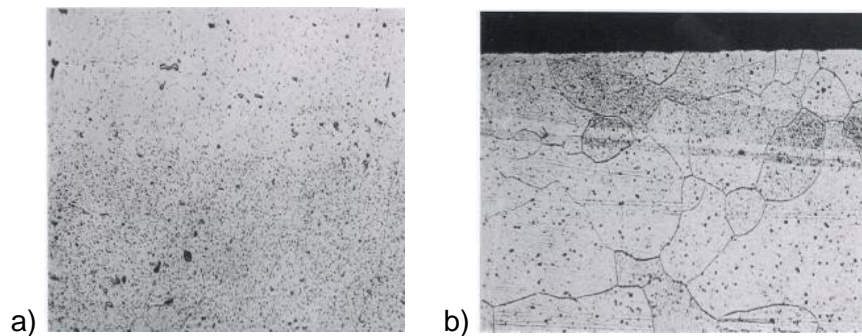
Figure 2.15. Bands defect microstructure (500x) on a) parallel and b) orthogonal plan to the defected surface, [100]

Also an extruded profile with thin streaks associated with small tearing aligned along the extrusion direction is shown in Figure 2.16.
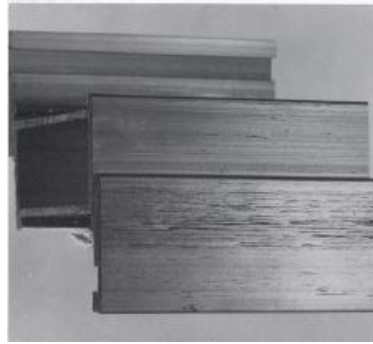
Figure 2.16. Streaks defect, [100]

The microstructure is analyzed on an orthogonal plan to the defected surface (Fig. 2.17a-b-c).

a) b) c)

Figure 2.17. Streaks defect microstructure (500x) on an orthogonal plan to the defected surface, [100]

Spots

The surface inhomogeneity is visible after anodizing treatment. The defect consists of spots with different reflectivity, shape and dimensions, which are found on the profile surface with a certain periodicity. It is due to a local re-precipitation of Mg_2Si, caused by a different cooling speed. It is locally expanded along the entire profile thickness and the material is not recoverable. This defect occurs when the profiles are positioned, still extremely hot, on pilger bench and the fans cooling is ineffective.
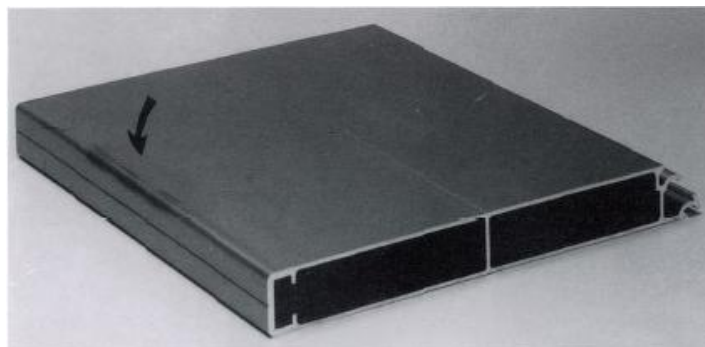
Figure 2.18. Spots defect, [100]

Metal reflux

Defect resulting in a backflow of metal with intermetallic compounds and oxides during the extrusion process. This is due to billet skin extrusion during the final ram stroke.
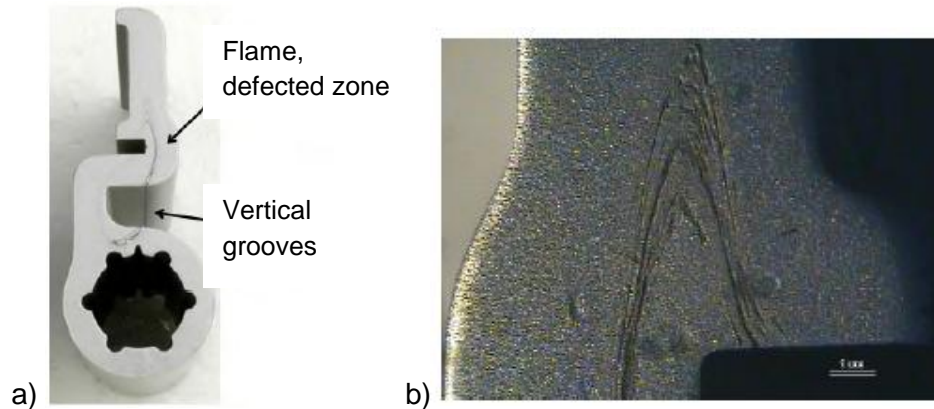
Figure 2.19. a) Metal reflux defect and b) detailed view (11x) of the defected zone, named *flame*, [100]

2.2 EXTRUSION PROCESS INVESTIGATION BY MEANS OF NUMERICAL APPROACHES

To simplify the research and to reduce costs and time, numerical analysis are performed. In such a way, set the parameters and modify them is simple and the outcomes investigation is instantaneous. In this work, FEM, Finite Element Methods, are considered; more in detail, Deform and HyperXtrude are the software used to simulate the extrusion process with 3D models in input, built with a CAD software, named Pro Engineer.

2.2.1 Numerical models generality

A substantial difference in the numerical models is about the evolution of the involved variables: their history can be time dependent or not. The developments of velocity, effective strain and temperature inside the deforming billet indicate that the process is non-steady, as result of continuous heat generation due to sticking condition at the billet-container interface, of billets cyclic loading and of dies changing [102]. Finite Element Method is becoming a predictive tool for die designer; it permits to save costs and time-consuming trial and error practice for the aluminum extrusion industry. The FEM models are based on two approaches: Lagrangian and Eulerian. The

Lagrangian one can well describe the free surface emerging from the die during the process, but it has serious limitations in handling complex geometries and large deformations because severe mesh distortions and frequent re-meshing requests. The Eulerian approach, instead, is well capable of working complex geometries and high deformations, but it does not permit the generation of free surface, which actually occurs throughout the whole extrusion process, thus being not suitable for simulating extrusion in the transient state. The more recently developed arbitrary Lagrangian Eulerian approach uses a free surface correction scheme to update the geometry so the bending, warping or twisting of the extrudate, can be predicted. However, it still has inherent limitations of the Eulerian approach, being incapable of describing: the transient-state characteristic of the process at the beginning stage when dramatic changes in temperature, stress, strain and strain rate occur; and the steady-state characteristics of shortening billet and elongating extrudate. Within the constraints of the size of data files generated and the computing time needed, the simulation of a complete extrusion cycle with a certain degree of geometric complexity and in its entirety is still a huge challenge. In the Lagrangian description the mesh follows the deforming material and also it deforms along with the shape changes of the material as extrusion proceeds. This imposes serious limitations on the complexity of the die and the wall thickness of the extrudate, relative to the dimension of the billet [103]. Transient effects include the loading of an empty die, the reduction in billet length and the heating and cooling of the material during a billet cycle. These kinds of calculations require unacceptably long calculation times. As an alternative, the stationary extrusion process can be simulated, for example, by means of HyperXtrude®, whose stationary solution gives the extrusion load at a certain billet length and it provides an upper limit for the temperature distribution. In this work Altair HyperXtrude® software is used also to simulate composite extrusion.

2.2.2 Material and process properties using Hyperxtrude® software

In most of the works in this thesis, Altair HyperXtrude® software is used to simulate the extrusion of profiles. In some cases, the influence of process and geometric parameters is analyzed on velocity field, load and temperature conditions; in other cases, the software is used to optimize the die design in order to avoid profile distortions with symmetric and non-symmetric cross shapes. Finally, it is possible to

simulate also composite extrusion, considering a non-symmetric profile reinforced with seven continuous wires.

Material law

The FEM used in metal forming can be generally categorized into viscoplastic FEM and elastic viscoplastic FEM, depending on which material constitutive equations are used. In simulation of aluminum extrusion, it is common to use a viscoplastic constitutive model because the high plastic strain during the process neglecting the elastic properties of the material even if, when the material enters the bearing channel, plastic deformations are minimal and elastic effects have a significant influence on the material behavior. The actual behavior of a specific aluminum alloy in the plastic domain is defined by an expression for the flow stress that describes the relation between the effective stress, the equivalent viscoplastic strain and equivalent viscoplastic strain rate. However, from the literature it is known that even at elevated temperatures a small elastic region is present. To include such an elastic region a modified Sellars-Tegart law is introduced:

$$\sigma_{f(k,T)} = s_m \arcsin \left(\left. \left(\dot{k} + \dot{k}o(T) \right) \middle/ A \exp\left(\frac{Q}{RT}\right) \right)^{\frac{1}{m}} \right) \qquad \text{(Eq. 2.1)}$$

$\dot{k}o(T)$ is a temperature dependent parameter and a small value of it between 0.001 and 0.01 is sufficient to obtain a realistic size of the elastic region; R is the universal gas constant, T is the temperature and s_m, A, Q and m are parameters that are used to fit the flow stress to experimental data. The testing methods used to determinate the parameters are torsion tests compared to compression tests, because the material during the extrusion process is loaded with these kinds of stresses. Secondly, small variations in alloy composition are possible and they should be considered [104].

In this work the billet is made up of AA6060 aluminum alloy taken from the software library, whereas the reinforcements, in case of reinforced profiles, are made up of high strength spring steel, taken also from the same library. The first one has a SyneHypInv behavior as the material property; the Sine Hyperbolic Inverse model is described by the following equation:

$$\sigma = \frac{1}{\alpha} Sinh^{-1}\left(\left[\frac{Z}{A}\right]^{\frac{1}{n}}\right)$$ (Eq. 2.2)

where $Z = \dot{\varepsilon} exp\left(\frac{Q}{RT}\right)$, n is the stress exponent, A the reciprocal strain factor, Q the activation energy, R the universal gas constant. Sine Hyperbolic Inverse law is among the material models implemented in HyperXtrude® solver and predicts a constant/steady-state flow stress for various strain rates and temperatures. Unless modified, this model does not account for strain-dependence and hence cannot predict stress softening. This law is the most widely used to describe thermo-viscoplastic behavior of metals during hot deformation.

The reinforcing wires have PowerLaw material constitutive equation. The generalized power law used in HyperXtrude® is given by the following expression:

$$\sigma = [Y(T) + (\varepsilon + \varepsilon_0)^n (\dot{\varepsilon} + \dot{\varepsilon}_0)^m C(T)]\alpha_T$$ (Eq. 2.3)

where $C(T)$ is the amplitude, m the strain rate exponent, n the strain exponent, T the temperature, $Y(T)$ the yield stress, $\alpha_T = e^{-\beta(T)}$ is the thermal expansion coefficient and temperature dependence whose possible values are summarized in Table 2.2, ε the strain, the strain offset, $\dot{\varepsilon}$ the strain rate, $\dot{\varepsilon}_0$ the strain rate offset, σ the stress.

None	Even for the case where there is no temperature dependence, a reference temperature should be specified. In this case, the properties are computed at this temperature.
Coefficients	With this option, the parameters **Amplitude** and **ConstantY** can depend on temperature and you can specify them using a TABLE or FUNCTION. The only difference between the **Coefficients** and **None** is that properties are constant in the case on **None**.
Exp(Q/RT)	In this case, in addition to **ReferenceTemperature** (T0), two other parameters, **ActivationEnergy** (Q) and **UniversalGasConstant** (R), are needed by the model. The following two lines should be added to the syntax. • ActivationEnergy= Q • UniversalGasConstant = R
Exp(-Beta(DeltaT))	In this case, in addition to **ReferenceTemperature** (T), parameters, **Beta** (beta) is needed by the model. The following line should be added to the original syntax. Beta = β

Table 2.2. Valid data for Temperature Dependence

Friction models

The information about the friction conditions during the numerical simulation of the extrusion process are set as sticking at the interface between the material and the full

matrix, unless in the bearing area, where a viscoplastic friction model is used to represent both sticking and slipping boundary conditions might be simultaneously present in the different parts of the bearing channel, with a friction coefficient of 0.3.

However, there are different kinds of friction models; some of these are below summarized.

- Coulomb friction model: the friction force is considered to be proportional to the normal pressure and can be expressed in terms of $f = \mu N$, where f is friction force, μ is friction coefficient and N the normal load. In extrusion process, due to high contact pressure at the workpiece/matrix interface, the friction stress tends to be higher than the shear flow stress of the workpiece material, so that the Coulomb friction model tends to overestimate the friction stress. For this reason, it is rarely used in FE simulation of the aluminum extrusion.

- Shear friction model: implemented into the FE simulations of extrusion process to avoid the overestimation of friction stress. It assumes that the friction stress is proportional to the shear flow stress of the deformed material, and it can be expressed as $f = mk$, where f is the friction force, m is the friction factor, which normally ranges between 0 (frictionless condition) and 1 (full sticking condition), k is the shear flow stress of the deformed material. However, it is not easy to determine the value of friction factor experimentally and thus its selection is based on assumptions.

- Empirical friction models material/container interface: Flitta and Sheppard [105] investigated the effects of initial billet temperature on the friction in hot aluminum extrusion process. The assumption of a constant value of friction factor for all extrusion temperatures is incorrect and a transition from sliding to sticking friction is observed when initial billet temperature increases, because also the friction increases. The authors obtained a linear relationship between the friction factor and the temperature: $m = A + BT$, where m is the average friction factor, T is the temperature, A and B are constants. A generalized form of the friction model was proposed for all extrusion variables, $\bar{m}_{\Delta Ln} = \left[\alpha + \alpha n ln\left(\frac{Zd}{A}\right) + b\right]_{\Delta Ln-1}$, where $\bar{m}_{\Delta Ln}$ is the average friction factor that varies with ram stroke, Z_d is the average of the Zener-Hollomon parameter, α, n and

A are the constants related to mechanical behavior of the workpiece material; finally, a and b are the constants for the friction model.

- Empirical friction models material/bearing channel interface: because the presence of a full sticking zone at the die entrance region and a sliding zone at the die exit region, Abtahi [106] developed an empirical friction model for the bearing channel of hot aluminum extrusion process. To get information about the friction conditions corresponding to the interface bearing land-material flow, the split-die technique was suited for measuring slip length and friction stress on the bearing land. The split-die extrusion tooling consists of three parts (Fig. 2.20): one die holder and two die inserts.
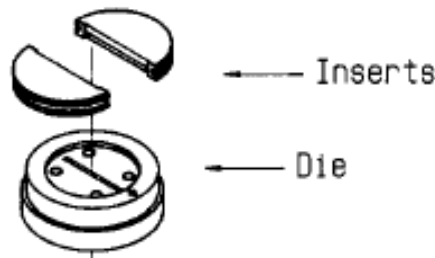
Figure 2.20. Split-die extrusion tooling, [106]

The two die inserts are held closely together in the die holder during extrusion (Fig. 2.21a), but split up afterwards (Fig. 2.21b), enabling direct characterization of the bearing surface [107].

a)   b)
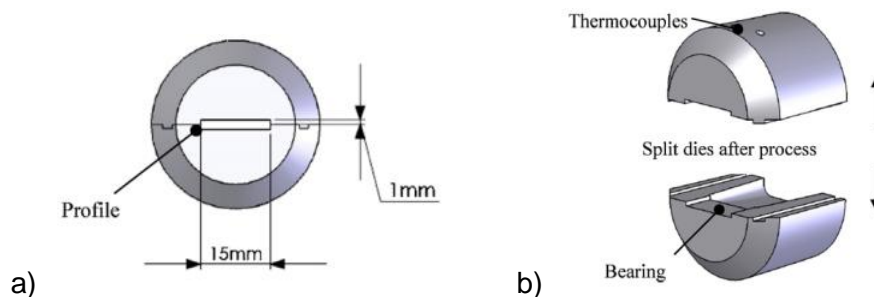
Figure 2.21. Die insert construction a) assembled during extrusion and b) split up for bearing surface characterization after extrusion, [107]

In particular, after the extrusion experiments, the die inserts are split up in order to measure the sticking length. Two different contact regimes exist in the bearing-extrudate contact during unlubricated aluminum extrusion process: sticking and slipping. Close to bearing entrance due to the large normal pressure, friction exceeds the shear strength of the extrudate and sticking

condition takes place between the bearing surface and the moving extrudate. As the normal pressure decreases towards the bearing outlet, the material surface starts to slide over the bearing once, the interface shear stress is slightly lower than the bulk shear strength, forming a slipping region [108]. In the sticking region, the extrudate surface is not yet formed since material is still sliding against itself, whereas in the slipping region effects like scratching of the surface start to take place [109]. It can be seen that the separation marking is bent towards the exit of the bearing (Fig. 2.22), due to an additional compressive stress in the center of the extrudate. The exiting speed of the different parts of the extrudate tends to equalize towards the bearing exit.
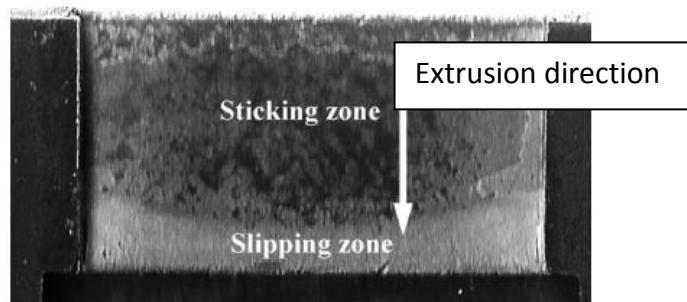
Figure 2.22. Separation of sticking and slipping zones on the bearing after aluminum extrusion, [107]

The profile surface is generated in the slipping region in which the friction conditions may vary considerably. The resulting friction force in the slipping region depends strongly on the die angle. The friction per unit of length increases with the die angle and decreases with both the profile's thickness and the exit speed. The surface quality of products depends properly on the lengths of these two regions.

Abtahi [106] determined the length of the slip zone as:

$$slipping\ length = (av+b)exp(\frac{\alpha}{cv+d})+(gv+h) \qquad\qquad \text{(Eq. 2.4)}$$

where α is the die angle, v the run-out speed and the others parameters are constants. The last model is applicable for die angle between 0 and 1°. While the following empirical friction model is proposed in the sticking region:

$$\tau_{st} = \tau_0 + kx \qquad\qquad \text{(Eq. 2.5)}$$

τ_0 is the friction at the inlet of the bearing channel, x the distance from the die entry and k is a function of exit speed. The lengths are controlled by several interacting parameters, such as extrusion conditions, die geometry and alloy properties [110]. The slipping zone decreases with the roughness of the bearing surface (Fig. 2.23). Moreover, if the bearing is choked there will be sticking conditions due to the pressure increase (Fig. 2.24a); if there is a parallel bearing there will be sticking conditions only if the length of the bearing is enough to create a high pressure in the bearing entrance.
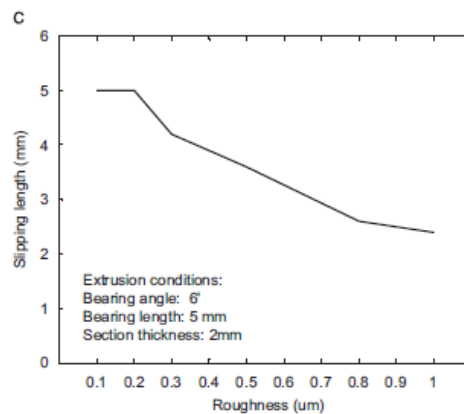
Figure 2.23. Slipping length related to bearing surface roughness, [110]

Therefore, if the length of the bearing is short than there will be only slipping conditions (Fig. 2.24b). The sticking zone can be completely eliminated if coefficient of friction is low enough and when the extrusion speed and extrudate surface temperature are very high.
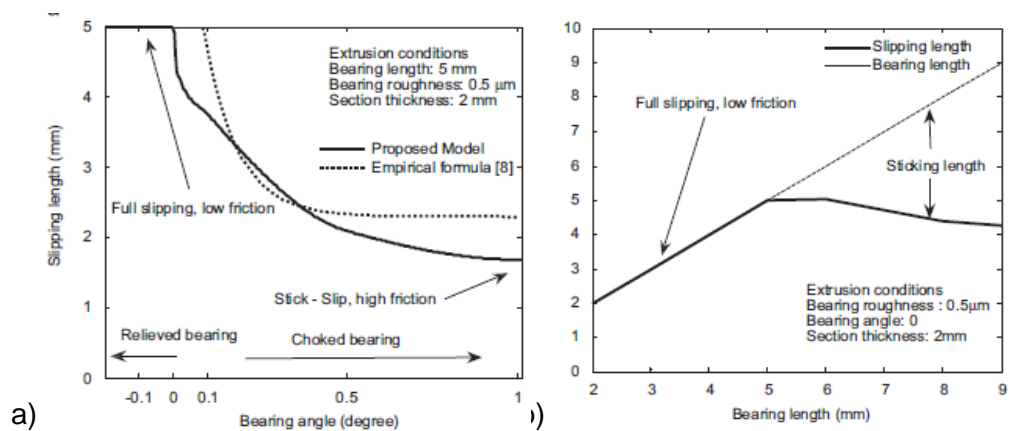
Figure 2.24. Slipping length related to a) bearing angle and b) bearing length, [110]

In the work of Bjork [108] is stated that the coefficient of friction in the bearing channel depends on local temperature, sliding velocity and surface contact conditions according to the following relation:

$$\tau_{int} = c_1 L_H \rho \ln \left({T_m}/{T_{int}} \right) exp\left(-c_2 v\right) \qquad \text{(Eq. 2.6)}$$

where L_H is the material latent heat, ρ is its density, T_m is the melting point and T_{int} is the interfacial temperature, c_1 and c_2 are constants.

Dead metal zone

Using square die, with 90 degrees angles, the material in the areas close to the matrix exit, named dead metal zones, is moving very slowly and a shearing of the material occurs on the dead zones surface. A larger dead metal zone is associated with increased internal friction, higher extrusion pressure, high temperatures and more inhomogeneous metal flow due also to profile complexity [111]. Dead metal zones are located also on the top surface of the bridges in case of porthole die; but, in that case, they could help the material to better flow into the feeders.

Extrusion load

Regarding the load reached during numerical and experimental tests there is a difference at the beginning of extrusion; in fact, during the first ones, the pressure quickly reaches a peak, while in practice it increases much less rapidly. This is because in the simulations the insider diameter of the container is identical to the diameter of the billet, and as result the upsetting to fill the container does not exist. After the peak, the process enters the steady-state stage with a gradual decrease of pressure, which is due to the reducing billet length and friction force at the container-billet interface. The relation between the peak pressure and the billet length is linear. This pressure drop is also partly due to the gradual temperature increase in the remaining billet.

Strain and stress conditions

The temperature is the parameter that more influence the material strain. At higher temperatures, the flow is faster and the resistance to deformation of the billet material decreases; consequently, the billet is more ductile and tends to easily fill the

container. Initially, the billet deformation is influenced by sticking condition along the container wall as shown in Fig. 2.25a.
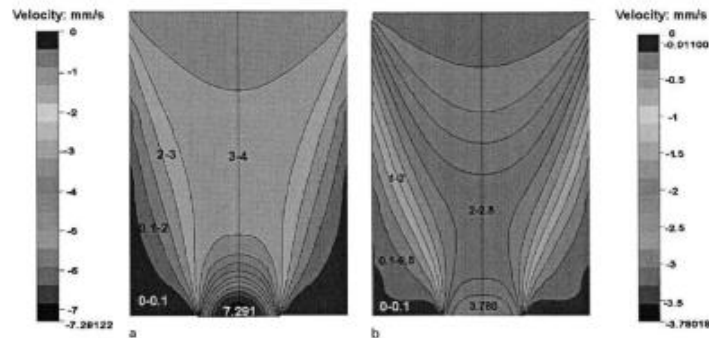
Figure 2.25. Effect of temperature and friction in extrusion process on material flow in case of a) high temperature, 400 °C; b) low temperature, 350 °C, [105]

Instead, at lower extrusion temperature, the billet is not so ductile and behaves in a relatively stiffer manner. The upsetting stage starts by sliding along most of the container wall and only one fifth of the billet length is sticking as shown in Fig. 2.25b. When the billet is fully compressed to fill the container, the elastic properties of the container and plastic properties of the material in contact have a significant effect on the difficulty of them to slide relatively to each other. The deformation zone is not stationary, the billet is deforming plastically while the shearing forces are operating to promote the burnishing effect at the interface between dead metal zone and billet.

Regarding the strain rate, it is higher at the interface material-container, than at the center, in the initial phase of the punch descent (Fig. 2.26); while the shear stress is higher at the interface material-container at low temperature and for every punch stroke (Fig. 2.27).
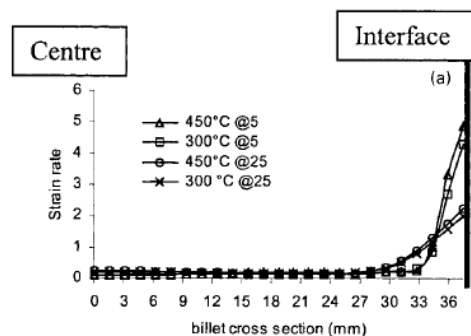
Figure 2.26. Strain rate on the profile cross section from the center to the external surface, [105]
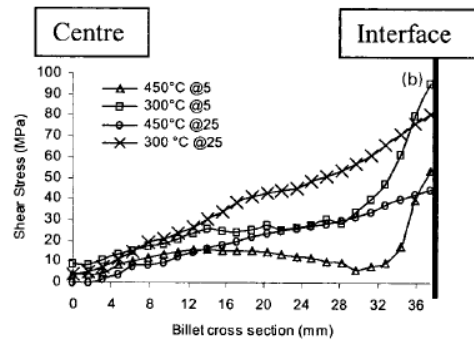
Figure 2.27. Shear stress on the profile cross section from the center to the external surface,
[105]

The zone of intense shear increases toward the die opening, separating the deformation zone from the dead metal zone. In this case, the frictional stress is identical to the flow stress of the billet material in pure shear, whereas the relative velocity increases from the ram speed at the top of the billet to the exit speed of the extrudate when approaching the die opening. The values of friction do not remain constant through the extrusion process. These changes are the consequences of an increase in the overall billet temperature within the deformation zone and of a decrease in the contact area with further ram travel. The die exit temperature of the extrudate is the most critical temperature; it increases if the heat produced by the work done in upsetting the billet and the work done against friction between material and tooling exceeds the heat losses. On the other hand, a lower extrusion temperature increases the resistance to deformation, reduces the volume of dead metal zone and decreases the work required to produce the desired surface [105]. Unlubricated aluminum extrusion is desirable in order to prevent impurity pick up from the tools.

Hyperbolic sine form correlating the effective flow stress with strain rate and temperature is considered appropriate to describe the hot deformation behavior of the material in hot conditions.

Mesh

During the simulation of extrusion processes, Lagrangian approach is usually used for large deformations; the elements become severely distorted during the process and, consequently, the need for re-meshing is necessary to continue the simulation. The frequency of re-meshing is controlled by the degree of deformation and is a user

variable. On the other hand, to reduce the computational time is possible to use the Eulerian approach to analyze variables such as pressure, temperature conditions and profile velocity. Finer mesh is applied in the FEM model where high deformation is expected to occur, whereas, a coarser mesh is used for the remainder parts. Therefore, coarse tetra mesh (elements with 4 nodes) is used when a lot of information are not necessary; finer hexa mesh (elements with 6 nodes) is used where the deformation is accentuate more information are needed. More in detail, coarse Tetra mesh is used for billet, finer tetra mesh for feeder, welding chamber and pocket, whereas fine Hexa mesh (Prisms) for bearing and profile (Fig. 2.28), remembering that HyperXtrude® model takes into account the internal volume of the die and the volume of the profile. Tetra mesh is created using the Volume Tetra subpanel to generate a shell mesh and fill the enclosed volume with solid elements. It is possible choose a shell mesh (2-D) using quads, trias, or mixed elements and a solid mesh (3-D) using only tetrahedral elements or mixed (tetras and penta) elements. In addition, there is the proximity meshing option, which refines the mesh in areas where the features are small and closer together.
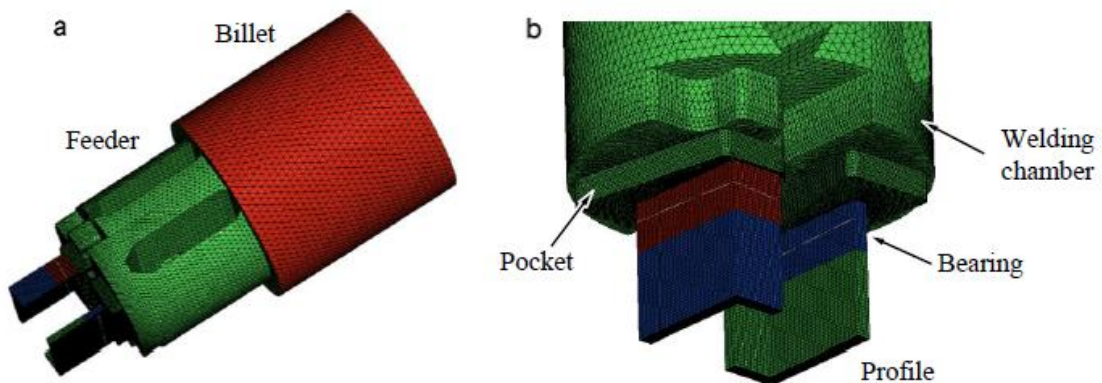
Figure 2.28. a) Model with mesh in HyperXtrude® and b) particular of the final part of the die

Reinforcing elements

Recently, lightweight materials and small sections are requested, as well as, manufacturing of reinforced profiles. The reinforcing elements have to be taken into account as meshed parts with hexa mesh matched with that of the surrounding material. The reinforcement material is characterized by plastic behavior and a specified velocity, given by the relation between the extrusion ratio and the punch speed, is considered the input velocity of the reinforcements.
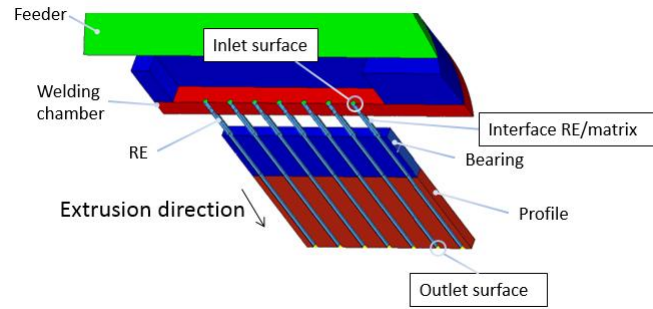
Figure 2.29. Meshed model in HyperXtrude®

Boundary conditions

Boundary conditions set during the numerical tests in HyperXtrude® consider friction model, temperature, punch speed and thermal exchanges. The punch speed usually is variable in the range 1-10 mm/s; a lower velocity limits the flow unbalance, a higher value, instead, increase the productivity. The extrusion usually is performed in hot conditions, so the billet pre heated temperature and the die temperature are between 400-500 °C, less than the melt aluminum temperature (≈700 °C). A convection heat exchange is set between the material and the die and adiabatic condition is set between material and bearing land region and between profile and external environment. No thermal exchange is established between the material flow and the wires because a FluidFluidInterface boundary condition is attributed at the elements located at that interface, as well as, no more information are required about friction condition and velocity constraint. This boundary type is used to describe interior interfaces among different fluid materials. These occur when solving co-extrusion problems. If free surface calculations are turned on, the deflection of this interface will be calculated. Additionally, if mesh update is turned on, this interface along with the mesh will be updated based on the calculated displacements. The profile surface is considered as a free surface. The friction between the die and the billet is fixed as sticking and at the interface material/bearing as viscoplastic with a coefficient of 0.3 in order to consider the sticking and following slipping conditions in between.

2.3 EXTRUSION PROCESS INVESTIGATION BY MEANS OF EXPERIMENTAL CAMPAIGNS

A lot of experimental campaigns are performed in order to validate the numerical outcomes or to better understand a particular phenomenon. Following, a description of the used equipment is made.

2.3.1 Furnace

In the investigations regarding this thesis, the working material, AA6060-T6 aluminum alloy, is firstly subjected to an annealing process (30 min at 415 °C, and then cooling at 260 °C decreasing 30 °C/h) and subsequently heated in an electrical furnace (Fig. 2.30) up to 500 °C and maintained at this temperature to homogenize the billet core for 1 hour. In fact, it is supplied in cylindrical billets with a diameter of 20-30 mm. The furnace is available in the Laboratory of the Department of Mechanical, Energy and Management Engineering at University of Calabria.

Figure 2.30. Electrical furnace

2.3.2 Hydraulic Press

A four pillars electro-hydraulic MTS/Instron 1276 machine with a load capability of 1000 kN is used for the extrusion experiments (Fig. 2.31). The tooling is heated by using a couple of band heaters placed around the holder and the welding chamber, while two thermocouples, located in the middle of the holder and close to the welding chamber, are used for the temperature feedback ring. The tests are carried out when the die temperature is equal to 450 °C; Al_2O_3 fiber based sheets are utilized for thermal insulating.
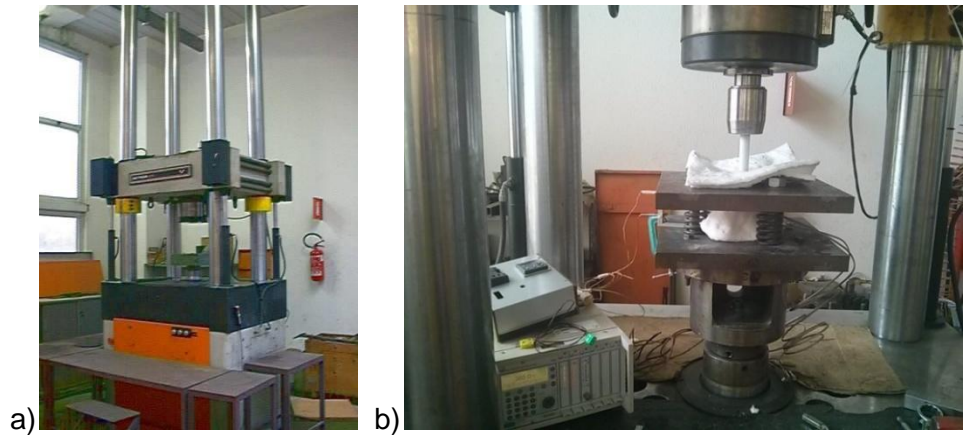
Figure 2.31. a) Electro-hydraulic MTS/Instron 1276 press and b) detailed view

With this press, the matrix has the feeding motion from down to up, and the punch is fixed.

2.3.3 Assembled die

The matrix (Fig. 2.32) is characterized of a container in which fill the billets, of a porthole die (Fig. 2.33a), welding chamber and pocket (where necessary, Fig. 2.32), and of a bearing land region (Fig. 2.33b).
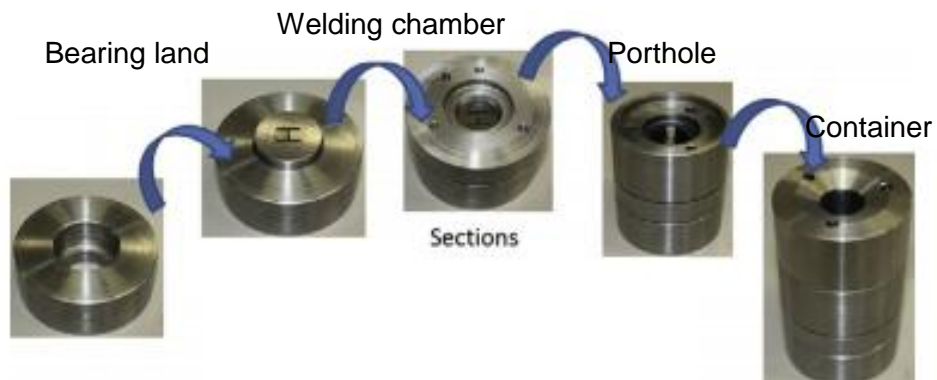
Figure 2.32. Exploded die
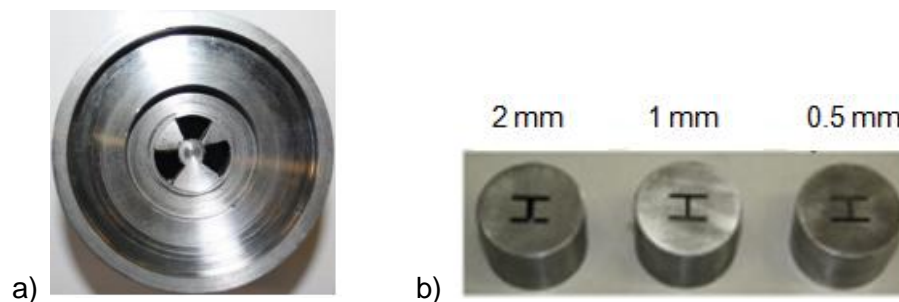
Figure 2.33. Detailed view of a) porthole die and b) bearing orifices with different profile thicknesses

For the extrusion experiments a proper set-up was designed and built for each investigated case study. After extrusion process, the extruded profiles are cooled down at room temperature.

2.3.4 AEG - ELOTHERM EDM (Electric Discharge Machine)

This machine (Fig. 2.34) is used to build the orifice inside the bearing die. The basic electrical discharge machining process consists of an electrical spark created between an electrode and a workpiece that is a visible evidence of the flow of electricity. This electric spark produces intense heat with temperatures reaching 8000-12000 °C, melting almost anything. The spark is very carefully controlled and localized so that it only affects the surface of the material. The EDM process usually does not affect the heat treat below the surface. With wire EDM the spark always takes place in the dielectric of deionized water. The conductivity of the water is controlled making an excellent environment for the EDM process. The water acts as a coolant and flushes away the eroded metal particles.

Figure 2.34. Electric discharge machine

2.3.5 SMS Meer extrusion press

A direct/indirect extrusion press SMS Meer with a load capability of 10 MN is used for the experiments performed in the Laboratory of the Institute of forming Technology and Lightweight Construction, in Dortmund, as shown in the following Figure 2.35.
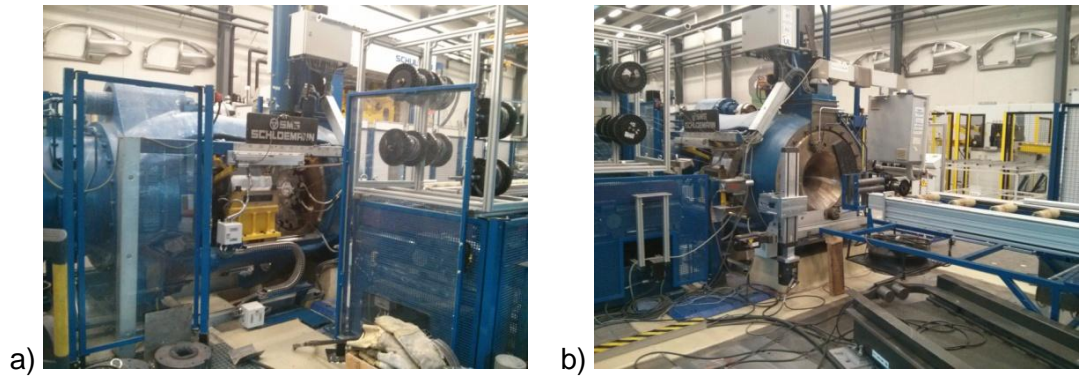
Figure 2.35. a) SMS Meer extrusion press and b) detailed exit view

2.3.6 Testing machine

In order to characterize the material mechanical properties corresponding to the profile welding surface after the porthole die extrusion process, some tensile tests are carried out. Tensile specimens are obtained by cutting the extruded profiles along their axis, orthogonally to the welding line, and clamped to a MTS/Instron testing machine, with a load capacity of 5 kN (Fig. 2.36).

Figure 2.36. Clamping system utilized for tensile tests

A properly designed equipment was built and mounted on the machine to allow the testing execution.

2.3.7 Equipment for microstructural analysis preparation and reagents

In order to analyze the welding line and the microstructure, the profiles are cut, polishing with diamond pastes and etched at Unical Laboratory. An abrasive cut-off saw is utilized for sectioning the extruded components and running water is used in this phase as coolant/lubricant in order to minimize the effects of cutting. Sometimes,

precipitates can be visible corresponding to the welding line but they do not represent defects [112]. The profiles extruded with porthole die in special conditions undergo more deformation than profiles without welding lines, and they are also more resistant to crack propagation. The metallographic preparation of aluminum and its alloys consists of: plane grinding with the finest possible SiC-Paper; diamond polishing to remove all embedded particles; final polishing with silicon dioxide suspension; anodizing with Barker's or Weck's reagent [113]. More in detail, regarding the mechanical grinding and polishing, it is recommended that plane grinding is carried out with the finest possible grid (1200# or 2400#) in order to avoid any excessive mechanical deformation. It is important that the force for grinding is also very low to avoid deep deformation and reduce friction between grinding paper and sample surface. Then, a diamond polishing has to be carried out until all deep scratches from grinding have been removed. The grinding and polishing phases are performed with a special tool (Fig. 2.37). Macro etchants are used for grain size evaluation; also to show flow lines from extrusion and for revealing weld seams. Different phases in cast alloys can either be identified by their characteristic color or by etching with specific solutions that attack certain phases preferentially.

Figure 2.37. Tool utilized for grinding and polishing phases of the extruded specimen, in order to consequently analyze its microstructure

In this thesis, color etchants developed by Weck is the technique used to highlight the grain borders. The etchant developed contains:

- 100 mL water
- 4 g potassium permanganate
- 1 g sodium hydroxide.

The specimen are immersed in the mix and gently agitated until the surface coloring.

2.3.8 Microscope

Grains distribution for each specimen is observed by a polarized light microscope (Fig. 2.38), that permits to investigate the recrystallization of aluminum alloys.

Figure 2.38. Leica Microscope

2.4 APPROACH USED IN THIS THESIS

This thesis regards the numerical and experimental investigation of composite extrusion in order to analyze the influence of continuous reinforcing elements on the material flow at the die exit.

Numerical campaign are performed with Deform^{TM} and HyperXtrude® software to investigate the influence of some process and geometric parameters on the material flow and experimental tests are carried out in order to validate the numerical outputs and clarify several phenomena.

Tensile tests are conducted to analyze the quality of the seam welds and microstructure analyses results are used to investigate the mechanical properties of the extruded profiles.

3. INVESTIGATION OF SEAM WELDS PHENOMENON IN PORTHOLE DIE EXTRUSION

In this chapter the influence of some process and geometric parameters on the seam weld quality is analyzed because its effect on profiles mechanical properties. Numerical analysis are performed by means of finite element software and experimental campaigns are, in some cases, carried out in order to verify the numerical results reliability. To make the work more comprehensive, microstructural analysis are performed by means of an optical microscope to scan the microstructural changes. The focus lies firstly on the bridge volume of the extrusion porthole die, whose shape influences the reinforcing elements feeding and the material entry in the welding chamber. More in particular, the influence of the flow distortion on the contact pressure inside the welding chamber is investigated designing a special test die with three mandrel supporting legs, each one of a different width. With the output considerations of the above case of study, the effect of some geometric and process parameters on the seam weld quality is analyzed, because the influence on the welding pressure value and contact time inside the welding chamber between the material streams, respectively. The considered geometric parameters were the leg size and the extrusion ratio related to the profile thickness changes; whereas, the ram speed is the process parameter taken into account. The welding line quality is analyzed by means of the weld width that is one of the possible indicator of the weld soundness. Finally, the influence of the above process and geometric parameters on the profile quality and on the seam weld strength is investigated extruding a 'I' shaped section with the welding line in the middle of the central tongue by means of microstructural observation and tensile tests, respectively. Numerical simulations are also utilized for locally calculate the pressure and temperature distributions in the die and at the exit of the bearing zone for a better explanation of the experimental evidence.

3.1 INFLUENCE OF MATERIAL FLOW DISTORTION ON THE PRESSURE CONDITIONS IN COMPLEX PORTHOLE DIES

As already known from the literature, in porthole die extrusion, seam welds are generated inside the welding chamber between the material streams that previously cross the porthole die ports. In order to have welding lines with good quality, particular pressure and temperature conditions must be reached into the welding chamber and bearing land region, setting properly process and geometric parameters. Some of these parameters are the billet temperature, the punch speed and the welding chamber, pocket and bearing design. In Kim's work [13], a strength improvement of the welding line was identified in case of high welding chamber height and tapered bottom surface of the bridge, because higher pressure values behind it. In Khan's work [35], the material flow in two porthole die models with non-symmetric feeders related to different bridge positions respect the die center, was analyzed. The work pointed out that the material flowed faster in the bigger feeder. Therefore, the strain rate, related to the flow speed, was higher where the feeder was wider; instead, pressure distribution was irregular especially when the bridge was in a more non-symmetrical position with respect to the die center. In fact, was difficult to define a welding plane between the two flows that joined behind the bridge with very different velocity values. Moreover, Pinter [43] analyzed the influence of the number of bridges, maintaining the same feeders volume in the considered die, on die deflection and welds generation during porthole die extrusion of tubular profiles. It was observed that there was a slight load increase rising number of the bridges because the bigger friction opposition to the flow, which got unbalanced. Moreover, if the holes section was bigger then also the pressure inside the welding chamber was higher and the charge weld was anticipated resulting in a minor amount of discarded profile. On the other hand, if the holes were flat, the load peak was related to total bridges surface and friction.

In this thesis the material flow and the contact pressure inside the welding chamber were analyzed considering a porthole die with a big number of feeders, in particular three, not symmetrically disposed. A numerical campaign was performed to analyze the influence of the complex porthole die with three bridges on the material flow inside the welding chamber in which three seam welds were visible. All the feeders had the same shape and volume, but they were not equidistant from one another;

more in detail, each distance was double than the other (Fig.s 3.1-3.2). This means that the bridges were characterized by different widths. The software utilized to run numerical simulations in steady state conditions was Altair HyperXtrude. The material investigated was AA6063 aluminum alloy, the temperature of the matrix was 460 °C, the billet temperature 540 °C, while 10 mm/s was set as ram speed. The model and the boundary conditions were the same of the work of Gagliardi et al. [114] and they are shown in the following Figure 3.1. The boundary conditions for the profile were heat exchange with environment and an outflow free surface.
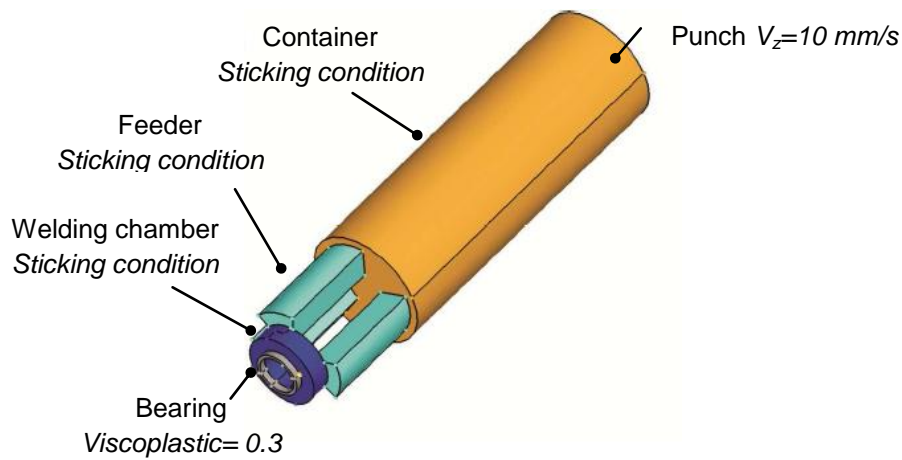
Figure 3.1. Model utilized in HyperXtrude®, [114]

Obviously, the material flow was more distorted between the furthest feeders, therefore behind the widest bridge. Concerning the profile quality linked to the quality of the seam welds, the considered output variable was the pressure on the welding plane, or the average stress on the same plane [115], inside the welding chamber. The numerical results shown that from the punch to the top of the welding chamber, pressure and mean stress values gradually decrease due to the friction forces, which feed the shear components, reaching, at the entry of the welding chamber, homogeneous values because the material flow was almost the same in each feeder (Fig 3.2).
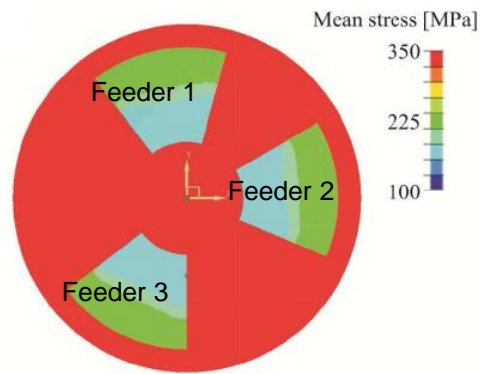
Figure 3.2. Average stress distribution at the entrance of the porthole section, [114]

Proceeding through the bottom welding chamber until the die exit, the contact pressure and mean stress increase reaching their highest value, as shown in Figures 3.3 and 3.4, respectively, between the closest feeders because the minor distortion of the material flows in a smaller welding chamber region.
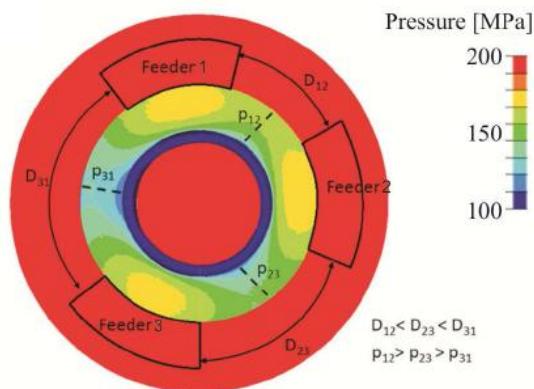
Figure 3.3. Pressure distribution inside the welding chamber, [114]
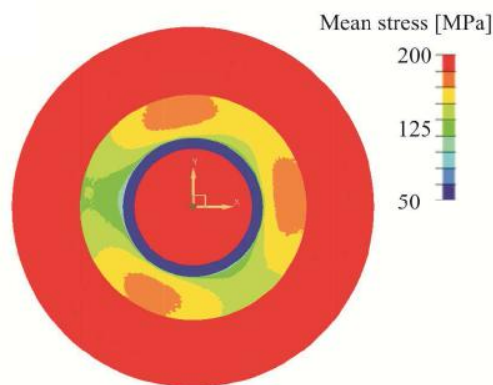
Figure 3.4. Average stress distribution at the bottom of the welding chamber, [114]

The reason for that is exactly due to the small bridge wide, therefore to the smaller volume to fill inside the welding chamber, and to the lower resistance and friction opposition by welding chamber walls to the flows movement. Considering the work of Gagliardi at al. [114], a tapered shape of the bridge at the entrance of the welding chamber could be helpful to reduce the distortion of the material flows that better weld together.

Afterwards, an experimental campaign was planned in order to analyze the pressure and temperature conditions inside the welding chamber considering this kind of matrix and verify the numerical results reliability. The details about the experimental tests are described in the following paragraph.

3.2. RELATIONSHIP BETWEEN PROCESS CONDITIONS AND SEAM WELD WIDTH IN EXTRUDED SHAPE THROUGH A PORTHOLE DIE WITH CUSTOMIZED GEOMETRY

To complete the previous work and to extend the above considerations to the general case, an experimental campaign and a new numerical investigation were performed. Taking into account the same die design, different were the input parameters changed in order to analyze the quality of the seam welds into the profiles related to the material pressure and temperature inside the welding chamber. More in detail, those parameters were the ram speed, the extrusion ratio and the bridges sizes, while the quality of the seam welds was evaluated experimentally by means of their width, checked by visual observation, and numerically by means of pressure and temperature conditions reached during the process. Ram speed because the influence on the productivity, while extrusion ratio because the necessity to reduce products section and weight.

3.2.1 Experimental campaign

A porthole die with three bridges of different shape and volume, but with both top and bottom flat surfaces, was built in reduced scale (Fig. 3.5) and assembled on a four pillars electro-hydraulic MTS/Instron 1276 machine with a load capability of 1000 KN. The investigation was carried out into the Laboratory of the Department of Mechanical, Energy and Management Engineering at University of Calabria.

Medium bridge MB,
67.5 °

Small bridge SB,
45 °

Large bridge LB,
90 °

Figure 3.5. Porthole die with different bridges

A hollow tube profile was extruded with several ram speed and extrusion ratio configurations. The billet material was AA6060 aluminum alloy with a pre heated temperature of 470 °C, whereas the temperature of the matrix was 450 °C. The thickness of the profile was 2-3 mm, with a constant inner diameter, and with an extrusion ratio of 6 and 3.5, respectively; while, the ram speed was set as 1-5-10 mm/s. More in detail, the attention was focused on the influence that both porthole die design and extrusion process parameters had on the three seam welding lines (Fig. 3.6), in particular, on the lines width in the middle of the thickness (Fig. 3.7).
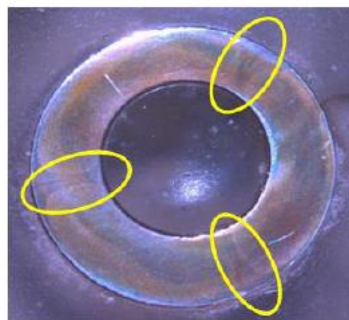
Figure 3.6. Extruded tube cross section with three seam welds and several charge welds

The last one was analyzed by means of visual observation, known that if the welding line visibility is lower, then the solid bonding is better [116]. At the end of each ram stroke, the extruded profiles were cut and the specimens quenched in cold water in order to avoid potential static recrystallization.
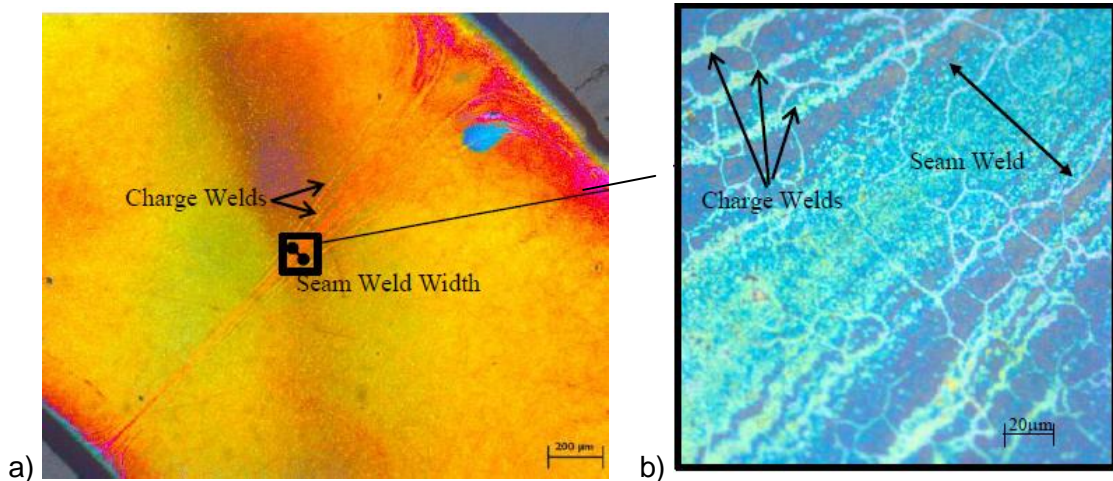
Figure 3.7. Visible welding line after etching with Weck's reagent after the fourth extruded billet

The specimens were then mounted using thermosetting resins, grounded and polished. The technique, which was utilized to highlight the grain boundaries, was based on colorful etchants developed by Weck [117]. The analyses of the grain distribution, carried out using a polarized light microscope, highlighted the presence of charge and seam welds as shown in Figures 3.7a-b, the first ones due to billet to billet extrusion process. As expected, the two kinds of welds had different microstructure [10]. The attention was focused on the seam welds; more in detail, the width of the welding lines was measured in the middle of the tube wall (Fig. 3.7a).

As already known the quality of the seam weld is related to its visibility; less evident is the welding and better is its quality [116]. In this case, the smallest width, 20 µm, was observed with high extrusion ratio (Fig. 3.8), as well as for all ram speeds between 1 and 5 mm/s, regardless of the bridges width. Instead, for higher values of ram speed, the welding line width increased from 40 µm to 60 µm, from small width of the bridge to the large one.
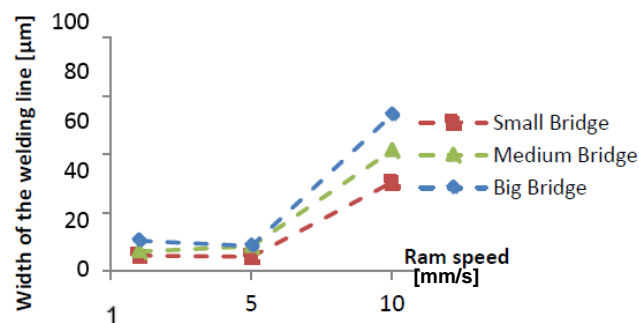
Figure 3.8. Welding line width for tube wall of 2 mm

For a lower extrusion ratio (Fig. 3.9), all results were comparable considering the ram speeds, and the welding lines were significantly wider than the higher extrusion ratio results (Fig. 3.10). Considering the lower extrusion ratio there were small differences only considering the bridges width: narrow seam weld lines corresponded to smaller bridges and wide weld lines corresponded to bigger bridges, as in the case of high extrusion ratio and high speed.
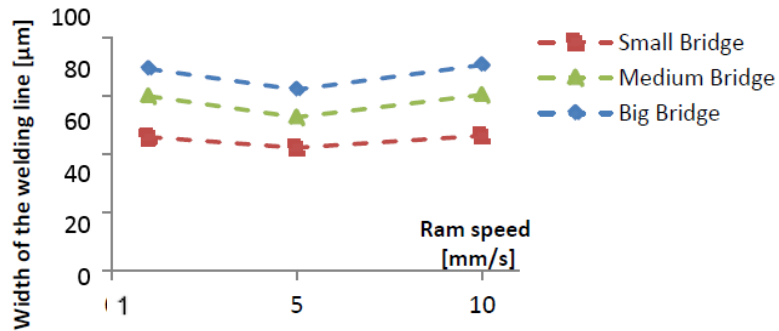
Figure 3.9. Welding line width for tube wall of 3 mm
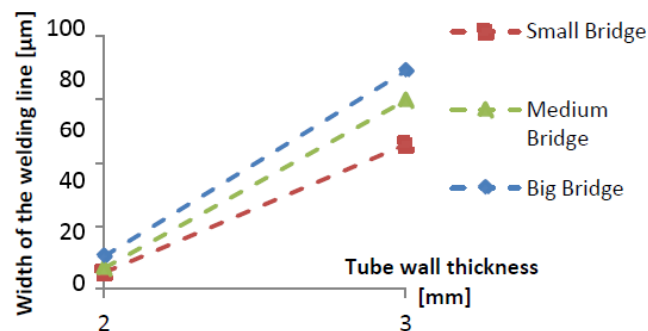
Figure 3.10. Welding line width for different extrusion ratios

However, for both thicknesses of the tubular profile, the influence of the ram speed on the welding line width was not linear. Finally, the parameters that promote longer contact time and higher contact pressure and temperature inside the welding chamber are respectively low ram speeds and high extrusion ratios. In order to confirm what previously said, a numerical campaign was performed.

3.2.2 Numerical investigation

Numerical simulations were conducted to investigate pressure and temperature local values of the material inside the welding chamber close to the bearing land region, as well as the time during which the material flows were in contact in the same chamber. The software used to run the numerical simulations in steady state condition, was

again HyperXtrude and the boundary conditions were the experimental ones, as shown in the next Figure 3.11. Ram temperature was set 470 °C, whereas the temperature for container and die was set 450 °C.
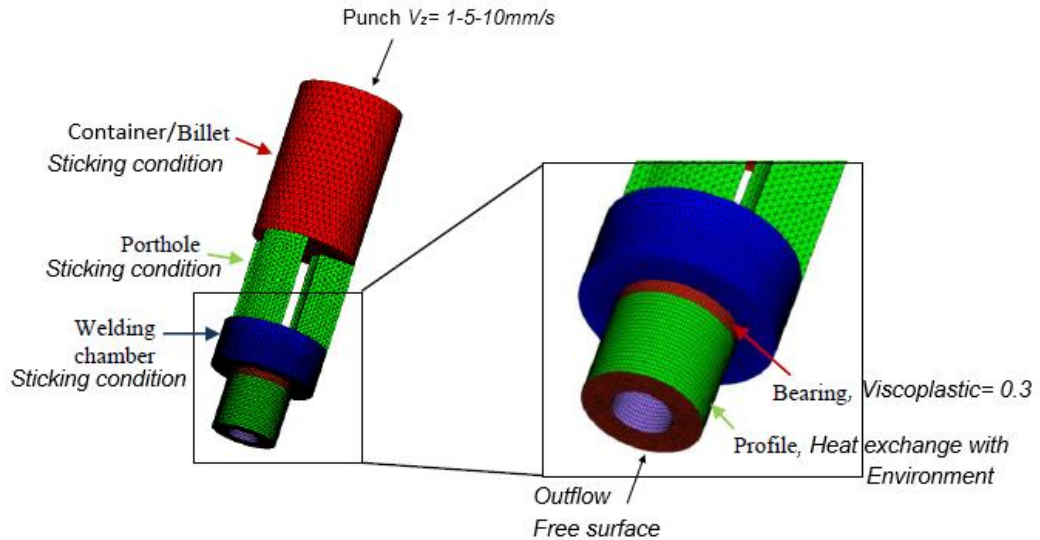
Figure 3.11. FEM model and boundary conditions used for numerical investigation

The input variables were the ram speed and the extrusion ratio related to the profile thickness. Numerical outcomes regarding the temperature and pressure conditions inside the welding chamber (Fig.s 3.12-3.13) were analyzed. It was possible to see that increasing the ram speed and maintaining a constant extrusion ratio, there was a significant increase of temperature (almost 100 °C) due to the reduced time contact between the billet and the container so that the hotter billet had not enough time to transfer heat to the cooler container (Fig. 3.12). Instead, considering the same inputs, the contact pressure slightly decreased (almost 30 MPa) (Fig. 3.13) because the material flow strength decreased due to temperature increase. This phenomenon was dominant over the increase of the yield strength (flow stress) value due to deformation at the higher strain rate. Maximum pressure and temperature conditions were behind the smaller bridge width because low was the flow distortion and friction opposition and short was the time for thermal transfer, respectively.
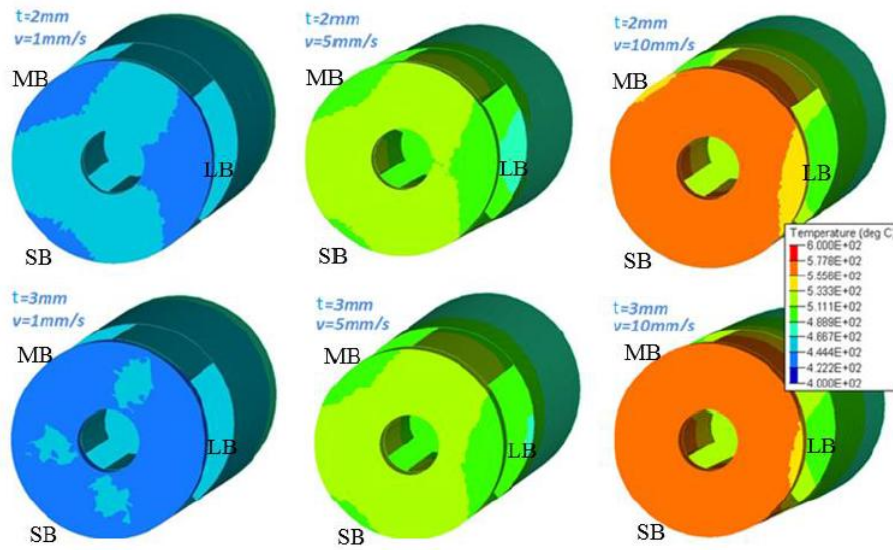
Figure 3.12. Numerical predicted temperature distribution within the welding chamber close to the bearing land for each analyzed case
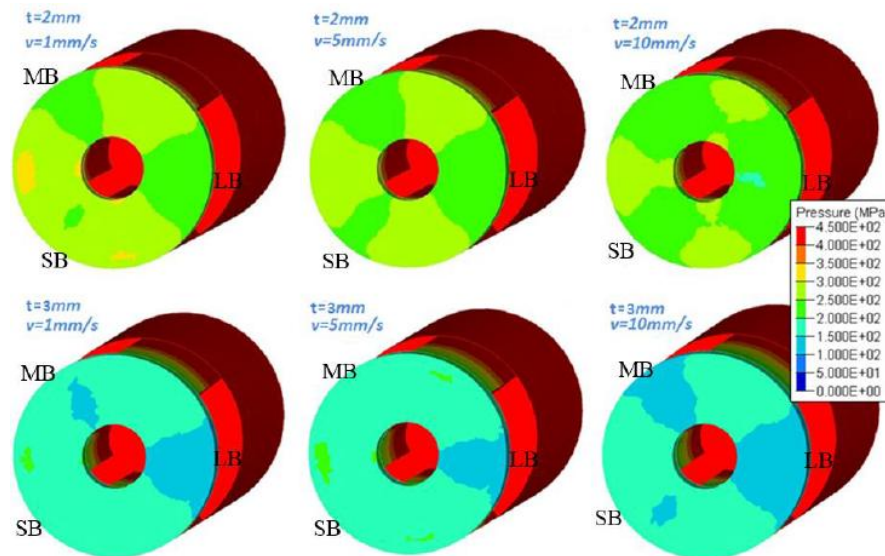
Figure 3.13. Numerical pressure distribution within the welding chamber close to the bearing land for each analyzed case

On the other hand, decreasing the extrusion ratio and maintaining a constant ram speed, there was a constant temperature inside the welding chamber and a huge contact pressure drop (almost 100 MPa), (Fig.s 3.14a-b). Also in this case, the maximum temperature and pressure values were behind the bridge with smaller volume because the same reasons of before.
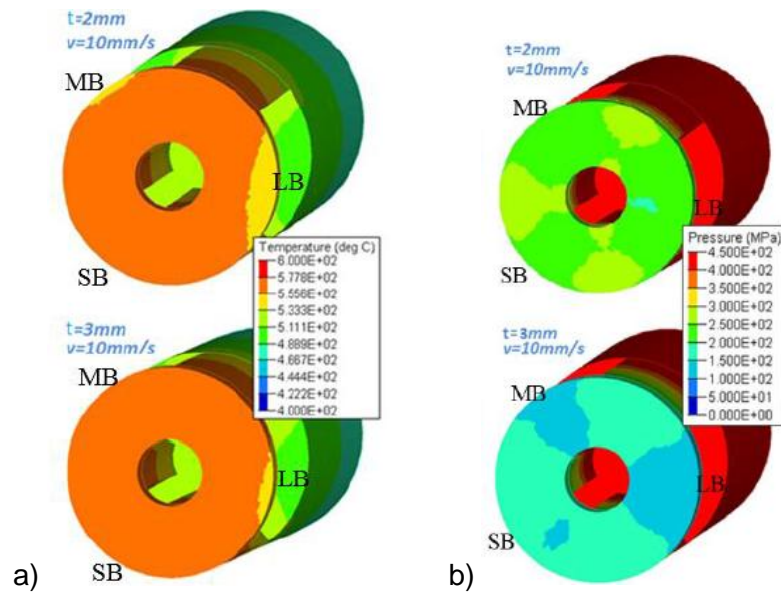
Figure 3.14. Numerical a) temperature and b) pressure distribution within the welding chamber close to the bearing land in case of v=10 mm/s

The variation in the width of welding lines observed in the experimental investigations was better understood with the support of numerical simulation analysis. In fact, thinner welding lines were obtained for the tube with the wall thickness of 2 mm due to the higher pressure within the welding chamber. The extrusion ratio is therefore a fundamental process parameter influencing the integrity of the seam welds. However, the effect of the extrusion ratio was less significant if the extrusion was carried out at high ram speeds. This was mainly explained by the fact that, for the higher extrusion ratio, the profile exit speed increased and therefore lowering the contact time within the welding chamber. It is important to point out that the influence of the ram speed on the welding line width was not linear. The width of the seam weld suddenly increased after increasing ram speed above 5 mm/s if proper process conditions with suitable pressure were considered. While ram speed was changed from 1 mm/s to 5 mm/s a slight decrement of the line width was observed due to the temperature growth and lowering of the yield strength of the material. However, a minimum contact time is always required in order to avoid any potential profile weakening due to poor quality of welds. Finally, the improvement in weld quality attributed to the bridge size reduction was quite complex. That could be accredited to the pressure increase, which was derived from simpler material flow and its lower distortion under the small bridge.

3.2.3 Conclusions about experimental and numerical outcomes comparison

Finally, numerical and experimental results could be related. Narrow seam welding lines, therefore better profile quality, are obtained with high extrusion ratios because the higher pressure on the welding plane, with not so high speeds and independently of the bridges volume. The effect of the extrusion ratio is less important if the extrusion is performed at high speed, because the contact time between the split flows into the welding chamber is reduced as consequence, generating a seam weld that has not a good quality and has a larger width, because the temperature rise and the material yield strength reduction. Moreover, the pressure increases behind the thinner bridge shape because the minor material flow distortion and friction opposition to the flow. In the last case the welding line is slimmer.

Extrusion ratio and ram speed influence the working conditions significantly but their individual change cannot be easily linked to immediate dimensional changes of the welding line. Additionally, the reduction of the bridge width allows the improvement of the welding conditions while other process parameters are kept constant and this determines for the carried out analyses a substantial reduction of the welding line width. Finally, while proper pressure and temperature conditions are guaranteed, a critical contact time can be identified. If the material leaves the welding chamber in shorter time, the seam weld width is more relevant.

3.3 INFLUENCE OF THE PROCESS SETUP ON THE MICROSTRUCTURE AND MECHANICAL PROPERTIES EVOLUTION IN PORTHOLE DIE EXTRUSION

The influence of the same variables of the above work (profile thickness [118] and ram speed [66]) on the temperature and pressure conditions inside the welding chamber was numerically analyzed, as deepening of Donati's work [28], and an experimental campaign was added to that. Moreover, microstructure evolution and mechanical characteristics were also investigated. Profile thickness was modified in order to maintain a constant extrusion ratio, (10.3÷13.8); instead, ram speed, which influences the strain rate, was varied in order to increase the productivity. A simple porthole die with two symmetric ports or feeders was considered in order to avoid any influence on the material flow and to have only one seam weld to analyze. Moreover, a profile with "I" cross section was taken into account because the extrusion ratio

could be maintained constant also changing the central tongue thickness. The bearing orifice was located in order to get an extruded profile with a seam weld line in the middle of its section, perpendicular to the central tongue and suitable for mechanical testing. The material taken into account was AA6060 aluminum alloy.

3.3.1 Experimental campaign

The investigated profile cross section had a variable central tong thickness with values a=0.5-1-2 mm, as shown in Figure 3.15.
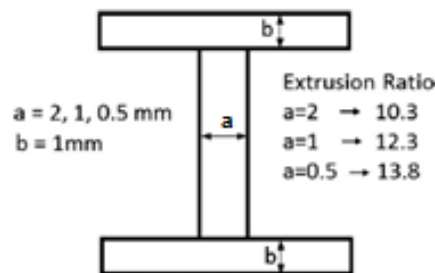
Figure 3.15. Extruded profile cross section

As already known, the material streams faster in the thick profile section and in the center of the die than in the other regions. In this case study the material flow could be distorted because the geometry changes, so a numerical optimization was performed for the optimal die design corresponding to each configuration of central tongue thickness. More in detail, the bearing land had different local lengths in order to get a homogeneous flow distribution. Subsequently, dies were built in modular way in order to substitute only the bearing module during the experimental campaign, using the same porthole die (Fig. 3.16).
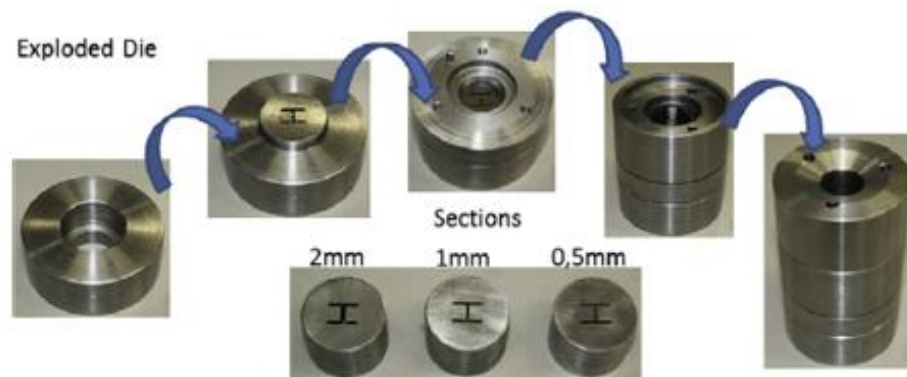
Figure 3.16. Exploded die used during the experimental campaign

The extrusion equipment (Fig. 3.17) was assembled on a four pillars electro-hydraulic MTS/Instron 1276 machine with a load capability of 1000 KN, and the tests were conducted into the Laboratory of the Department of Mechanical, Energy and Management Engineering at University of Calabria. The temperature of the die was 450 °C, the billet temperature was 500 °C; while at the end of the process the profile was cooled at room temperature.

Figure 3.17. Equipment used during the experimental campaign

The values for the ram speed were 1-5-10 mm/s. After extrusion process, specimens cut from the profiles were analyzed by both microstructural investigation and tensile tests, in order to compare the results corresponding to the grain size with weld and profile strength [98].

3.3.2 Microstructural investigation

For microstructural investigation, parts of extruded profiles were cut orthogonally to the extrusion direction in order to analyze grains evolution into the profile cross section, especially close to the seam weld. After grinding, polishing, and etching phases, the grains distribution was observed by polarized light microscope. The Figure 3.18 shows that the grain dimensions increased (50 µm) for reduced profile thickness and for high extrusion speed, because more energy was supplied during the process. More in detail, there was deformation energy due to the thinner thickness of the central tongue, and thermal energy due to the high ram speed that reduced the contact time between the material and the container, as well as between the material and the die, reducing also the exchanged heat. In that case, the profile at the exit had high energy that it gave way to the external environment, generating static recrystallization at the end of the process, further the dynamic recrystallization during it [18], because no quenched treatment was applied. Consequently, grains size grew because the energy lost during the static recrystallization.
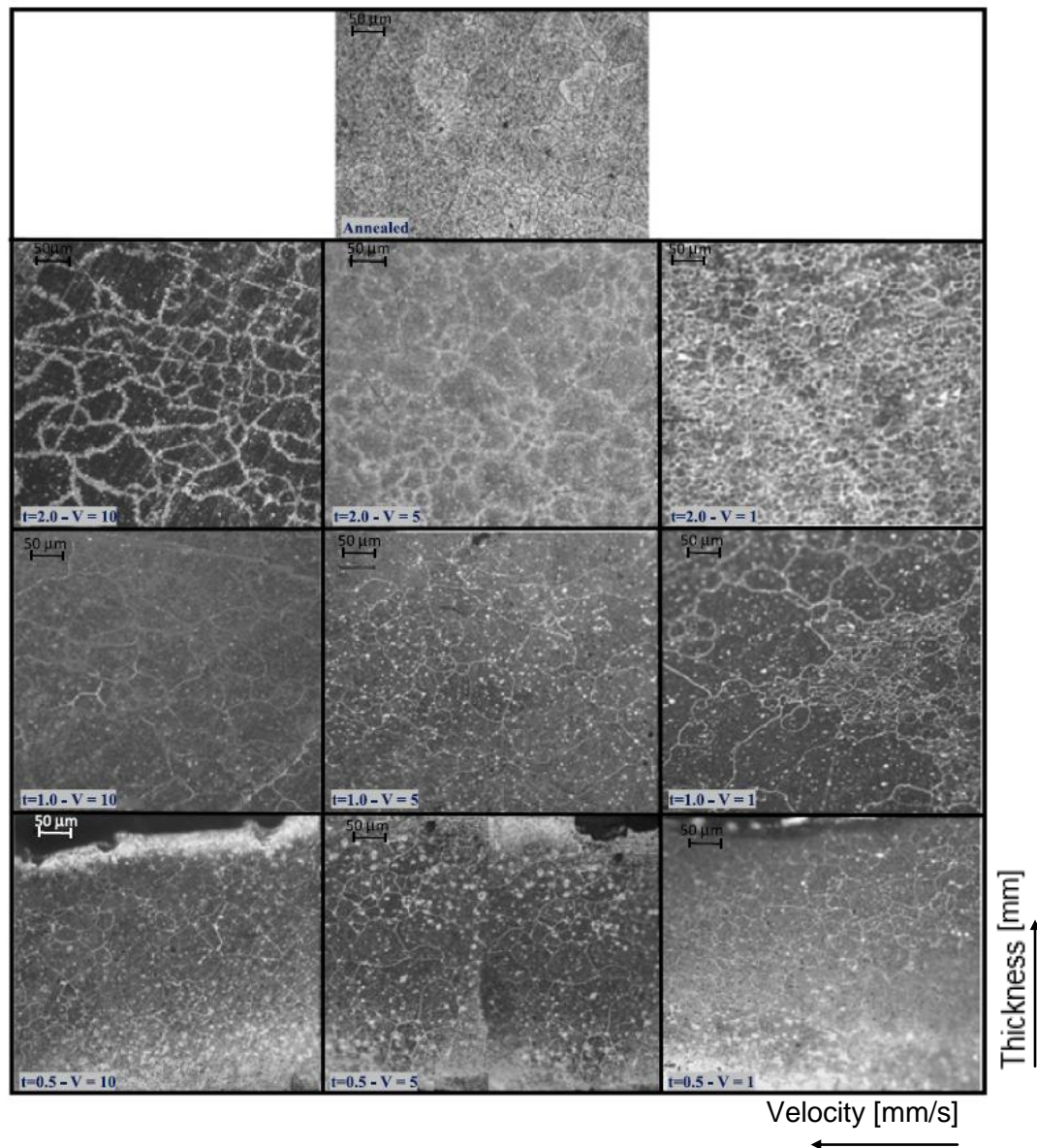
Figure 3.18. Microstructural evolution due to the changes of profile thickness, t [mm], and process velocity, V [mm/s]

Finer grains distribution (10 µm) was gained with a thickness of the central tongue of 2 mm and a ram speed of 1 mm/s (Fig. 3.18), due to the lower energy supplied during the extrusion. In fact, less was the deformation energy, due to a lower extrusion ratio, as well as the thermal energy, because the long contact time between the material and the matrix for thermal exchange. For that reason, the static recrystallization was avoided, and small grains were visible on the profile cross section, subsequently to the dynamic recrystallization during the process.

Therefore, the observed microstructural variations depended of the different working conditions, which the material was subjected at. More in detail, if the ram speed

increased, going from 1 to 10 mm/s, the material temperature inside the welding chamber and in the bearing zone raised due to two phenomena: less interaction time with the dies (reduced cooling) and greater deformation work, since aluminum alloy is characterized by a higher strength when strain rates increase. Consequently, the extruded profiles, cooled down at room temperature, suffered different static recrystallization; this grain evolution can be considered as a post-deformation phase with a growth, which is bound to the stored forming energy. Taking into account also the extruded geometry, the variation of the middle tongue from thicker (t=2 mm) to thinner (t=0.5 mm/s) thicknesses shown that also profile geometry influenced the material deformation, shear forces and resulting temperature variation. Moreover, if the flow section was changed, dynamic recrystallization resulted to have a different impact on the grain size distribution in the profiles at the exit of the die. According to the above observations and considering the obtained results, it was possible to say that the grains dimension gradually increases with the increment of the punch speed due to higher temperatures and thermal energy, which encourage the recrystallization post-deformation. This result is more evident for smaller thicknesses because narrow flows promote the conditions for grains growth due to stored deformation energy lost after the process if no one treatment is performed to freeze the microstructure. More in particular, the average grain size for the finest distribution resulted to be lower than 10 μm; this was observed for the configuration where less energy was supplied to the process (bigger thickness, t=2 mm, and lower ram speed, V=1 mm/s). The grain size distribution gradually grew exceeding the average of 50 μm for higher energy configurations, which were obtained reducing the profile thickness and increasing the punch velocity.

3.3.3 Tensile tests properties

Tensile tests were performed on other specimens cut from the same profiles with a MTS/Instron testing machine, with a load capacity of 5 KN (Fig. 3.19). The specimens were designed to fracture them close to the welding line, in the central tongue, in order to point out the weld influence on profile mechanical properties.

Figure 3.19. Tensile tests equipment

Analyzing the results was highlighted that the main strength and strain to failure were achieved with a tongue thickness of 1 mm, independently from the ram speed value (Fig.s 3.20-3.21). On the other hand, the worst conditions were obtained with the thinnest tongue.
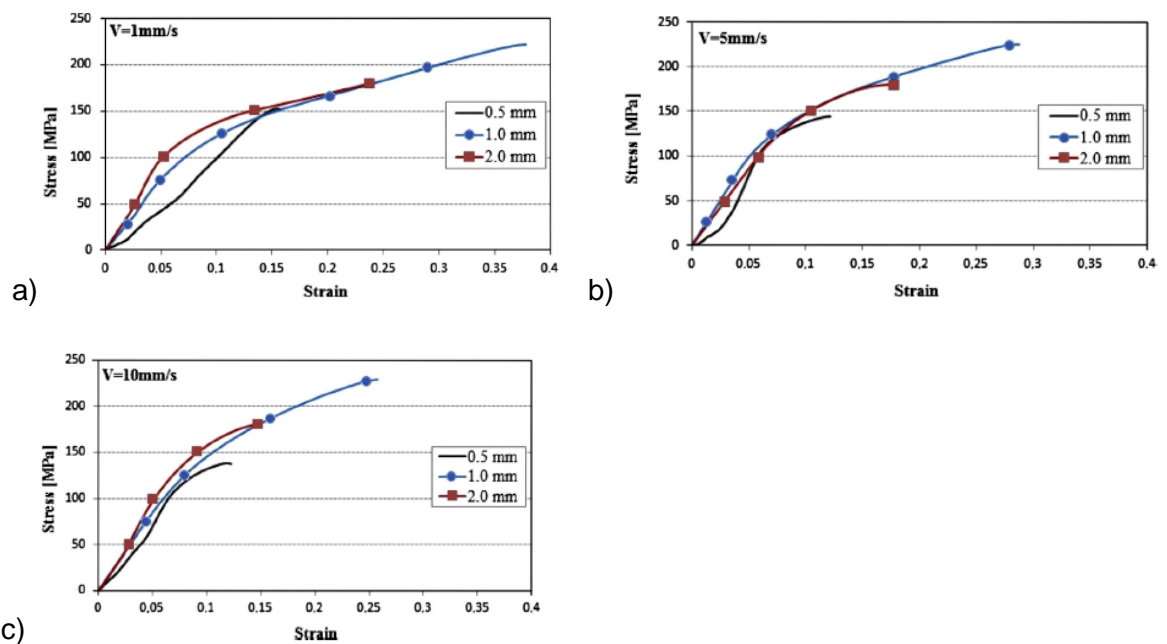
Figure 3.20. Stress-strain curves for the three analyzed thicknesses for different ram speeds: a) 1 mm/s; b) 5 mm/s; c) 10 mm/s, respectively
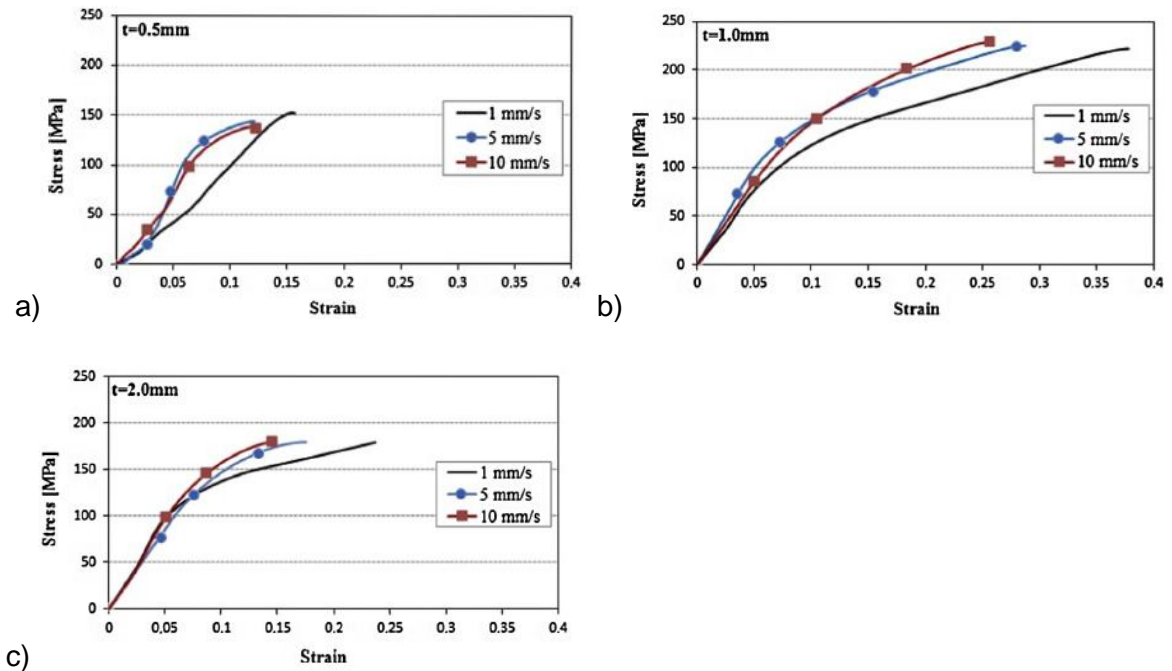
Figure 3.21. Stress-strain curves for the three analyzed ram speeds for different profile thicknesses: a) 0.5 mm; b) 1 mm; c) 2 mm, respectively

The results about the value of strength and strain to failure for each configuration are summarized in Table 3.1.

t [mm]	0.5	0.5	0.5	1	1	1	2	2	2
V [mm/s]	1	5	10	1	5	10	1	5	10
Strength [MPa]	151.44	144.14	137.75	221.94	224.84	229.39	179.67	179.77	180.26
Strain to failure	0.1589	0.1214	0.1222	0.3778	0.2861	0.2575	0.2370	0.1755	0.1453

Table 3.1. Strength and strain to failure after the tensile tests for each investigated configuration

The ram speed did not influence the ultimate tensile strength, whereas if the ram speed increased the strain to failure decreased. With lower speed, the quality of the seam weld is better because the contact time between the material flows inside the welding chamber is higher.

Therefore, the best trends were represented by the configurations with the tongue thickness of 1 mm for each investigated ram speed; this can be explained considering that the narrower sections (0.5 mm) bring to excessive grain growth while

the larger ones cannot generate suitable conditions for a very good material joining. The relevance of the welding line quality on the obtained results can be clearly understood analyzing Figure 3.21 where, for same tongue thickness, the achievable strength was almost the same for different process velocities while the maximum strain to failure gradually increased for reduced extrusion ram speeds. This evidence is clearly due to an improvement of the welding line, which can be justified by the higher contact time between the material streams inside the welding chamber if slower processes are carried out. The above considerations are supported whereas contact time and pressure are the main variables, which have to be taken into account for the numerical evaluation of the welding line quality.

3.3.4 Comparison between microstructural observations and tensile tests outcomes

Because the mismatch between the outcomes regarding the extruded profiles microstructure related to the profile mechanical properties, and the highest strength and strain to failure values linked to a good weld quality, a monotonic trend coherent with only energetic considerations cannot be identified. In fact, if a lower energy is suitable for the grain dimension, it is not possible to forget the quality of the welding line which is related to the internal pressure. This point has to be deeply investigated because the tensile tests were set for allowing the specimen breaks precisely on the welding plane. Therefore, even if small grains are desired for the improvement of the profile mechanical properties [119]; this evidence seems to be not related to the seam weld effectiveness. The results, therefore, have to be analyzed including the effect that the quality of the welding lines gives to the stress–strain curves. Numerical analyses provided a valuable support predicting the pressure distribution inside the welding chamber for different working conditions.

3.3.5 Numerical investigation and correlations with experimental outcomes

Because the final different considerations about the microstructural and tensile tests analysis, a numerical campaign was carried out to get more information about the pressure and temperature conditions inside the welding chamber from which depends the quality of the material streams joining phase. The numerical software used to get information about the only stress and strain distributions was Altair

HyperXtrude [120], with Eulerian formulation, whose meshed model is shown in Figure 3.22, with the imposed boundary conditions.
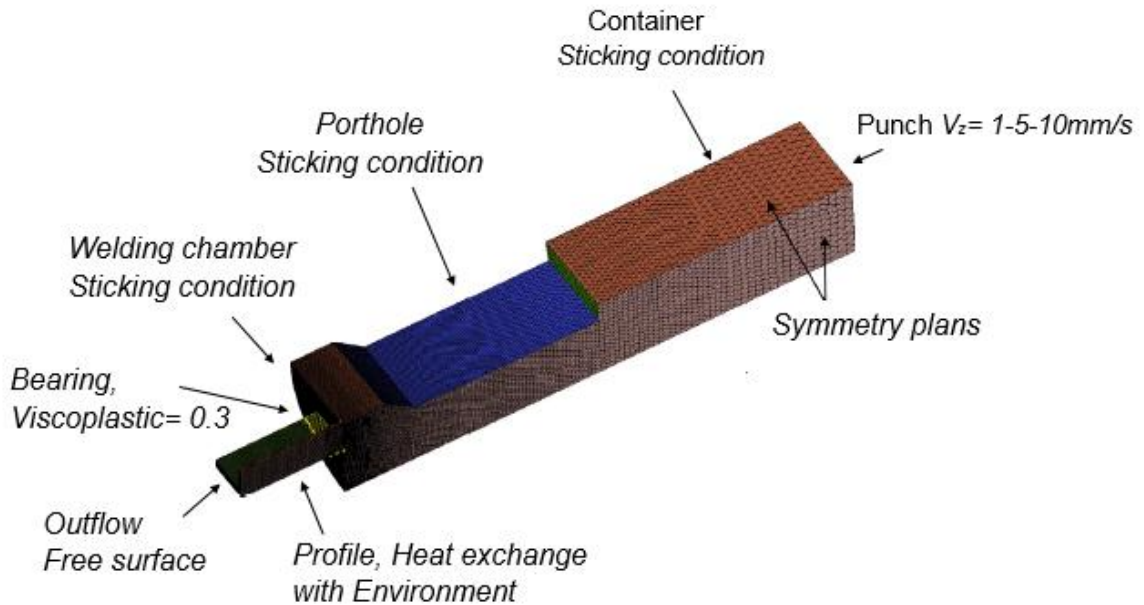
Figure 3.22. Meshed model in HyperXtrude®

The numerical results showed pressure and temperature distribution changing the thickness of the central tongue and the ram speed, as in the experimental campaign. The pressure on the welding surface into the welding chamber depended of profile cross section: it had a value of 70 MPa if that section had a thick central tongue and a value of 150 MPa if the thickness of that tongue was thinner (Fig. 3.23). This was due to the higher resistant that the small cross section of the bearing land opposed to the material flow. Because the ram speed did not influence the welding pressure, than it is possible to use a high speed in combination with a small thickness to increase the productivity, manufacturing competitive products.
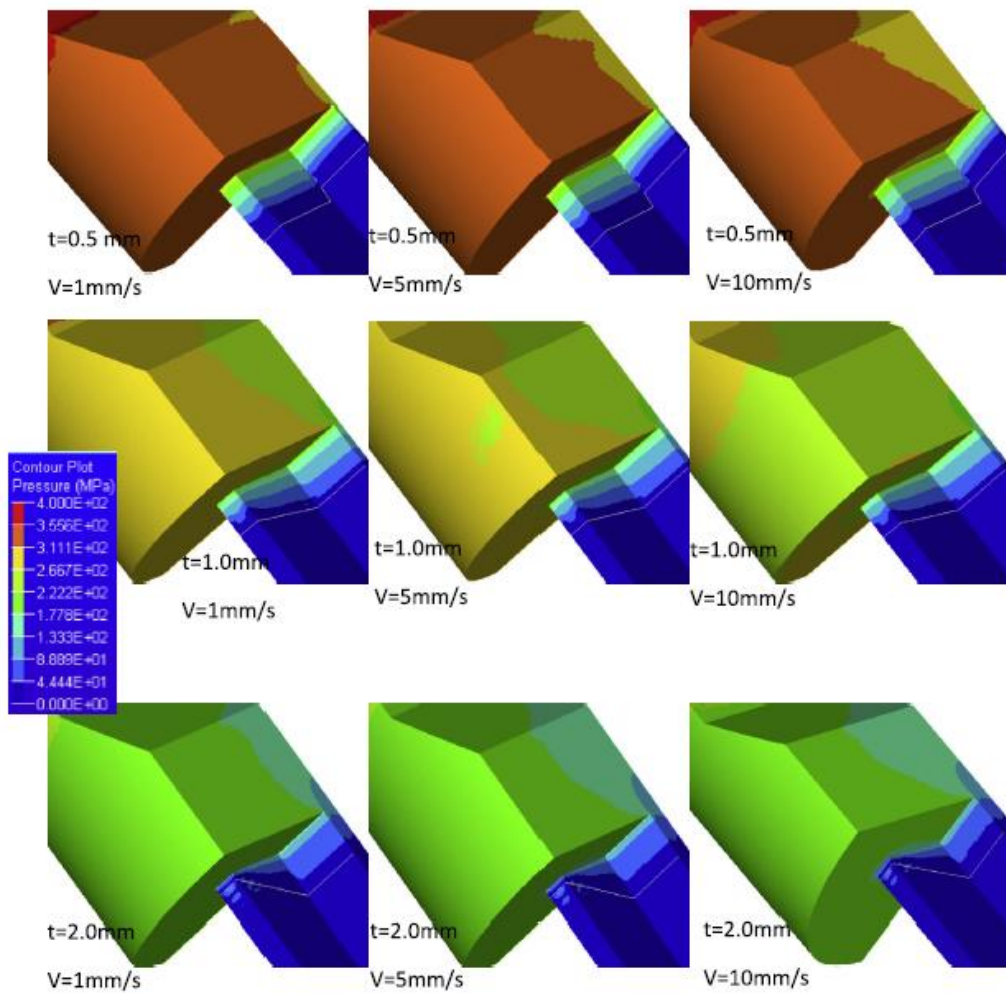
Figure 3.23. Pressure distribution inside the welding chamber and the bearing area for each analyzed case

Despite the temperature was more influenced by the extrusion speed than the profile geometry (Fig. 3.24). In fact, the material temperature increased raising the ram speed because the material had not enough time to exchange heat with the cooler container. Moreover, the temperature increased, although less, reducing the profile thickness because the plastic deformation at the bearing entrance [66].
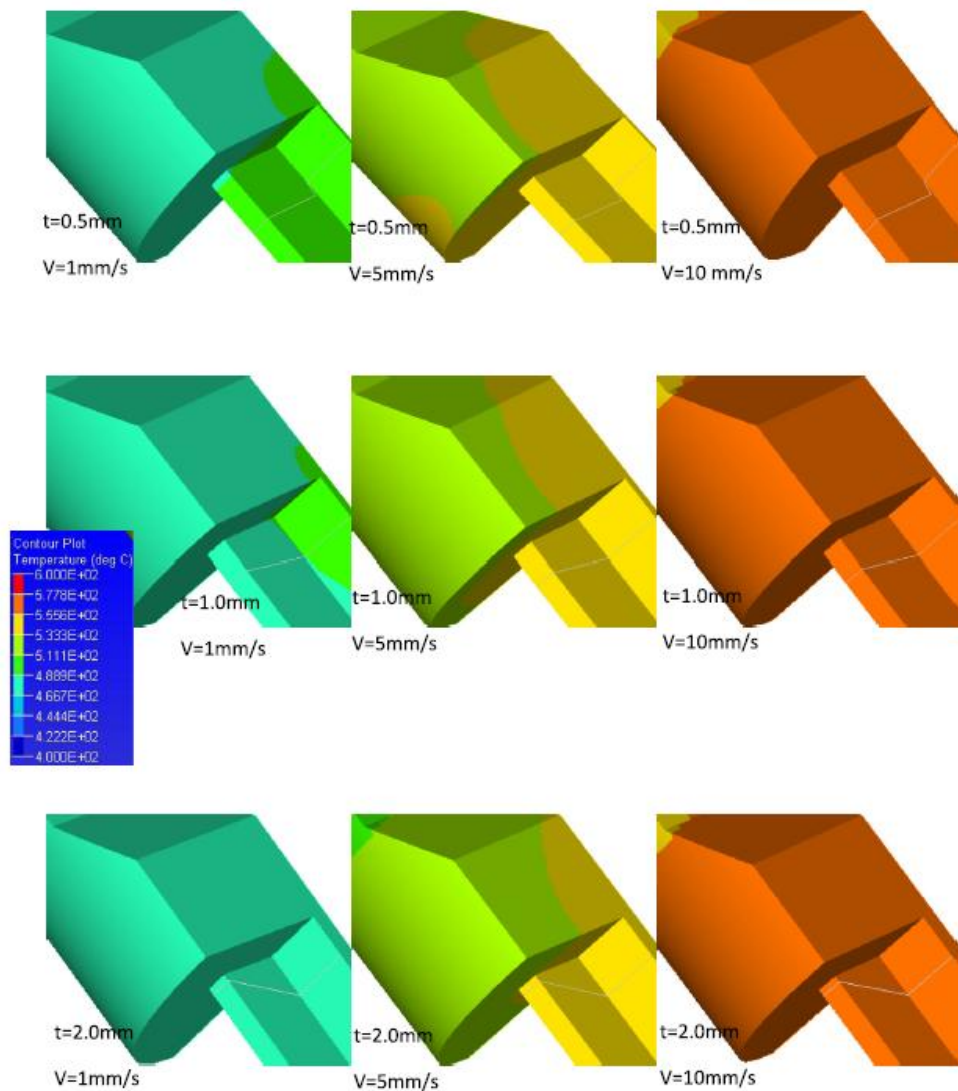
Figure 3.24. Temperature distribution inside the welding chamber and the bearing area for each analyzed case

As seen, the numerical outcomes confirm that obtained by tensile tests.

3.3.6 Conclusions

It is not correct to analyze the only microstructure of the profile, depending of the deformation and thermic energy accumulated during the process, or the only results about tensile tests to draw conclusions about the profile strength and the quality of the seam weld. In fact, a lower energy produces profiles characterized by a microstructure with small grains but with a poor weld quality because the low welding pressure. Moreover, the ram speed, and then the profile temperature, must not be too high, otherwise the profile could be affected by surface defects, cracks and coarse grain growth. The increasing of the ram speed, whose value is important for

the process productivity, has to be properly chosen not just for its impact on superficial defects, but also for the microstructural changing that the increment of material temperature can determine. Instead, the reduction of profile thickness emphasizes the critical issues of the previous results due to higher shear forces in the gate zone. However, the pressure distribution inside the welding chamber increases for narrower sections and, therefore, the critical contact time necessary to reach perfect seam welds is lower. Considering just this last thought, the ram speed could be higher for thinner parts respect to thicker ones. In conclusion, the relationship between extruded profile thickness and ram speed has to be taken into account for a suitable optimization of porthole die extrusion. Cryogenic fluid, immediately downstream of the bearing area, or other cooling systems could be valid solutions to mitigate some encountered drawbacks, increasing the feasibility working area of thin parts extrusion at higher process velocities.

4. INVESTIGATION OF PROFILE PROPERTIES AND DISTORTION IN PORTHOLE DIE EXTRUSION

High productivity and thin and complex profile shapes are a consequence of the process speed increment and the profile thickness reduction, respectively. Increasing the ram speed there is an increase of the temperature that can lead to superficial defects, such as hot shortness. Whereas, reducing the profile thickness there are strain and stress states that can originate ductile fractures such as shear tearing or speed cracking on the external profile surface. In this chapter results about defects growth are shown considering a ductile fracture criterion to highlight the relation between thickness reduction and punch velocity changes with superficial defects in extruded components. Secondarily, the main reasons of profiles distortion are highlighted. More in detail, the material flow distortion and the process load in steady state conditions are analyzed in case of non-symmetric profiles evaluating the most influential geometric parameters. These considerations permit to increment the knowledge of designers and die formers about the design of a die able to minimize the efforts during extrusion process.

4.1 NUMERICAL ANALYSIS ON SURFACE DUCTILE FRACTURES CHANGING PROFILE THICKNESS AND PROCESS SPEED

In this part of the work, a ductile fracture criterion, whose terms are replaced by values determined by numerical campaigns, is used to highlight how the extruded profiles surface quality, so the surface tearing and speed cracking defects occurrence, depends on profile thickness reduction and process speed increase. As known, the extrudate can be affected by defects on the external surface, such as hot shortness, surface tearing and speed cracking, which are generated by specific working conditions [121, 122]. In fact, hot shortness is due to metal heating with temperature that increases above the incipient melting point; surface tearing and speed cracking are generated by local tensile stresses. The profile thickness reduction is considered because the growing market demand of lighter weight and volume products; the process speed increase has the aim of rising the productivity. More in detail, the shape of the analyzed profile was "I" beam section used also in the previous chapter to investigate the relation between process setup and extrudate microstructural and mechanical properties.

4.1.1 Ductile criterion for damage analysis

Lou et al. [123] developed a ductile fracture criterion by taking into account damage accumulation due to nucleation, growth and shear coalescence of voids. More in detail, the void nucleation was considered proportional to the equivalent plastic strain $\bar{\varepsilon}_f$, the void growth was represented as a function of the stress triaxiality ($\varphi = \frac{(\sigma_2 + \sigma_1 + \sigma_3)/3}{(\sigma_{eq\,Von\,Mises})}$) and shear coalescence of voids (related to Lode parameter equal to $L = \frac{(2\sigma_2 - \sigma_1 - \sigma_3)}{(\sigma_1 - \sigma_3)} = \sqrt{(\frac{\bar{\sigma}}{\tau_{max}})^2 - 3}$) was described by the normalized maximum shear stress, τ_{max}. This theory can be discretized by the following equation [124]:

$$(\frac{2\tau_{max}}{\bar{\sigma}})^{C_1}(\frac{\langle 1+3\varphi\rangle}{2})^{C_2}\bar{\varepsilon}_f = C_3 \qquad \langle x\rangle = \begin{bmatrix} x\;when\;x \geq 0 \\ 0\;when\;x < 0 \end{bmatrix} \qquad \text{(Eq. 4.1)}$$

where $\bar{\sigma}$ is the equivalent stress, C_1, C_2 and C_3 are positive constants which depend on the worked material. This equation can be modified introducing the Lode parameter (L) [125] and it can be rewritten as:

$$(\frac{2}{\sqrt{L^2+3}})^{C_1}(\frac{\langle 1+3\varphi\rangle}{2})^{C_2}\bar{\varepsilon}_f = C_3 \qquad \langle x\rangle = \begin{bmatrix} x\;when\;x \geq 0 \\ 0\;when\;x < 0 \end{bmatrix} \qquad \text{(Eq. 4.2)}$$

Analyzing the last one, it is possible to state that the equivalent plastic strain monotonically decreases if triaxiality increases; this can be explained because higher triaxiality encourages the void growth reducing the material ductility. On the other hand, the equivalent strain can reach a minimum value for L= 0 [124], while it symmetrically increases moving away in both positive and negative *L* values. Moreover, has to be highlighted that if *stress triaxiality* has a value lower than -1/3, theoretically, no ductile fracture happens [123].

4.1.2 Numerical campaign

Taking into account the ductile criterion, a numerical investigation was carried. More in detail, *effective strain* is the principal variable that was investigated for considering voids nucleation; regarding voids growth, instead, *triaxiality* is monitored. Finally, shear coalescence is analyzed by means of the Lode parameter. The shape and dimensions of the profile are following illustrated (Fig. 4.1); the profile had "I" cross section, as in a work already described in the previous chapter, in order to change the extrusion ratio in a not so marked way varying the central tongue thickness that

could assume three values a=0.5-1-2 mm. Also in this case, the ram speed was a variable of the process and the values investigated were 1-5-10 mm/s.
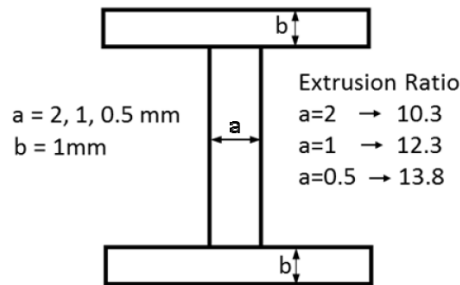
Figure 4.1. Extruded profile cross section

Numerical simulations were performed by means of Altair HyperXtrude® software with Eulerian formulation, and in Figure 4.2 is represented the meshed model with the set boundary conditions.
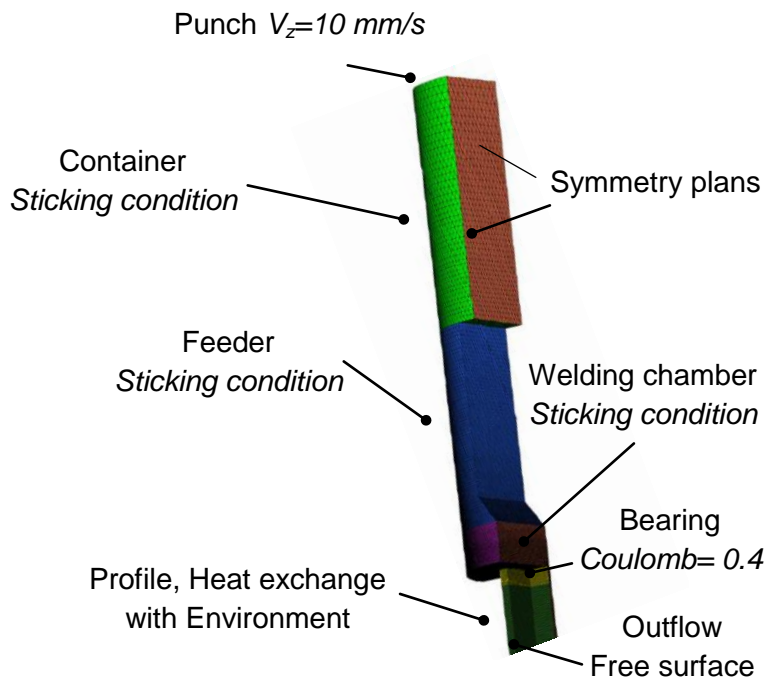
Figure 4.2. Meshed model used in HyperXtrude® with Eulerian formulation with set boundary conditions

The billet, with a diameter of 20 mm and a length of 30 mm, was made up of AA6060 aluminum alloy, and, also in this case, billet and die temperatures were 500 and 450 °C, respectively. The first phase of the numerical campaign aimed at optimizing the bearing shape, taking into account a welding chamber height of 5 mm. In particular, the bearing local lengths were identified in order to get a homogeneous material flow

at the die exit with a constant velocity value on the profile cross section and along the profile length, except the length of the central tongue. The last one was 2 mm constant, for each configuration, so that this geometric variable did not influence the investigated outputs (Fig. 4.3).
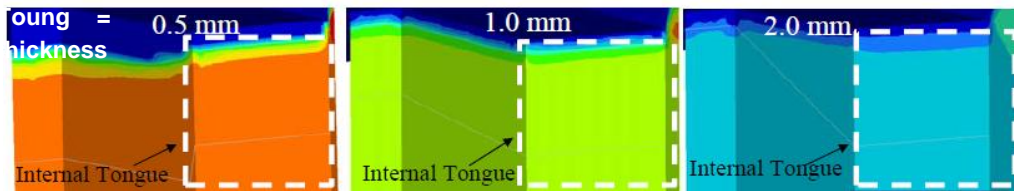
Figure 4.3. Optimized bearing local lengths with the same central tongue length for each configuration, with a punch speed of 1 mm/s

As expected, strain increment, (therefore voids nucleation increment and ductility raising), was observed for the smallest investigated thickness (Fig. 4.4); for that configuration, moreover, the strain increment was slightly influenced by the process velocity, differently from what happened with the other thicknesses where the velocity effect was negligible.
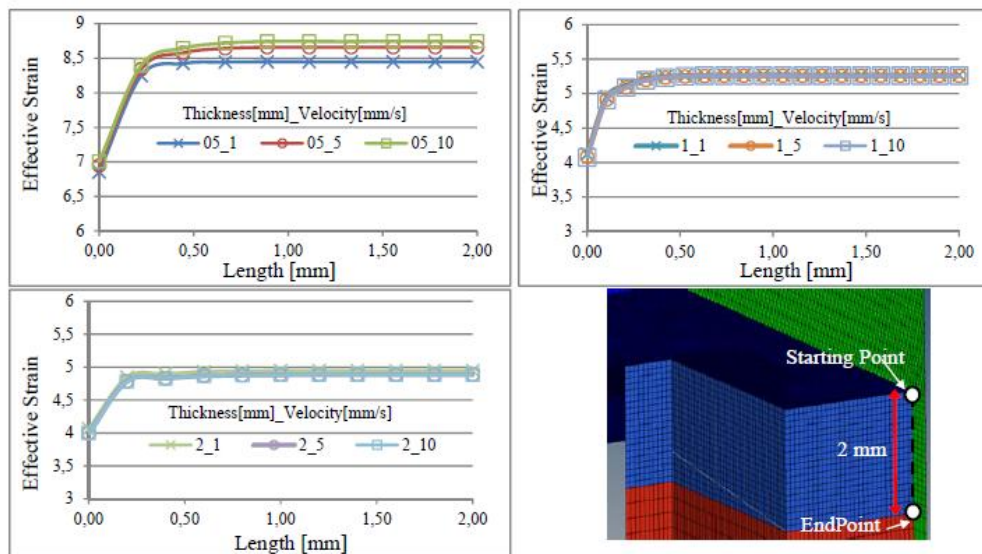
Figure 4.4. Strain distribution in the middle of the external surface in the central tongue for each analyzed configuration

Triaxiality value on the extruded surface was higher than -1/3, for each investigated extrusion condition (Fig. 4.5); this meant that voids growth for those specific working settings could take place. In detail, the trend of the variable did not clearly depend on thickness tongue; however, the small thickness (0.5 mm) brought to triaxiality value higher than zero especially close to the die gate (EndPoint, Fig. 4.5) and, as consequence, thickness reduction facilitated the voids growth. Instead, it was not

affected by the strain rate related to the process speed; which instead affected the temperature increment that can bring to other typologies of surface failure, such as hot shortness.
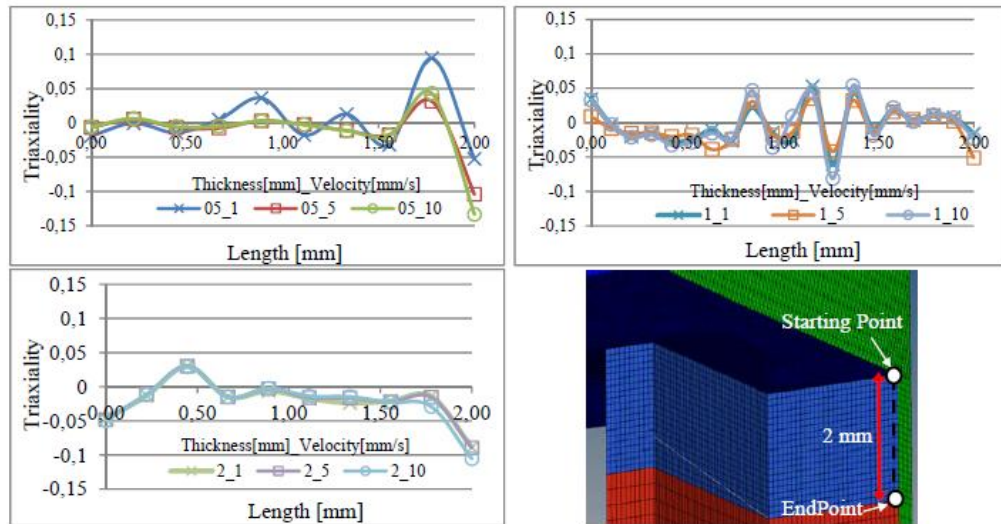
Figure 4.5. Triaxiality in the middle of the external surface in the central tongue for each analyzed configuration

Finally, Lode parameter was the indicator used to evaluate shear coalescence. Conditions which facilitate the voids coalescence result to be for L= 0, as said, and looking the results (Fig. 4.6), the shear coalescence did not influence significantly the fracture on surface with the smallest thickness, because the Lode values were closer to zero especially for bigger thicknesses.
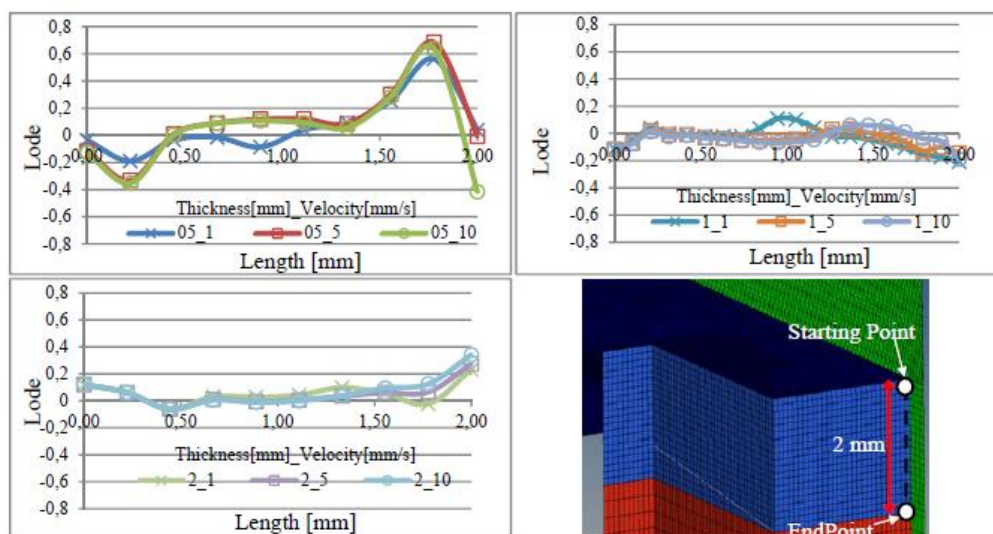
Figure 4.6. Lode parameter in the middle of the external surface in the central tongue for each analyzed configuration

4.1.3 Conclusions

Concluding, the defects due to ductile fractures, which can appear if thinner sections have to be produced, are mainly linked to the strain distribution on the extruded surfaces. Particular strain conditions, in fact, allow the voids nucleation which can grow due to favorable triaxiality; on the contrary, the shear coalescence does not give any considerable contributes to defect propagations if thin profiles are manufactured. Also the process speed, related to the strain rate, is not useful to predict the investigated surface defects, such as surface tearing and speed cracking, but it has to be considered if other typologies of surface failure, such as hot shortness, are taken into account, because its effect on the temperature.

4.2 NUMERICAL ANALYSIS ON SURFACE DUCTILE FRACTURES IN CASE OF A DIE WITH VARIABLE BEARING LENGTH

According with the previous results about strain distribution, a die with a profile characterized by the smallest thickness of middle tongue, 0.5 mm, was used to analyze the influence of different bearing heights, with a constant length along the entire profile in each configuration, on the voids nucleation. A numerical campaign was carried out considering a flat die with the same "I" beam profile, with 0.5 mm constant thickness of central tongue because the most critical case for defects presence. Three different bearing heights, with a constant length along the profile perimeter in each configuration, were analyzed with a value of 0.5-1-2 mm. The strain distribution on the surface is strongly influenced by the bearing height (Fig. 4.7): it decreases with short bearings, because minor friction forces are opposed to the material flow at the interface material/bearing die.
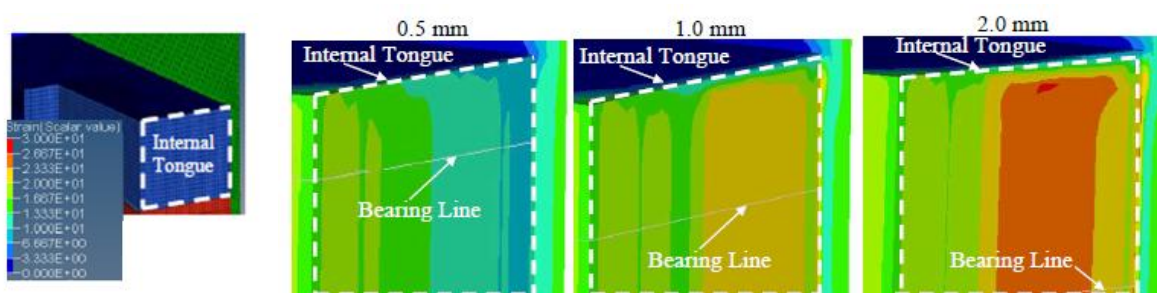
Figure 4.7. Strain distribution for different bearing heights with a constant length along the profile perimeter in each configuration

Concluding, the value of the bearing height affects the strain distribution on the profile surface; therefore, it has to be taken into account regarding the analysis of some defects, such as surface tearing and speed cracking, because its influence on voids nucleation using a ductile fracture criterion.

4.3 INFLUENCE OF BEARING AND POCKET DESIGN ON VELOCITY DISTRIBUTION INSIDE THE PROFILE AT THE DIE EXIT AND ON PROCESS LOAD EXTRUDING NON-SYMMETRIC PROFILES

To manufacture extrudates with good quality, they must be free of defects. The last ones can be surface defects or defects due to distortion inside the profile because inhomogeneous velocity distribution at the die exit. To avoid distortion a right die design has to be identified [48, 66, 68]. In the present work is described a numerical analysis carried out to investigate how some geometric parameters can influence the material flow, the velocity distribution inside the profile and also the extrusion load reached during the process to avoid die wearing and breaking and to reduce press capacity. The considered geometric parameters are bearing local lengths, pocket height and pocket cross section. The profiles had the same shape and properties listed in the previous task making the problem more complex because their asymmetry. A statistical method was subsequently used to analyze the numerical outcomes and to find the optimized die design for manufacturing a profile undistorted in one case and for working with minimum load conditions in another case.

4.3.1 Numerical plan and simulations set up

The study was performed in a numerical way using the finite element code HyperXtrude®, in steady state condition, taking into account the contemporary extrusion of two profiles with non-symmetric "L" cross section, whose location and dimensions are shown in Figure 4.8.
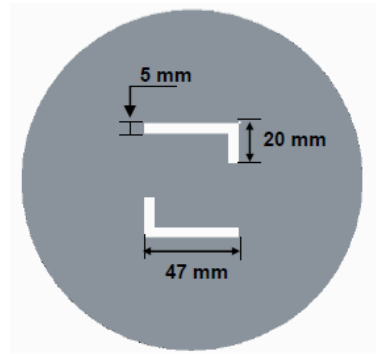
Figure 4.8. Back view of the die and profiles shape sizes

The geometry of the die was defined analyzing numerically the material flow at the exit of a die without pocket and with constant bearing length. Parameterized dimensions of pocket greatnesses, such as height (H_{pocket}, Fig. 4.10) and cross section (D_{pocket}, Fig. 4.9), and of bearing local lengths ($H_{bearing}$, Fig. 4.10) were planned.
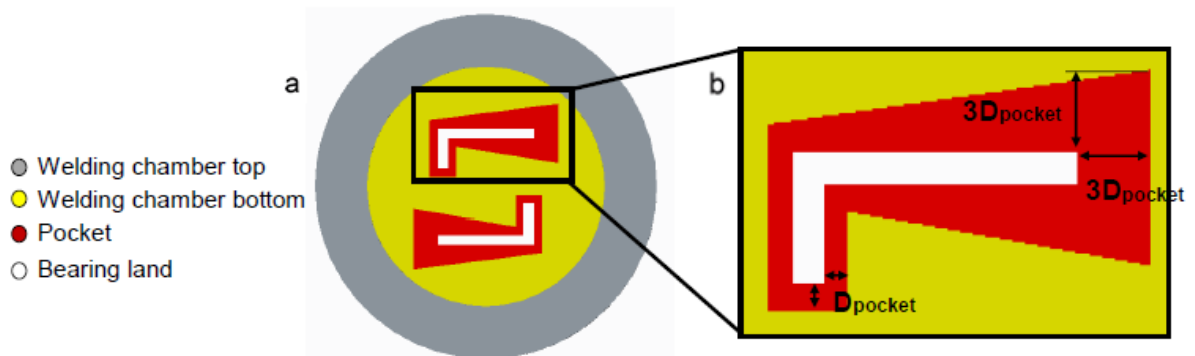
Figure 4.9. a) Top view of the die; b) detailed view
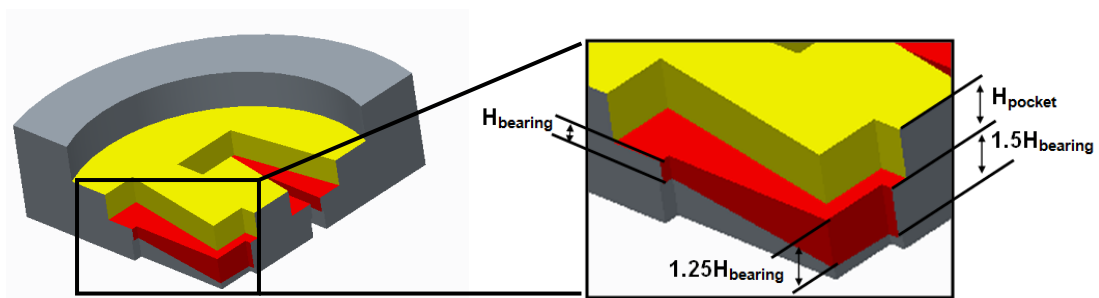
Figure 4.10. a) CAD model of the die; b) pocket and bearing particular

Moreover, multiplicative constants were set as shown in Table 4.1, to change the die design in a logical way in order to optimize the material flow at the bearing exit varying also the extrusion load. A full orthogonal plan of 27 tests was performed and then solved by using Design Expert statistical tool to confirm the results reliability.

H$_{bearing}$ [mm]	D$_{pocket}$ [mm]	H$_{pocket}$ [mm]
3	2.5	3
6	5	7
9	7.5	11

Table 4.1. Multiplicative constants

The extruded material was AA6060 aluminum alloy, the preheated billet temperature was 500 °C, while the temperature of the container and of the other parts was 450 °C and 420 °C, respectively. Punch speed was set to 1 mm/s for an extrusion ratio of 27. Friction was sticking at the interface material/matrix and viscoplastic, with a coefficient of 0.3, at the interface material/bearing.
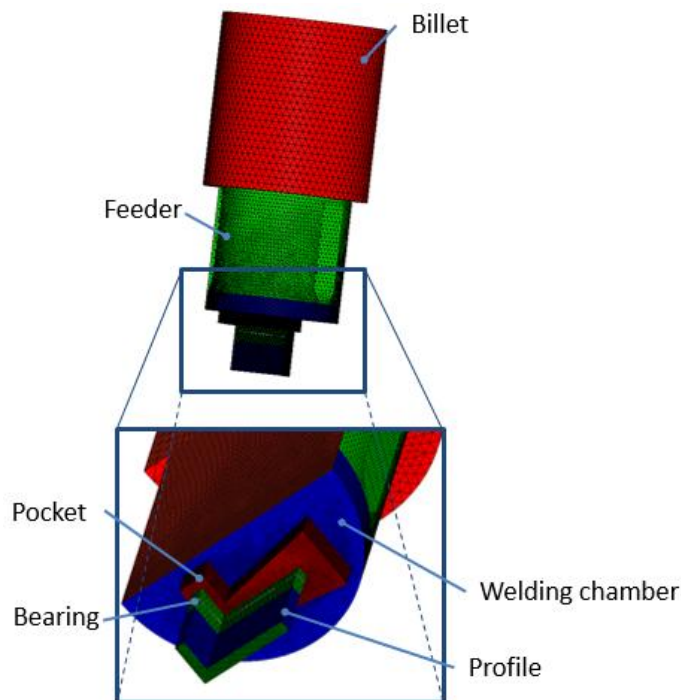
Figure 4.11. HyperXtrude® meshed model and particular of the die exit

The attention was then focused on two outputs: velocity distribution on the profile cross section, and maximum load reached during the process in steady state conditions. The first one because can create distorted profiles; the second one because can generate an excessive stress field on the die and can require a press with high capacity.

4.3.2 Influence of the geometric parameters on velocity distribution

Regarding the speed distribution, the velocity discrepancy ΔV between two points belonging to the profile cross section was taken into account. The two points were chosen to maximize that discrepancy (Fig. 4.12), which range was 0.17÷29.99 mm/s after testing all the cases of the full orthogonal plan.
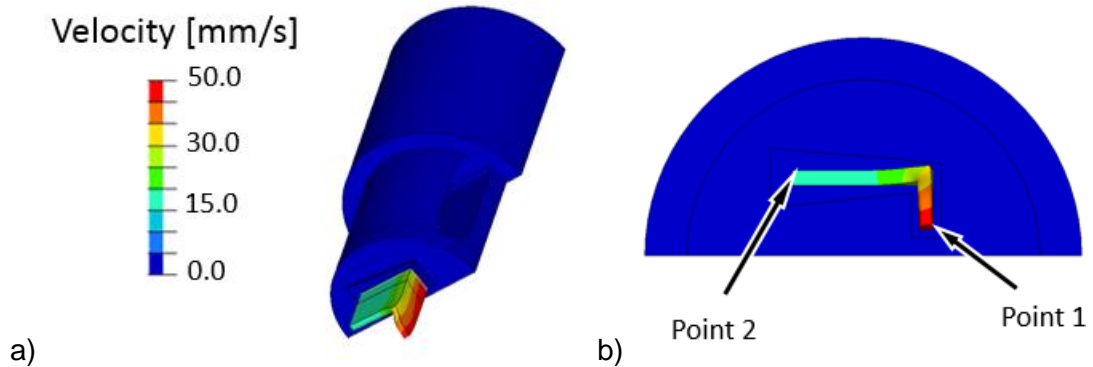
Figure 4.12. a) Velocity distribution in one test of the numerical campaign; b) considered points to calculate ΔV, on the profile cross section

The influence of the geometrical parameters on the exit velocity was evaluated by using ANOVA data [126], and afterwards Response Surfaces were built to emphasize the more significant variables interactions and graphically justify the outputs variation [127]. ANOVA findings are shown in Table 4.2, and stated that all the first order factors influence the output, as well as the ΔV significantly varies with the second order factor of the pocket section.

Factors	A	B	C	AB	AC	BC	A^2	B^2	C^2
Influence on ΔV	High	High	High	Low	Low	Medium	Medium	High	No

Table 4.2. *ΔV*, ANOVA evidence, A= H$_{pocket}$, B= D$_{pocket}$, C= H$_{bearing}$

On the other hand, also the interaction of the local bearing lengths configuration and the pocket section influences the velocity discrepancy as shown in Figure 4.13. More in particular, if the pocket section is smaller, the bearing setup influence is large; while, for wider pocket dimensions the bearing configuration is less influent. The material flow is not homogeneous especially when both previous parameters are small. Finally, the pocket height is not significant to get velocity changes.
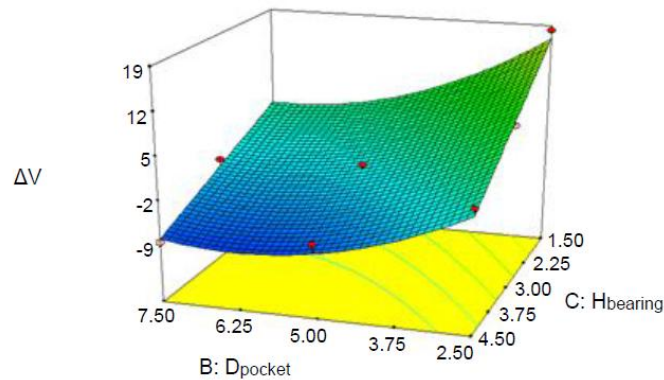
Figure 4.13. Response Surface of local bearing lengths and pocket cross section interaction

4.3.3 Influence of the geometric parameters on extrusion load in steady state conditions

The variability range of the punch load reached during the numerical tests was 6.85÷8.93 MN. Instead, regarding ANOVA analysis about the influence of the geometric parameters on process load value (Table 4.3), it was possible to see that the first order factors strongly affect it, as well as the second order ones with the exception of the bearing height, which does not have effect on the response.

Factors	A	B	C	AB	AC	BC	A^2	B^2	C^2
Influence on Ram Load	Medium	High	High	High	No	No	High	High	No

Table 4.3. *Load*, ANOVA evidence, A= H_{pocket}, B= D_{pocket}, C= $H_{bearing}$

As concerns the factors interactions, the only one that plays a relevant role in the process force variation is between H_{pocket} and D_{pocket}, as shown in Figure 4.14 that reports the Response Surface of the above specified interplay. The maximum process load is reached by designing a die with smaller pocket sections, in agreement with Li at al. [128], and higher pocket heights. The minimum load, instead, can be achieved if both the factors are set to their highest value. Finally, considering the Response Surface and looking at the curve gradient, the pocket section is the variable whose changes more affect the extrusion load.
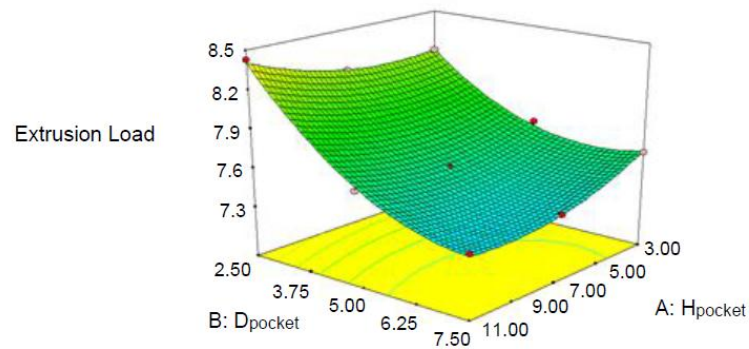
Figure 4.14. Response Surface of pocket height and pocket cross section interaction

4.3.4 Verification tests with the optimized dies

Finally, the optimized dies design, one to minimize the velocity discrepancy into the exit profile and the other one to minimize the extrusion load on the punch, were identified by using the Desirability function and the Design Expert optimization tool [129], considering the structural constraints. The geometric sets of both the dies are reported in Table 4.4 and Table 4.5, for the minimum profile distortion (Setting 1) and the minimum load (Setting 2), respectively. Therefore, verification tests were run to confirm the made observations.

Setting 1	
$H_{bearing}$ [mm]	4.9
H_{pocket} [mm]	10.84
D_{pocket} [mm]	4.08

Table 4.4. Setting 1: optimized die for minimizing the velocity distribution discrepancy

Setting 2	
$H_{bearing}$ [mm]	3,06
H_{pocket} [mm]	9.11
D_{pocket} [mm]	7.44

Table 4.5. Setting 2: optimized die for reaching the minimum process load in steady state conditions

As said, in the initial tests the velocity discrepancy range was 0.17÷29.99 mm/s; while in Setting 1 this value is 0.12 mm/s (almost null), and the profile seems be completely undistorted (Fig. 4.15). The load reached during the process in case of Setting 1 is 7.65 MN.
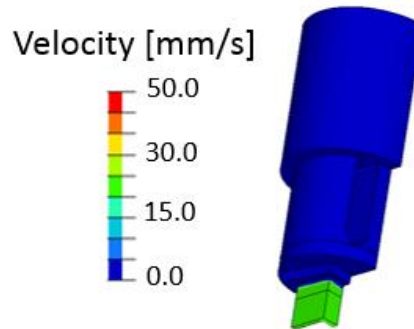
Figure 4.15. Homogeneous profile velocity distribution, Setting 1

On the other hand, the load reached in case of die built with the dimensions reported in Setting 2, is 6.82 MN, lower than the minimum value obtained during the previous numerical analysis, which was 6.85 MN. Instead, the velocity discrepancy for Setting 2 is 0.48 mm/s.

4.3.5 Conclusions

A careful analysis about the right die design aimed at extruding simultaneously two profiles with non-symmetric cross section and without any distortion, exalts that the variable that has more influence on process performances is the pocket cross section. Moreover, the interaction between pocket shape and bearing configuration has to be taken into account to guarantee a certain material flow homogeneity. Finally, a depth study of the pocket volume is necessary to extrude a profile with minimal effort in terms of loads.

5. INFLUENCE OF REINFORCING ELEMENTS ON THE MATERIAL FLOW DISTORTION DURING COMPOSITE EXTRUSION

Composite extrusion process is taken into account, which aims at improving the mechanical properties of extrudates by embedding continuous reinforcing elements into the profiles using a modified porthole die. The influence of high reinforcing volumes on the material flow is evidenced. An experimental campaign is carried out and a modeling approach is identified in order to simulate the composite extrusion process. Several issues are highlighted regarding the unbalanced material flow inside the final profile and the high load on the reinforcing elements that can bring to their breaking.

5.1 NEW MODELING APPROACH TO SIMULATE THE COMPOSITE EXTRUSION PROCESS

Reinforced extruded profiles (Fig. 5.1) manufacturing by experimental tests during a collaboration with the Institute of Forming Technology and Lightweight Construction (IUL) of Dortmund, which has already carried out research on composite extrusion for several years, were the starting point in order to find a numerical setting model capable of approximating the real behavior of composite extrusion.
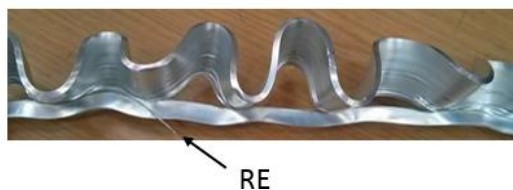
Figure 5.1. Reinforced extruded profile

Two profiles reinforced with continuous wires, as shown in Figure 5.2, with non-symmetric shape, were simultaneously extruded. Numerical investigations were performed by means of Altair HyperXtrude® software (Fig. 5.3). The billet was made up of AA6060 aluminum alloy and it had a length of 200 mm and a diameter of 146 mm; whereas the wires were made up of high strength spring steel AISI 301.
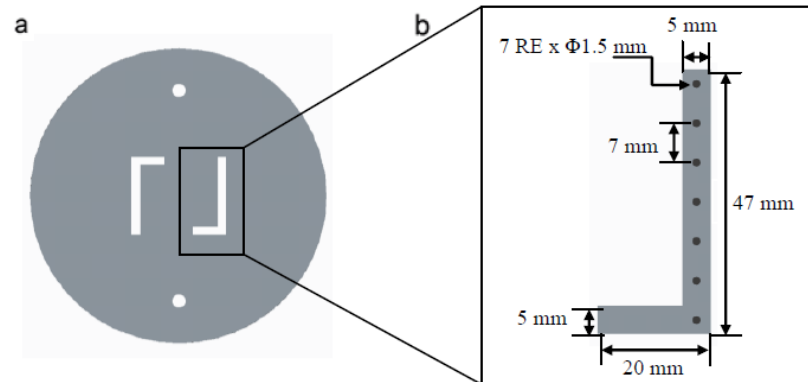
Figure 5.2. a) Die bottom surface; b) profile shape cross section with reinforcing elements and main geometric parameters

The preheating billet temperature was 470 °C, while the container and die temperatures were 450 °C and 420 °C, respectively. Ram speed was set 1 mm/s. Viscoplastic friction, with a friction coefficient of 0.3, was assumed at the interface material-bearing to represent sliding contact in the gate zone [107]. Sticking friction conditions were set at the interface material-container and material-die walls.
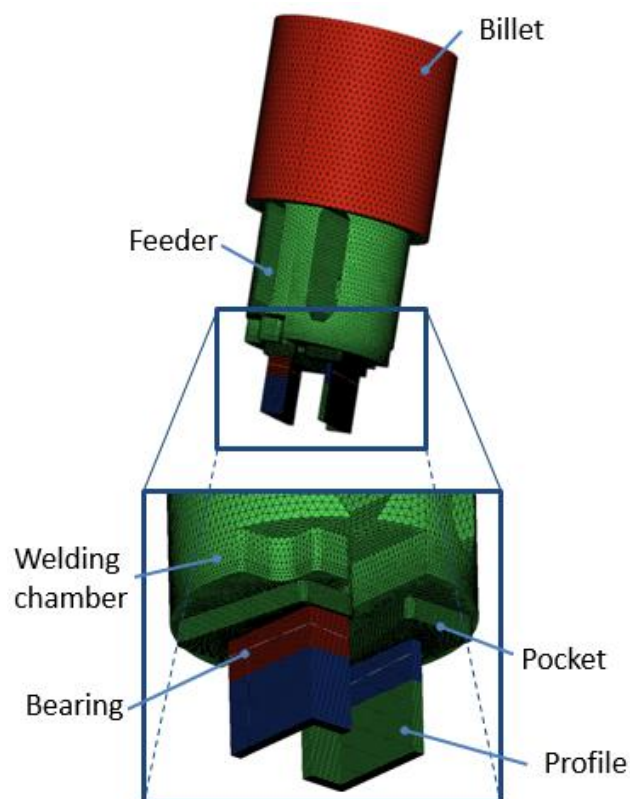
Figure 5.3. HyperXtrude® meshed model and particular of the die exit

The investigated setting are below summarized.

Setting 1) Firstly, to consider the reinforcements, appropriate constraints are set; in particular, a SolidWall boundary condition is specified at the interface between the material and the RE with sticking friction and adiabatic thermal condition. In such a way, the REs behave as rigid bodies that move with a velocity v_{RE} equal to the final profile velocity, related to extrusion ratio, $ex = (\frac{D^2_{container}}{4}\pi/(hb - n\frac{D^2_{RE}}{4}\pi))$, and ram speed, v_{punch}, as shown in the following equation:

$$v_{RE} = v_{punch} * ex \qquad \text{(Eq. 5.1)}$$

The extrusion ratio is the ratio between the initial cross section of the billet and the cross section of the profile devoid of REs. The material velocity distribution (Fig. 5.4) ensured a homogeneous flow at the bearing exit. In detail, following the aluminum flow from the tip of the mandrel, it was observed how the material velocity increased up to the die orifice. A velocity peak was highlighted in the core of the bearing entrance while a zero velocity was observed along the external borders of the section, due to friction sticking conditions at the interface aluminum/bearing walls; the mass conservation principle was, therefore, respected. Instead, the velocity of the profile at the exit of the die was almost homogeneous; in fact, the difference between maximum and minimum velocity values in that region resulted less than 3%.
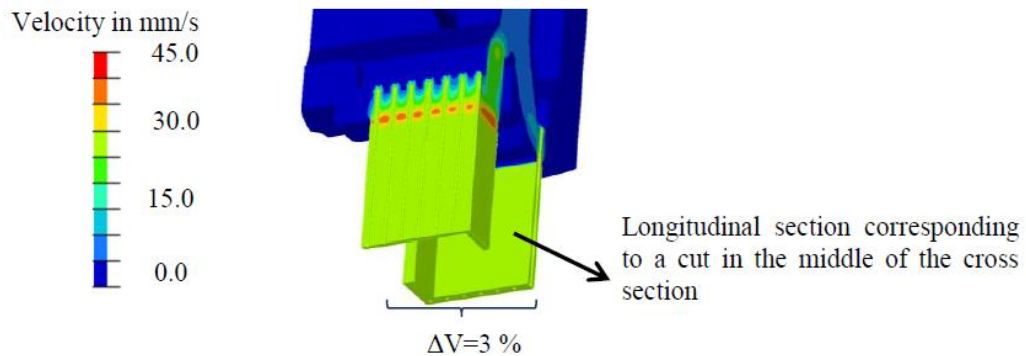
Figure 5.4. Profile velocity distribution, Setting 1

That result disagreed with the experimental evidence, clearly showing the numerical outcomes inaccuracy for the used boundary conditions chosen to define the interaction between steel wires and aluminum matrix.

New investigations were then carried out using both stationary and transient model, in order to find a configuration of boundary conditions allowing the simulation of composite extrusion. Because the same static and transient outcomes, steady state

simulations were preferably run due to shorter computational times. Moreover, a half of the model was built (Fig. 5.5) because of the similarity between the results obtained during the simultaneous extrusion of the two profiles. Three different setups were analyzed considering the reinforcing elements as meshed parts inside the welding chamber, bearing and profile.
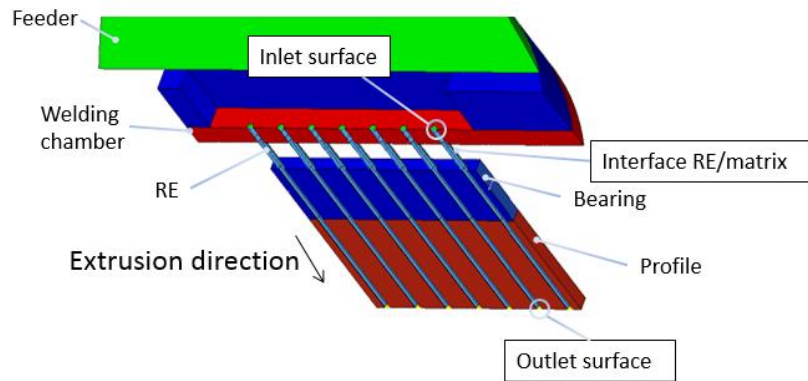
Figure 5.5. Half of the model in HyperXtrude® and surfaces to consider for boundary conditions setting

Setting 2) The reinforcement material is considered as a tool material with elastic behavior, by using the software library. A SolidFluidInterface boundary condition is set at the interface material-wire with slip velocity friction and a slip coefficient of about 10^{10}; moreover, a zero velocity along the extrusion direction is set at the same interface. The inlet and outlet surfaces of the wires are finally implemented by tool surface boundary condition with zero traction value in the extrusion direction, which allows the wires to freely move. Applying that Setting, inhomogeneous velocity distribution was obtained on the profile cross section (Fig. 5.6). More in detail, the velocity in the shorter side of the shape was faster than in the other side, which was in disagreement with experimental results.
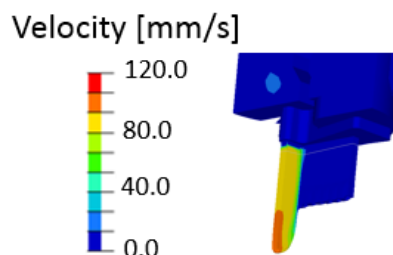
Figure 5.6. Profile velocity distribution, Setting 2

Setting 3) The same properties described in the previous model (Setting 2) are utilized with the exception of the condition at the interface between wires and matrix material. In fact, SolidFluidInterface is replaced by FluidFluidInterface and no more information are required about friction condition and velocity constraint. Considering Setting 3, the final velocity distribution on the profile cross section was characterized by the same trend of the experimental results; in fact, the material velocity was faster in the longer region of L shape (Fig. 5.7). However, the discrepancy between maximum and minimum velocity values was not so marked as observed during the experimental tests.
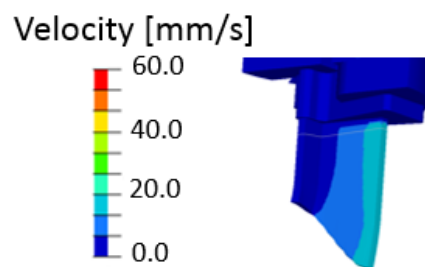
Figure 5.7. Profile velocity distribution, Setting 3

Setting 4) In the last analyzed configuration, the reinforcement material is considered as a workpiece material. The wires are made of steel, taken from software library. The material is characterized by plastic behavior; a specific velocity, given by the extrusion ratio and the punch speed (Eq. 5.1), is the input velocity and a FluidFluidInterface boundary condition is attributed at the elements located at the interface material-reinforcements. In case of Setting 4, the final velocity distribution on the profile cross section was not homogeneous as the experiments shown; it was faster in the longer region of L shape similar to the extruded profile velocity (Fig. 5.8).
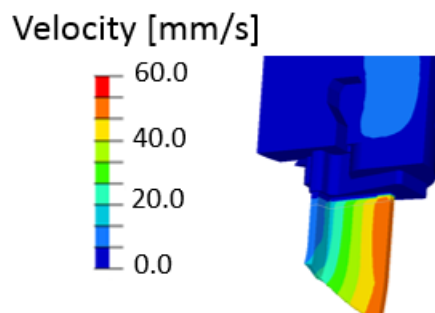
Figure 5.8. Velocity distribution into the profile, Setting 4

5.1.1 Conclusions

A composite extrusion process of non-symmetric profiles was numerically analyzed identifying the approach to simulate the extrusion of reinforced profiles.

5.2 HOT EXTRUSION OF COMPOSITE PROFILES WITH HIGH REINFORCING VOLUMES

Afterwards, composite extrusion process was carried out in order to analyze the influence of the reinforcing elements on material flow distortion and profile defects trying to increase the reinforcing volume currently inserted inside the profile, as described in the work of Shwane et all [78]. The investigation was conducted in collaboration with the Institute of Forming Technology and Lightweight Construction (IUL) of Dortmund. An experimental campaign was performed in the IUL Laboratory and a numerical investigation was subsequently carried out in order to explain the experimental outcomes regarding the material flow and the load on the reinforcing elements.

5.2.1 Experimental campaign

Known the advantages of composite extrusion, aluminum profiles reinforced with continuous elements are actually used in manufacturing lightweight products. One factor of interest, in the last years, is increasing the reinforcing volume, that is the ratio between the total reinforcements cross area and the profile cross area, maintaining a reduced profile section and increasing its strength (Fig. 5.9).
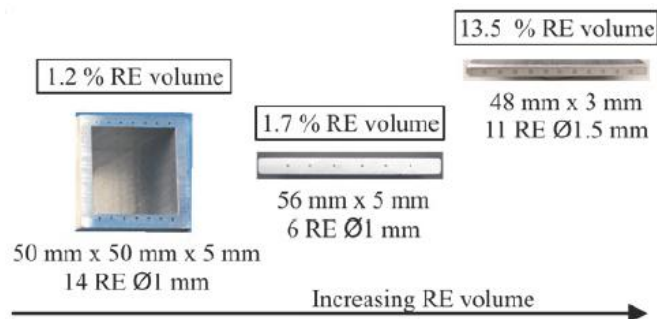
Figure 5.9. Composite profiles cross sections, [78]

A profile with a rectangular section and reinforced with 12 wires, for a reinforcing volume of 16.4% (Fig. 5.10b), already extruded in the past with 11 REs (Fig. 5.10a), was manufactured with a 10 MN capacity press into the IUL Laboratory.

48 mm x 3 mm, 11 RE Ø1.5 mm
13.5 % RE volume

48 mm x 2.7 mm, 12 RE Ø1.5 mm
16.4 % RE volume

a)

b)
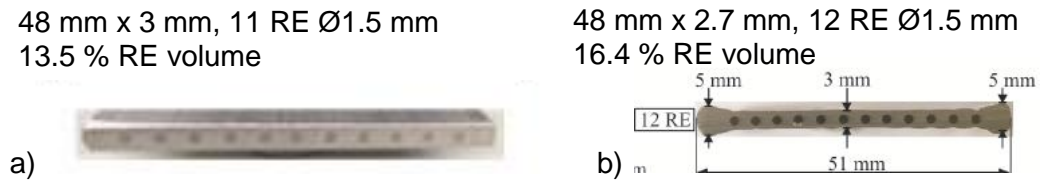
Figure 5.10. a) Reinforced profile with 11 REs; b) desired profile cross section with 12 REs, [78]

An optimized die designed to extrude a not reinforced profile with the same cross section and homogeneous material flow at the die exit, was used and the effect of the reinforcing elements on the material flow was analyzed. The billet material was AA6060 aluminum alloy, while the reinforcing elements material was steel.

A thickness thickening (Fig. 5.10b), especially at the section edges of the profile, was observed. Another critical issue could be the reinforcing element breaking due to the stess distribution. To better explain the thickness increase and to investigate the load distribution on the wires, a numerical campaign was performed considering velocity field and load on reinforcements as outputs.

5.2.2 Numerical investigation about profile velocity field and load distribution on the reinforcing elements

Numerical simulations were run by means of Altair HyperXtrude® software in steady state conditions (Fig. 5.11). The aluminum billet had a diameter of 106 mm and a length of 200 mm; its preheated temperature was 500 °C, whereas container and die temperature was 450 °C and 420 °C, respectively. The punch speed was set 0.5 mm/s and the friction model between the matrix and the material was sticking condition. The bearing had a length of 7 mm and the friction condition between it and the material was set as viscoplastic with a friction coefficient of 0.3.
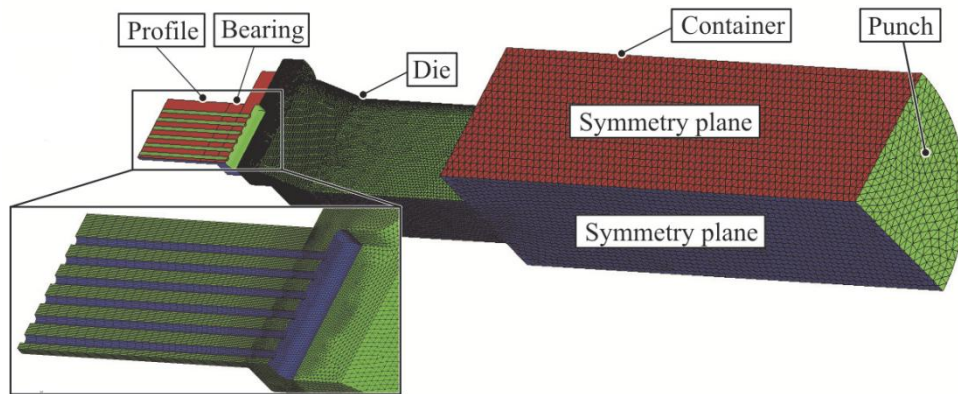
Figure 5.11. HyperXtrude® meshed model and some boundary conditions, [78]

To run the simulations twelve meshed bodies were considered inside the welding chamber, bearing and profile, with a proper material. A temperature of 470 °C and a proper velocity, dependent on ram speed and extrusion ratio as in the previous Eq. 5.1, were set as input boundary conditions on the top surface of the REs into the welding chamber. The other boundary conditions corresponding to the elements are that identified in Setting 4 in the previous paragraph. Analyzing the numerical results regarding the velocity distribution, as shown in Figure 5.12a, is possible to explain the experimental ones.
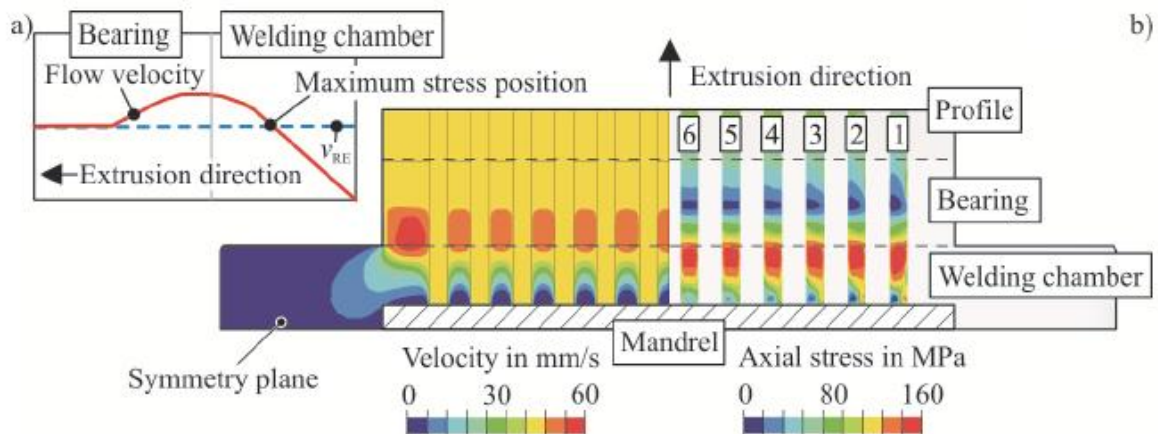
Figure 5.12. a) Velocity distribution and b) axial stress in the REs, [78]

More in detail, a higher velocity values corresponding to the end edges of the profile cross section due to the minor opposition to the material flow movement, is the main reason of the thickness increase. The faster material cannot flow into the already cooled and sound profile, so it locally accumulates. Numerical outcomes confirmed as Kloppenborg stated [88]: the velocity gradient was more pronounced at the bearing entrance than at the bearing exit due to the transition from sticking to sliding

friction [107]. At the entrance, the aluminum sticks to the bearing surface (velocity is zero) as well as to the RE surface (velocity corresponds to RE velocity). Due to the velocity gradients and the volume invariability property, the material is accelerated in the remaining cross section area (Fig. 5.12a).

Instead, concerning load distribution on the reinforcements, it was clear that the highest axial stress acted on the more external reinforcements (1, Fig. 5.12b) because the wider discrepancy between RE speed and material flow velocity at the edges, so they are the elements that easily can be broken.

5.2.3 Conclusions

The extrusion of a profile with 16.4% reinforcing content was taken into account. Reinforcing elements number and location influence the material flow. Higher is the difference between material and reinforcement velocity values and greater is the load on the reinforcing element that could break.

CONCLUSIONS

Currently, the market demands are increasingly oriented towards customized products characterized by complex shapes, thin sections, reduced encumbrances. Automotive field is one of the sectors of most interest whose requirements are related to the reduction of weights and volumes for fuel saving; therefore, companies need to manufacture lightweight profiles ensuring good quality, reduced volumes, low production costs and short working time, to be competitive.

In this regard, extrusion can be properly designed to satisfy the over exposed requirements. More in detail, extruded profiles with hollow and complex shapes can be manufactured by porthole die improving the product mechanical properties. A current challenge is to extrude reinforced components in order to improve the profile mechanical properties keeping reduced weight and volume. An undistorted profile missing of defects and reinforced with continuous elements can be manufactured with a porthole die geometry carefully designed. Therefore, a high knowledge about porthole die extrusion process is needed. One of the materials of interest is aluminum and its alloys because of its outstanding mechanical properties.

Several critical aspects related to aluminum extrusion have to be taken into account. More in detail:

- the influence of seam welds integrity and quality on the profile mechanical properties. Specific temperatures and contact pressures inside the welding chamber must be guaranteed in order to have solid bonding;
- the detection of defects into the profile and on its surface, such us central bursting and speed cracking, surface tearing and hot shortness, respectively;
- distortions due to inhomogeneous material flow at the die exit influenced by process and geometric parameters and by insertion of reinforcing elements inside the stream in case of composite extrusion;
- high loads reached during the process.

The work of this thesis have regarded some of the above issues. The main considerations are below summarized.

Composite extruded profile with a high reinforcing content can be manufacture with a special porthole die.

A new approach of modeling extrusion aluminum profiles reinforced with steel wires, by means of Altair HyperXtrude® software, is identified in order to analyze the material flow and predict the reinforcement fracture.

Flow distortion due to the interaction between the material and the reinforcing elements can affect the reinforced profile.

Continuous wires with highest gradient velocity between them and the surrounding material are the most loaded elements, that can break during the process.

In order to avoid the reinforcing elements breaking due to high stresses, a die with an optimized geometry should be designed and the influence of the wires location inside the profile should be investigated.

Future developments

Some future developments to enrich the work of this thesis and the knowledge about the extrusion research field, are below summarized.

The outcomes of the numerical model identified in this thesis, to simulate the extrusion of reinforced profiles, can be validate with an experimental campaign.

On the other hand, statistical tools can be used improving the research; the most significant process and geometric parameters that influence the material flow distortion and process load in case of composite extrusion, can be investigated.

After that the extrusion process using the optimized die able to manufacture such kind of profile can be numerically and experimentally re-analyzed.

REFERENCES

[1] G. Berti, M. Monti, A. Del Lago, Simulazione numerica del processo di microestrusione idrostatica di un acciaio a basso tenore di carbonio, 2010.

[2] F. Micari, Processi di formatura dei metalli, Materiali e tecnologie, 2004, Ed. Flaccovio Dario.

[3] http://thelibraryofmanufacturing.com/extrusion.html

[4] J. Zhou, L. Li, J. Duszczyk, 3D FEM simulation of the whole cycle of aluminum extrusion throughout the transient state and the steady state using the updated Lagrangian approach, Journal of materials Processing Technology 134 (2003) 383-397.

[5] Ding Tang, Qingqing Zhang, Dayong Li, Yinghong Peng, A physical simulation of longitudinal seam welding in micro channel tube extrusion, Journal of Materials Processing Technology, 214 (2014) 2777–2783.

[6] M. Foster, D. Joseph, M. Fiderer, Using finite element modeling to better understand extrusion material flow and die stress, International Conference on Extrusion and Benchmark (2013).

[7] R. Akeret, Extrusion welds-quality aspects are now center stage, Fourth international aluminum extrusion technology seminar, Chicago, 2 (1988) 357-67.

[8] N. Nanninga, C. White, T. Furu, O. Anderson, R. Dickson, Effect of orientation and extrusion welds on the fatigue life of an Al-Mg-Si-Mn alloy, International Journal of Fatigue, 30 (2008) 1569-1578.

[9] J.V. Rijkom, P.H. Bolt, A review of new approaches and technologies in extrusion welds related to the background of existing knowledge, Seventh international aluminum extrusion technology seminar, Chicago, (2000) 249-60.

[10] X. Zhang, D. Feng, X. Shi, S. Liu, Oxide distribution and microstructure in welding zones from porthole die extrusion, Trans. Nonferrous Met. Soc. China, 23 (2013) 765-772.

[11] Y. Mahmoodkhani, M. A. Wells, N. Parson, W.J. Poole, Numerical modeling of the material flow during extrusion of aluminum alloys and transverse weld formation, Journal of materials processing technology, 214 (2014) 688-700.

[12] R. Akeret, Extrusion welds—quality aspects are now center stage, Proc. ET, I (1992) 319-336.

[13] K.J. Kim, C.H. Lee, D.Y. Yang, Investigation into the improvement of welding strength in three-dimensional extrusion of tubes using porthole dies, Journal of Materials Processing Technology, 130-131 (2002) 426-431.

[14] H.H. Jo, C.S. Jeong, S.K. Lee, B.M. Kim, Determination of welding pressure in the non-steady-state porthole die extrusion of improved Al7003 hollow section tubes, Journal of Materials Processing Technology, 139 (2003) 428-433.

[15] J. Liu, G. Lin, D. Feng, Y. ZOU, L. Sun, Effect of process parameters and die geometry on longitudinal welds quality in aluminum porthole die extrusion process, J. Cent. South Univ. Technol., 17 (2010) 688-696.

[16] G. Liu, J. Zhou, J. Duszczyk, FE analysis of metal flow and weld seam formation in a porthole die during the extrusion of a magnesium alloy into a square tube and the effect of ram speed on weld strength, Journal of Materials Processing Technology, 200 (2008) 185-198.

[17] G. Buffa, L. Donati, L. Fratini, L. Tomesani, Solid state bonding in extrusion and FSW: process mechanics and analogies, Journal of Materials Processing Technology, 177 (2006) 344-347.

[18] L. Donati, A. Segatori, M. El Mehtedi, L. Tomesani, Grain evolution analysis and experimental validation in the extrusion of 6XXX alloys by use of a lagrangian FE code, International Journal of Plasticity, 46 (2013) 70-81.

[19] P. Saha, Aluminum extrusion technology, ASM International, The Materials Information Society, 2000.

[20] T. Sheppard, Extrusion of aluminum alloy, Kluwer academic publisher, Dordrecht, Holland, 1999.

[21] H. Valberg, T. Loeken, M. Hval, The extrusion of hollow profiles with a gas pocket behind the bridge, Int. J. Mater. Prod. Tech., 10 (1995) 222-267.

[22] B. Bourqui, A. Huber, C. Moulin, A. Brunetti, Improved weld seam quality using 3D FEM simulations in correlation with practice, Proceedings of First European Aluminum Association, (2002).

[23] Y.T. Kim, K. Ikeda, T. Murakami, Metal flow in porthole die extrusion of aluminum, Journal of Materials Processing Technology 121 (2002) 107-115.

[24] Q. Li, C. Harris, M.R. Jolly, Finite element modelling simulation of transverse welding phenomenon aluminum extrusion process, Material and Design, 24 (2003) 493-496.

[25] A. Loukus, G. Subhash, M. Imanejad, Mechanical properties and microstructural characterization of extrusion welds in AA6082-T4, Journal of Material Science, 39 (2004) 6561-6569.

[26] L. Donati, L. Tomesani, The prediction of seam welds quality in aluminum extrusion, Journal of Materials Processing Technology, 153-154 (2004) 366-373.

[27] E. Ceretti, L. Fratini, , F. Gagliardi, C. Giardini, A new approach to study material bonding in extrusion porthole dies, CIRP Annals, Manufacturing Technology, 58 (2009) 259-262.

[28] L. Donati, L. Tomesani, The effect of die design on the production and seam weld quality of extruded aluminum profiles, Journal of Materials Processing Technology, 164-165 (2005) 1025-1031.

[29] L. Donati, L. Tomesani, Simulation of welding conditions in porthole die extrusion, Proceedings of the AMST Conference on Advanced Manufacturing System and Technology, (2002) 437.

[30] S. Bingol, M.S. Keskin, Effect of different extrusion temperature and speed on extrusion welds, Journal of Achievements in Materials and Manufacturing Engineering, 23 (2007).

[31] J.H. Zhu, B. Young, Effects of trasverse welds on aluminum alloy columns, Thin-Walled Structures 45 (2007) 321-329.

[32] Donati L., Tomesani L., Minak G., Characterization of seam weld quality in AA6082 extruded profiles. J. Mater. Proc. Tech. 191 (2007) 127-131.

[33] Y.A. Khan, H. Valberg, I. Irgens, Joining of metal streams in extrusion welding, Int J Mater Form, 2 (2009) 109-112.

[34] T Hatzenbichler, B. Buchmayr, Finite element method simulation of internal defects in billet-to-billet extrusion, Proceedings of the Institution of Mechanical Engineers Part B Journal of Engineering Manufacture, 224 (2010) 1029-1042.

[35] Y.A. Khan, H.S. Valberg, Metal flow in idealized a-symmetric 2D extrusion welding, Int J Mater Form, 3 (2010) 383-386.

[36] Y.Mahmoodkhani, M. Wells, N. Parson, C. Jowett, W.J. Poole, Modeling the Formation of Transverse Weld during Billet-on-Billet Extrusion, Materials, 7 (2014) 3470-3480.

[37] B. Reggiani, A. Senatori, L. Donati, L. Tomesani, Prediction of charge welds in hollow profiles extrusion by FEM simulations and experimental validation, Int J Adv Manuf Technol, 69 (2013) 1855-1872.

[38] Y. Mahomoodkhani, M.A. Wells, N. Parson, W.J. Poole, Numerical modeling of the material flow during extrusion of aluminum alloys and transverse weld formation, Journal of Materials Processing Technology, 214 (2014) 688-700.

[39] P.F. Fisher, Developments in Spatial Data Handling, Springer Verlag, (2005) Berlin/Heidelberg.

[40] A.J. den Bakker, R.J. Werkhoven, W.H. Sillekens, L. Katgerman, The origin of weld seam defects related to metal flow in the hot extrusion of aluminum alloys EN

AW-6060 and EN-AW-6082, Journal of Materials Processing Technology, 214 (2014) 2349-2358.

[41] M. Schwane, F. Gagliardi, A. Jager, N.B. Khalifa, A.E. Tekkaya, Modeling approach for the determination of material flow and welding conditions in porthole die extrusion with gas pocket formation, Trans Tech Publications, (2013) 787-793.

[42] C.P. Dick, Y.P. Korkolis, Strength and ductility evaluation of cold-welded seam in aluminum tubes extruded through porthole dies, Materials and Design, 67 (2015) 631-636.

[43] T. Pinter, B. Reggiani, L. Donati, L. Tomesani, Numerical assessment of the influence of process and geometric parameters on extrusion welds and die deformation after multiple-cycles, ICEB 2015.

[44] M. Endelhart, D. Behne, N. Grittner, A. Neumann, W. Reimche, C. Klose, Non-destructive testing of longitudinal and charge weld seams in extruded aluminum and magnesium profiles, ICEB 2015.

[45] R. Akeret, Properties of pressure welds in extruded aluminum alloy sections, J. Inst. Met, 10 (1972) 202.

[46] M. Plata, J. Piwnik, Theoretical and experimental analysis of seam weld formation in hot extrusion of aluminum alloys, in: Proceedings of Seventh International Aluminum Extrusion Technology Seminar ET, I (2000) 205-211.

[47] A.F.M. Arif, A. K. Sheikh, S.Z. Qamar, M.K. Raza, K.M. Al-Fuhaid, Product defects in aluminum extrusion and their impact on operational cost, The 6th Saudi Engineering Conference, Dhahran, 5 (2002) 137.

[48] D. Lesniak, W. Libura, Extrusion of section with varying thickness through pocket dies, Journal of Materials Processing Technology, 194 (2007) 38-45.

[49] Q. Li, C.J. Smith, C. Harris, M.R. Jolly, Finite element investigations upon the influence of pocket die designs on metal flow in aluminum extrusion: Part I. Effect of pocket angle and volume on metal flow, Journal of materials processing technology, 135 (2003) 189-196.

[50] G. Fang, J. Zhou, J. Duszczyk, FEM simulation of aluminum extrusion through two-hole multi-step pocket dies, Journal of materials processing technology, 209 (2009) 1891-1900.

[51] Q. Li, C.J. Smith, C. Harris, M.R.Jolly, Finite element investigations upon the influence of pocket die designs on metal flow in aluminum extrusion: Part II. Effect of pocket geometry configurations on metal flow, Journal of materials processing technology, 135 (2003) 197-203.

[52] Y. He, S. XIE, L. CHENG, G. HUANG, Y. FU, FEM simulation of aluminum extrusion process in porthole die with pockets, Trans. Nonferrous Met. Soc. China 20 (2010) 1067-1071.

[53] G. Fang, J. Zhou, J. Duszczyk, Fem simulation of aluminum extrusion through two-hole multi-step pocket dies, Journal of materials processing technology 209 (2009) 1891-1900.

[54] N. Negendank, S. Muller, W. Reimers, Extrusion of aluminum tubes with axially graded wall thickness and mechanical characterization, Procedia CIRP (2014) 3-8.

[55] L. Donati, A. Segatori, M. El Mehtedi, L. Tomesani, Grain evolution analysis and experimental validation in the extrusion of 6XXX alloys by use of a lagrangian FE code, International Journal of Plasticity 46 (2013) 70-81.

[56] G. Fang, J. Zhou, J. Duszczyk, Extrusion of 7075 aluminum alloy through double-pocket dies to manufacture a complex profile, Journal of materials processing technology, 209 (2009) 3050-3059.

[57] R. Mayavaram, U. Sajja, C. Secli, S. Niranjan, Optimization of bearing lengths in aluminum extrusion dies, Procedia CIRP, 12 (2013) 276-281.

[58] X. Wu, G. Zhao, Y. Luan, X. Ma, Numerical simulation and die structure optimization of an aluminum rectangular hollow pipe extrusion process, Materials Science and Engineering, 435–436 (2006) 266–274.

[59] G.J. Huang, Y. Fu, Y.F. He, S.S Xie, L. Cheng, FEM simulation of aluminum extrusion process in porthole die with pockets, Transactions of Nonferrous Metals Society of China, 20 (2010) 1067–1071.

[60] G. Fang, J. Zhou, J. Duszczyk, FEM simulation of aluminum extrusion through two-hole multi-step pocket dies, Journal of Materials Processing Technology, 209 (2009) 1891-1900.

[61] Y. Aue-u-lan¸ K. Khansai, 3D Numerical simulation to investigate the influential factors causing die failure in hot aluminum extrusion of square hollow profile. Journal of Science and Engineering, 2 (2012) 11- 17.

[62] G. Fang, J. Zhou, J. Duszczyk, Extrusion 7075 aluminum alloy through double-pocket dies to manufacture a complex profile, Journal of Materials Processing Technology, 209 (2009) 3050–3059.

[63] Q.C. Hsu, K.H. Kuo, C.P. Hsu, Solid welding conditions for seam and hollow extrusion process of 7075 aluminum alloy, Key Engineering Materials, 479 (2011) 62-73.

[64] Q.C. Hsu, K.H. Kuo, P.H. Tsai, Square tube manufacturing by forward extrusion of AA7075 with porthole die, Advanced Materials Research, 579 (2012) 92-100.

[65] Q.C. Hsu, K.H. Kuo, B.F. Sheng, Study on welding strength and die life assessment for hollow extruded Aluminum Alloy 7075, Proceedings of the ASME 2012 International Mechanical Engineering Congress & Exposition, IMECE 2012-85689.

[66] C. Zhang, G. Zhao, Z. Chen, H. Chen, F. Kou, Effect of extrusion stem speed on extrusion process for a hollow aluminum profile, Mater Sci Eng B, 177 (2012) 1691-7.

[67] M.J. Wang, C.L. Gan, X.Y. Liu, Deformation behavior of 6063 aluminum alloy during high-speed compression, Journal of Wuhan University of Technology, 20 (2005) 40-43.

[68] Q.C. Hsu, Y.L. Chen, T.H. Lee, Non-symmetric hollow extrusion of high strength 7075 aluminum alloy, Procedia Engineering, 81 (2014) 622-627.

[69] T. Nakamura, S. Tanaka, M. Hiraiwa, H. Imaizumi, Y. Tomizawa, K. Osakada, Friction-assisted extrusion of thin strips of aluminum composite material from powder metals, CIRP Annals - Manufacturing Technology, 41 (1992) 281–284.

[70] Y. Sanomura, M. Kawamura, Fiber Orientation Control of Short-Fiber Reinforced Thermoplastics by Ram Extrusion, Polymer composites, Vol. 24 (2003) No. 5.

[71] M. Plancak, W.Z. Misiolek, V.K. Sikka, Physical and Numerical Analysis of Extrusion Process for Production of Bimetallic Tubes (2006).

[72] B. Vamsi Krishna, P. Venugopal, K. Prasad Rao, Co-extrusion of dissimilar P/M preforms – An explored route to produce bimetallic tube, Materials Science and Engineering: A, 407 (2005) 77–83.

[73] K.S. Lee, S.H. Kang, Y.S. Lee, Coextrusion of a crystalline aluminum alloy with a Zr-based bulk metallic glass, Materials Processing Division, Materials Deformation Group, Korea Institute of Materials Science, 531 Changwondaero, Changwon, Gyeongnam 641-831, South Korea.

[74] M. Paramsothy, N. Srikanth, M. Gupta, Solidification processed Mg/Al bimetal macrocomposite: Microstructure and mechanical properties, Journal of Alloys and Compounds, 461 (2008) 200–208.

[75] Z. Chen, K. Ikeda, T. Murakami, T. Takeda, Extrusion behavior of metal–ceramic composite pipes in multi-billet extrusion process, Journal of Materials Processing Technology, 114 (2001) 154–160.

[76] J. Muehlhause, S. Gall, S. Mueller, Simulation of the co-extrusion of hybrid Mg/Al profiles, Key Engineering Materials, 424 (2010) 113-119.

[77] M. Schikorra, A.E. Tekkaya, M. Kleiner, Experimental investigation of embedding high strength reinforcements in extrusion profiles, CIRP Annals – Manufacturing Technology 57 (2008) 313-316.

[78] M. Schwane, T. Citrea, C. Dahnke, M. Haase, N.B. Khalifa, A.E. Tekkaya, Simulation of Composite Hot Extrusion with High Reinforcing Volumes, 11th International Conference on Technology of Plasticity, ICTP 2014, 19-24 October 2014, Nagoya Congress Center, Nagoya, Japan, Procedia Engineering, 81 (2014) 1265–1270.

[79] M. Schikorra, M. Kleiner, Simulation-Based Analysis of Composite Extrusion Processes, CIRP Annals – Manufacturing Technology, 56 (2007) 317-320.

[80] D. Pietzka, N. Ben Khalifa, S. Gerke, A.E. Tekkaya, Composite extrusion of thin aluminum profiles with high reinforcing volume, Key Engineering Materials, 554-557 (2013) 801-808.

[81] T. Sheppard, A. Jackson, Constitutive Equation for use in Prediction of Flow Stress during Extrusion of Aluminum Alloys, Materials Science and Technology, 13 (1997) 203-209.

[82] M. Kleiner, M. Schikorra, Simulation of welding chamber conditions for composite profile extrusion, Journal of Materials Processing Technology, 177 (2006) 587–590.

[83] M. Schwane, C. Dahnke, M. Haase, N. Ben Khalifa, A.E. Tekkaya, Composite Hot Extrusion of Functional Elements, Advanced Materials Research, 1018 (2014) 223-228.

[84] M. Kleiner, M. Schikorra, Simulation of welding chamber conditions for composite profile extrusion, Journal of Materials Processing Technology, 177 (2006) 587–590.

[85] D. Pietzka, N. Ben Khalifa, S. Gerke, A.E. Tekkaya, Composite extrusion of thin aluminum profiles with high reinforcing volume, Key Engineering Materials, 554-557 (2013) 801-808.

[86] M. Kleiner, M. Schikorra, Simulation-Based Analysis of Composite Extrusion Processes, Annals of the CIRP, 56 (2007) 317-320.

[87] T. Kloppenborg, N. Ben Khalifa, A.E. Tekkaya, Accurate Welding Line Prediction in Extrusion Processes, Key Engineering Materials, 424 (2010) 87-95.

[88] T. Kloppenborg, Analyse- und Optimierungsmethoden für das Verbundstrangpressen, PhD thesis, Institute of Forming Technology and Lightweight Construction, TU Dortmund University, Shaker Publishing, ISBN 978-3-8440-1384-9, (2012, in German).

[89] K.A. Weidenmann, E. Kerscher, V. Schulze, D. Löhe, Characterization of the interfacial properties of compound-extruded lightweight profiles using the push-out-technique, Material Science and Engineering, 424 (2006) 205-211.

[90] M. Haase, N. Ben Khalifaa, A.E. Tekkayaa, W.Z. Misiolek, Improving mechanical properties of chip-based aluminum extrudates by integrated extrusion and equal channel angular pressing (iECAP), Materials Science and Engineering, 539 (2012) 194–204.

[91] A.R. Eivani, A.K. Taheri, A new method for producing bimetallic rods, Materials Letters, 61 Issues 19–20 (2007) 4110–4113.

[92] H.J. Choi, S.J. Lim, H.T. Shin, S. Choi, CNC extruder for varied section extrusion, Journal of Achievements in Materials and Manufacturing Engineering, 29 (2008) 2.

[93] A. Selvaggio, M. Haase, N. Ben Khalifa, A.E. Tekkaya, Extrusion of Profiles with variable wall thickness, Procedia CIRP, 18 (2014) 15-20.

[94] V. Güley, N.B. Khalifa, A.E. Tekkaya, Direct recycling of 1050 aluminum alloy scrap material mixed with 6060 aluminum alloy chips by hot extrusion, Int J Mater Form, 3 (2010) 853–856.

[95] J. Gronostajski, H. Marciniak, A. Matuszak, New methods of aluminium and aluminium-alloy chips recycling, Journal of Materials Processing Technology, 106 Issues 1–3 (2000) 34–39.

[96] R. Chiba, T. Nakamura, M. Kuroda, Solid-state recycling of aluminum alloy swarf through cold profile extrusion and cold rolling, Journal of Materials Processing Technology, 211 Issue 11 (2011) 1878–1887.

[97] F. Zanatta, D. Colombo, Tesi: Alluminio, processi di produzione innovativi e tecnologie meccaniche, Università degli Studi di Trento, Facoltà di Ingegneria dei Materiali (2003).

[98] N. Hansen, Hall-Petch relation and boundary Strengthening, Scripta Materialia, 51 (2004) 801-806.

[99] N. Negendank, S. Muller, W. Reimers, Extrusion of aluminum tubes with axially graded wall thickness and mechanical characterization, Procedia CIRP 18 (2014) 3-8.

[100] R. Boi, G. Barbarossa, R. Barbato, S. Valzano, Schede difetti, Qualitat & CIOA (Aital), 2008.

[101] P. Garbacz, T. Giesko, A. Mazurkiewicz, Inspection method of aluminium extrusion process, Archives of Civil and Mechanical Engineering, 15 (2015) 631-638.

[102] J. Lof, Developments in finite element simulations of aluminum extrusion, 2001.

[103] J. Zhou, L. Li, J. Duszczyk, 3D FEM simulation of the whole cycle of aluminum extrusion throughout the transient state and the steady state using the updated

Lagrangian approach, Journal of Materials Processing Technology, 134 (2003) 383-397.

[104] J. van de Langkruis, J. Lof, W.H. Kool, S. van der Zwaag, J. Huetink, Comparison of experimental AA6063 extrusion trials to 3D numerical simulation, using a general solute-dependent constitutive model, Computational Materials Science 18 (2000) 381-392.

[105] I. Flitta, S. Sheppard, Nature of friction in extrusion process and its effect on material flow, Material Science and Technology, 19 (2003) 837-846.

[106] S. Abtahi, T. Welo, S. Storen, Interface Mechanisms on the Bearing Surface in Extrusion, Proc. 6th Int. Al. Extr. Techn. Sem., Cicago, 2 (1996) 125-131.

[107] X. Ma, M.B. De Rooij, D.J. Schipper, Friction conditions in the bearing area of an aluminum extrusion process, Wear, 278-279 (2012) 1-8.

[108] T. Bjork, Tribological aspect of aluminum extrusion dies, Comprehensive Summaries of Uppsala Dissertations from the Faculty of Science & Technology, 2001.

[109] S. Tverlid, Modelling of friction in the bearing channel of dies for extrusion of aluminum sections, Doctoral Thesis, 1997.

[110] X. Ma, , M.B. De Rooij, D.J. Schipper, Modelling of contact and friction in aluminum extrusion, Tribology International, Special Issue on Second International Conference on Advanced Tribology, 43 (2010) 1138-1144.

[111] S.Z. Qamar, FEM study of extrusion complexity and dead metal zone, Archives of Materials Science and Engineering, 36 (2009) 110-117.

[112] S. Bingol, A. Bozact, Investigation of the formation extrusion welds in aluminum extrusion, 10th International Research/Expert Conference "Trends in the Development of Machinery and Associated Technology", Spain, 2006.

[113] www.struers.com.

[114] Francesco Gagliardi, Martin Schwane, Teresa Citrea, M. Haase, N.M Khalifa, A.E. Tekkaya, Bridge Design Influences on the Pressure Conditions in the Welding chamber for Porthole Die Extrusion, Key Engineering Materials Vols. 622-623 (2014) pp 87-94.

[115] R. AKERET, in Proceedings of 5th International Aluminum Extrusion Technology Seminar, Chicago, Vol. 1 (1992) 219.

[116] N. Alharthi, S. Bingöl, A. Ventura, W. Misiolek, Analysis of Extrusion Welding in Magnesium Alloys – Numerical Predictions and Metallurgical Verification, Procedia Engineering, 11th International Conference on Technology of Plasticity, ICTP 2014, 19-24 October 2014, Nagoya Congress Center, Nagoya, Japan, 81 (2014) 658-663.

[117] M. Warmuzek, Metallographic techniques for aluminum and its alloys, Metallography and microstructure, Vol. 9ASM Handbook, ASM International, Materials Park (OH) (2004).

[118] D. Lesniak, W. Libura, Extrusion of sections with varying thickness through pocket dies, J Mater Process Technol, 194 (2007) 38-45.

[119] W.S. Lee, Z.C. Tang, Relationship between mechanical properties and microstructural response of 6061–T6 aluminum alloy impacted at elevated temperatures, Mater Des, 58 (2014) 116–24.

[120] M. Schwane, F. Gagliardi, A. Jäger, N. Ben Khalifa, A.E. Tekkaya, Modeling approach for the determination of material flow and welding conditions in porthole die extrusion with gas pocket formation. Key Eng Mater, 554-557 (2013) 787-93.

[121] J. Zhou, L. Li, J. Duszczyk, Computer simulated and experimentally verified isothermal extrusion of 7075 aluminum through continuous ram speed variation, Journal of Materials Processing Technology, 146 (2004) 203-212.

[122] L. Li, J. Zhou, J. Duszczyk, Prediction of temperature evolution during the extrusion of 7075 aluminum alloy at various ram speeds by means of 3D FEM simulation, Journal of Materials Processing Technology, 145 (2004) 360-370.

[123] Y.S. Lou, H. Huh, S. Lim, K. Pack, New ductile fracture criterion for prediction of fracture forming limit diagrams of sheet metals, International Journal of Solids Structures, 49 (2012) 3605-3615.

[124] Y. Lou, H. Huh, Extension of a shear-controlled ductile fracture model considering the stress triaxiality and the Lode parameter, International Journal of Solids and Structures, 50 (2013) 447-455.

[125] Lode, Versuche Uber den Einfluss der mittleren Hauptspannung auf das Fliessen der Metalle Eisen, Kupfer, und Nickel. Z. Phys, 36 (1926) 913-939.

[126] R. Cornish, One way Analysis of Variance, Mathematics learning Support Centre, 2006.

[127] R.H. Myers, D.C. Montgomery, C.M. Anderson-Cook, Ed. Wiley Response Surface Methodology: Process and Product Optimization Using Designed Experiments, 2009.

[128] Q. Li, C.J. Smith, C. Harris, M.R. Jolly, Finite element investigations upon the influence of pocket die designs on metal flow in aluminum extrusion, Part I. Effect of pocket angle and volume on metal flow, Journal of Materials Processing Technology, 135 (2003) 189-196.

[129] M. J. Anderson, P. J. Whitcomb, DOE Simplified: Practical Tools for Effective Experimentation, 2007.

SCIENTIFIC CURRICULUM VITAE

Teresa Citrea

Data di nascita   04/04/1988

Luogo di nascita   Rossano (CS)

Tel: 3475591908

E-Mail: teresa.citrea@unical.it

Journal Publications

1. Gagliardi F., Citrea T., Ambrogio G., Filice L., Influence of the Process Setup on the Microstructure and Mechanical Properties Evolution in Porthole Die Extrusion, Materials and Design, 60 (2014) 274-281;

2. Gagliardi F., Citrea T., Ambrogio G., Filice L., Numerical Analysis on Surface Ductile Fractures for Some Extrusion Conditions, Key Engineering Materials, 585 (2014) 51-58;

3. Francesco Gagliardi, Martin Schwane, Teresa Citrea, M. Haase, N.M Khalifa, A.E. Tekkaya, Bridge Design Influences on the Pressure Conditions in the Welding chamber for Porthole Die Extrusion, Key Engineering Materials Vols. 622-623 (2014) pp 87-94;

4. T. Citrea, C. Dahnke, F. Gagliardi, M. Haase, G. Ambrogio, A. Erman Tekkaya, Optimization of porthole die for non-symmetric composite profiles, Proceedings Aluminium Two Thousand World Congress and International Conference on Extrusion and Benchmark ICEB 2015 12-16 May 2015, Florence, Italy, submitted to Materials Today: Proocedings;

5. F. Gagliardi, T. Citrea, G. Ambrogio, L. Filice, W. Z. Misiolek, Relationship between process conditions and seam weld width in extruded shapes through a porthole die with customized geometry, Proceedings Aluminium Two Thousand World Congress and International Conference on Extrusion and Benchmark ICEB 2015 12-16 May 2015, Florence, Italy, submitted to Materials Today: Proocedings.

Conference proceedings published in journals

1. Schwane M, CITREA T., Dahnke C, Haase M, Khalifa NB, Tekkaya AE, Simulation of composite hot extrusion with high reinforcing volumes, 11th International Conference on Technology of Plasticity, ICTP 2014, 19-24 October 2014, Nagoya Congress Center, Nagoya, Japan, Procedia Engineering 81 (2014) 1265-1270;

2. Ciancio C., Citrea T., Ambrogio G., Filice L., Gagliardi F., Musmanno R., Design of a high performance predictive tool for forging operations, 9th CIRP Conference on Intelligent Computation in Manufacturing Engineering, Procedia CIRP, 33 (2015) 173 – 178;

Congresses and Conferences

1. Ambrogio G., Citrea T., Filice L. and Gagliardi F. (2014) "Numerical simulation of high speed incremental forming aluminium alloy" proceedings of Numisheet 2014, The 9th International Conference and Workshop on Numerical Simulation of 3D Sheet Metal Forming Processes, January 6-10, 2014 Melbourne, Australia;

2. T. Citrea, F. Gagliardi, G. Ambrogio, L. Filice, Influence of some geometrical variables on profile distortion and ram load in the extrusion process, Proceedings XII A.I.Te.M Conference, 7-9 september 2015, Palermo, Italy.

Attendance at:

1. SMART, 3rd Summer School on Sheet Metal Advanced Research & Teaching, September 29th to October 4th, Cefalù, Sicilia, 2013;

2. ICEB 2013, International Conference on Extrusion and Benchmark, 8th-9th October 2013 in Dortmund, Germany;

3. ManuLight 2014,Conference on Manufacture of Lightweight Components, 3th-4th April 2014, Dortmund, Germany;

4. Aluminum 2000 & ICEB 2015, 12nd-16th May 2015, Palazzo degli Affari, Florence, Italy.